# DEVELOPMENT OF MULTIDIMENSIONAL CHROMATOGRAPHY FOR COMPLEX (METH)ACRYLATE-BASED COPOLYMERS USED IN COSMETIC APPLICATIONS

Vom Fachbereich Chemie

der Technischen Universität Darmstadt

zur Erlangung des akademischen Grades eines

Doktor-Ingenieurs (Dr.-Ing.)

genehmigte Dissertation

vorgelegt von

**Dipl.-Ing. Jacques-Antoine Raust**

aus Nîmes, Frankreich

| | |
|---|---|
| **Referent:** | **Prof. Dr. Harald Pasch** |
| **Korreferent:** | **Prof. Dr. Markus Busch** |
| **Tag der Einreichung:** | **17. 10. 2008** |
| **Tag der mündlichen Prüfung:** | **15. 12. 2008** |

**Darmstadt 2008**

**D17**

I would like to express my gratitude to all the people who played an active role in the achievement of this PhD thesis. I thank Prof. Harald Pasch who gave me the opportunity to work in his group and who devoted me a lot of his time during my stay at DKI. I am also thankful for his trust in me and for the liberty that I had for performing my research.

I would like to thank Dr. Claudine Moire, Dr. Céline Farcet and Dr. Michel Valtier from L'Oréal for the successful collaboration, for providing the polymer samples and for the financial support of this work. I am particularly grateful to them as they entrusted me with this interesting and challenging research. I thank all L'Oréal employees whom I met during my different stays in Paris for the work together and for their enthusiasm.

I acknowledge the persons who helped me to find my way at the different stages of my education career. Here, I particularly want to mention Prof. Lucette Bardet, Prof. Patrice Prognon, Dr. Bernard Do, Prof. Pierre Gareil and Prof. Bernadette Charleux. They encouraged me and evoked my interest for science, especially in the field of chemistry.

I express my heartfelt gratitude to all my past and present colleagues of DKI who made my stay at the institute so pleasant. I appreciate the friendly atmosphere during the work as well as during the leisure activities. Thank you for having made me feel more than welcome in Germany.

Enfin je remercie tous mes proches (ma femme Agnès, ma famille et mes amis), à qui je souhaite exprimer toute ma tendresse et l'immense joie qui m'habite lorsque je suis avec eux.

Diese Arbeit wurde am Deutschen Kunststoff-Institut unter Leitung von Prof. Dr. H. Pasch in der Zeit von Februar 2006 bis Dezember 2008 durchgeführt.

Publication:

Jacques-Antoine Raust, Adele Brüll, Claudine Moire, Céline Farcet and Harald Pasch

"TWO-DIMENSIONAL CHROMATOGRAPHY OF COMPLEX POLYMERS 6: METHOD DEVELOPMENT FOR (METH)ACRYLATE-BASED COPOLYMERS"

*Journal of Chromatography A*, **1203** (2008), 207-216

Oral presentation:

1. "DEVELOPMENT OF MULTIDIMENSIONAL CHROMATOGRAPHY FOR COMPLEX TERNARY COPOLYMERS"
   *SCM-3 (Third International Symposium on the Separation and Characterization of Natural and Synthetic Macromolecules),*
   30.01.-02.02.2007, Amsterdam, The Netherlands
2. **"**DEVELOPMENT OF MULTIDIMENSIONAL CHROMATOGRAPHY FOR (METH)ACRYLATE-BASED TERNARY COPOLYMERS"
   *YES 2007 (3rd Young European Scientists Workshop)*
   08.-13.07.2007, Krakow, Poland

Posters:

1. "DEVELOPMENT OF MULTIDIMENSIONAL CHROMATOGRAPHY FOR (METH)ACRYLATE-BASED TERNARY COPOLYMERS"
   *YES 2007 (3rd Young European Scientists Workshop)*
   08.-13.07.2007, Krakow, Poland
2. "2D-LC SEPARATION OF FATTY ALCOHOL ETHOXYLATES SIMULTANEOUSLY BY ENDGROUP AND CHAIN LENGTH WITH ON-LINE $^{1}$H-NMR CHARACTERIZATION"
   *10th Annual UNESCO/IUPAC Conference on Macromolecules & Materials*
   08.-11.09.2008 Mpumalanga, South Africa

# CONTENT

# I. German Summary

Der schnell wachsende Markt für kosmetische Erzeugnisse und der Bedarf an innovativen Produkten mit neuen und verbesserten Eigenschaften führen zur Entwicklung von immer komplexeren Polymerstrukturen. Die Strukturvariationen können durch unterschiedliche Monomerkombinationen oder durch unterschiedliche Polymerisationsverfahren erreicht werden. Sie führen häufig zu Copolymeren mit ungewöhnlichen Eigenschaften. Für das detaillierte Verständnis der molekularen Struktur dieser neuen Produkte bzw. für die Erarbeitung von Struktur-Eigenschaftsbeziehungen sind neue und bessere Charakterisierungsverfahren erforderlich. Nur so können Syntheseparameter und letztendlich die Produkteigenschaften gezielt optimiert werden.

Das Ziel der vorliegenden Arbeit war die Entwicklung von analytischen Methoden zur umfassenden Charakterisierung der molekularen Heterogenität von Copolymeren auf der Basis unterschiedlicher Acrylate und Methacrylate. Der Fokus lag dabei auf der Entwicklung von mehrdimensionalen chromatographischen Methoden, die es gestatten, die unterschiedlichen molekularen Parameter (z. B. Molmassenverteilung, MMD, und chemische Heterogenität, CCD) quantitativ zu bestimmen.

Die untersuchten Copolymere unterschieden sich in ihrer Monomerzusammensetzung und in der Art der Herstellung. Die erste Probenserie wurde durch eine zweistufige freie radikalische Polymerisation (FRP) hergestellt. Dabei bestand der erste Syntheseschritt in der Copolymerisation zweier Monomere. In einem zweiten Schritt wurde das Vorprodukt mit dem dritten Monomeren umgesetzt, wobei ein komplexes terpolymer entstand. Folgende fünf Monomere wurden miteinander kombiniert: Isobornylacrylat (iBorA), Isobornylmethacrylat (iBorMA), Isobutylacrylat (iBuA), Isobutylmethacrylat (iBuMA) und 2-Ethylhexylacrylat (2EHA).

Die zweite Probenserie enthielt zwei Arten von Diblockcopolymeren, die durch kontrollierte radikalische Polymerisation (CRP) hergestellt wurden. Im ersten Fall erfolgte die Synthese durch eine zweistufige Atom Transfer Radical Polymerization (ATRP), wobei im ersten Schritt iBuA zu einem Homopolymeren mit enger Molmassenverteilung umgesetzt wurde. Dieser erste Block wurde anschließend als Makroinitiator mit iBorA und iBorMA copolymerisiert, wobei ein iBorA-iBorMA-Copolymerblock gebildet wurde. Im zweiten Fall wurden Blockcopolymere durch Reversible Addition Fragmentation Chain Transfer (RAFT)

hergestellt. Dabei wurde der erste Block aus 2EHA mit Dithiobenzoat-Endgruppe gebildet. Der zweite Block wurde durch Umsetzung mit Methylacrylat (MA) erhalten.

Die Ergebnisse der vorliegenden Arbeit können wie folgt zusammengefasst werden:

1. Es wurden chromatographische Methoden für die Analyse von komplexen segmentierten Copolymeren entwickelt, die durch einen zweistufigen FRP-Prozess hergestellt wurden. Die Molmassenverteilungen der Produkte wurden durch SEC bestimmt. Wie zu erwarten wurden breite Verteilungen gefunden, da die Polymerisation nicht kontrolliert war. Zusätzlich erhöhte sich die Polydispersität durch die angewandte zweistufige Polymerisation, es wurden aber in allen Fällen monomodale Verteilungen erhalten. Zur Bestimmung der chemischen Heterogenität wurde eine Methode für die Gradienten-HPLC entwickelt. Mit dieser Methode gelang es, alle Produktkomponenten aufzutrennen und zu identifizieren. Es zeigte sich, dass die Reaktionsprodukte neben den erwarteten Terpolymeren auch Copolymere aus dem ersten Polymerisationsschritt und Homopolymer aus dem zweiten Polymerisationsschritt enthielten. Über die Peakflächen wurde eine erste grobe Quantifizierung der Komponenten vorgenommen. Dabei zeigte sich, dass die Produktzusammensetzung erheblich von der Art der eingesetzten Monomere abhing. Für eine vollständige Beschreibung der komplexen Zusammensetzung der Polymere musste jedoch eine Methode der 2D-LC entwickelt werden. Diese trennte die Produkte nach der chemischen Zusammensetzung in der ersten Dimension und nach der Molmasse in der zweiten Dimension. Auf diese Weise konnten die Molmassen für alle Produktkomponenten bestimmt werden. Ein weiteres Ziel war die Erarbeitung einer schnellen Methode, die zukünftig in der prozess- und Qualitätskontrolle eingesetzt werden kann.

2. Für eine Validierung der Peakzuordnung in der Chromatographie und für quantitative Aussagen zur Copolymerzusammensetzung wurde eine Methode entwickelt, bei der die chromatographischen Trennungen mit einem off-line FTIR-Detektor gekoppelt wurden. Ein LC-Transform-Interface wurde verwendet, um die chromatographisch getrennten Fraktionen lokal getrennt auf eine Germaniumscheibe aufzusprühen. Nach Verdampfen des Lösungsmittels lagen die Polymerfraktionen als dünne Filme vor und konnten entsprechend durch FTIR vermessen werden. Die Methode wurde eingesetzt, um Proben unterschiedlicher Zusammensetzung aus iBorMA, iBorA (erster Schritt) and iBuA (zweiter Schritt) zu analysieren. Die Kalibration der FTIR wurden mit Referenzpolymeren durchgeführt. Es wurde eine lineare Abhängigkeit zwischen dem Anteil an iBorA + iBorMA und den entsprechenden FTIR-Peakflächen gefunden. Durch SEC-FTIR war es anschließend möglich,

die chemische Zusammensetzung als Funktion der Molmasse quantitativ zu bestimmen. Die Analyse der unterschiedlichen Produktkomponenten (Homopolymere, binäre und ternäre Copolymere) gelang durch Gradienten-HPLC-FTIR. Durch die Methodenkopplungen wurde die Existenz einer erheblichen Menge binärer Copolymere nachgewiesen, die aus dem ersten Polymerisationsschritt stammen. Weiterhin konnte die Verteilung der iBor(M)A-Wiederholungseinheiten im Terpolymeren bestimmt werden. Es konnte nachgewiesen werden, dass der Anteil des im zweiten Polymerisationsschritt addierten Monomeren einen entscheidenden Einfluss auf die Produktzusammensetzung hat.

3. Durch Verwendung von stationären Phasen unterschiedlicher Polarität konnte die Elutionsreihenfolge der Polymerkomponenten eingestellt werden. Auf diese Weise konnte eine möglichst hohe Selektivität der Trennungen erreicht werden. Im vorliegenden chromatographischen System gelang es, die binären Copolymere (aus iBorA und iBorMA) im SEC-Modus zu eluieren, während alle iBuA enthaltenden Komponenten auf der stationären Phase (Cyano-modifiziertes Kieselgel) adsorbiert wurden. Für die quantitative Auswertung wurde der ELSD-Detektor mit binären Copolymeren kalibriert. Auf diese Weise konnte der Massenanteil dieser Komponenten quantitativ bestimmt und mit den Bruttozusammensetzungen der Reaktionsprodukte aus der $^{1}$H-NMR korreliert werden. Schließlich ließ sich aus den HPLC-FTIR- und NMR-Daten die Zusammensetzung der Terpolymere selektiv ermitteln. Die erhaltenen Strukturinformationen trugen zu einem besseren Verständnis der Polymerisationsprozesse bei und bewiesen, dass die Terpolymerisation im zweiten Reaktionsschritt nicht vollständig abläuft.

4. Zur Charakterisierung der ternären Diblockcopolymere, die durch ATRP hergestellt wurden, konnte das bereits entwickelte chromatographische System angewandt werden, da die gleichen Monomere zum Einsatz kamen. Hier wurde erwartet, dass relativ einheitliche Produkte erhalten werden, da die kontrollierte radikalische Polymerisation eingesetzt wurde. Dies war tatsächlich für den ersten Polymerisationsschritt der Fall. Für kinetische Proben, die während des zweiten Reaktionsschrittes erhalten wurden, ergaben sich aber bimodale Molmassenverteilungen, die auf einen Verlust der Polymerisationskontrolle hinwiesen. Diese Annahme wurde durch die Gradienten-HPLC and und 2D-LC bestätigt. Anscheinend wurden zu Beginn des zweiten Polymerisationsschritts als Folge eines Kettentransfers des Broms (aus dem ATRP-Kettenregler) im wesentlichen Oligomere aus iBorA und iBorMA gebildet. Im weiteren Verlauf der Polymerisation nimmt der Oligomeranteil ab und höhermolekulare binäre und ternäre Copolymere werden gebildet. Auch bei diesen Untersuchungen zeigte sich, dass nur durch selektive und leistungsfähige Produktanalytik ein Verständnis der bei der

Polymerisation ablaufenden Prozesse erreicht werden kann. Dabei haben sich die Gradienten-HPLC und die 2D-LC als besonders wertvoll erwiesen.

5. In einer weiteren Produktserie wurden als Monomere 2EHA und Methylacrylat (MA) eingesetzt. Diese Monomere wurden wiederum in einem zweistufigen Prozess durch RAFT polymerisiert. Dabei sollten sich Diblockcopolymere bilden, die während der Reaktion unter Partikelbildung assoziieren. Im ersten Schritt wurde 2EHA unter Bildung eines Makro-RAFT-Agens polymerisiert, gefolgt von der Polymerisation des MA im zweiten Schritt. Im vorliegenden Fall mussten neue HPLC-Verfahren entwickelt werden, um die Produkte nach der chemischen Zusammensetzung zu trennen. Schon aus der SEC ergab sich, dass die Reaktionsprodukte heterogen aufgebaut sind. Bimodale Verteilungen legten den Verlust der Kontrolle während der Polymerisation nahe. Durch die optimierte HPLC wurde bestätigt, dass ein großer Teil des 2EHA als Homopolymer aus dem ersten Polymerisationsschritt vorlag. Die UV-Detektion zeigte, dass diese Homopolymermoleküle kein aktives Kettenende aufwiesen (keine DTB-Gruppe) und dementsprechend im zweiten Polymerisationsschritt inaktiv waren. Ein noch besseres Verständnis über die bei der Polymerisation ablaufenden Prozesse wurde durch die 2D-LC (Gradienten-HPLC x SEC) erhalten. Die erhaltene Produktverteilung legte die Annahme nahe, dass eine der wesentlichen Nebenreaktionen die Rekombination von zwei P2EHA-Radikalen an der Oberfläche der gebildeten Partikel ist. Dabei setzt die Partikelbildung zu Beginn des zweiten Polymerisationsschrittes ein, so dass unter diesen Bedingungen zum erheblichen Teil die Rekombination des P2EHA und eine unkontrollierte radikalische Polymerisation des MA unter Bildung von PMA abläuft.

6. Neben den bereits diskutierten chromatographischen Methoden wurde die Chromatographie unter kritischen Bedingungen (LC-CC) zur selektiven Auftrennung der Reaktionsprodukte eingesetzt. Am kritischen Punkt der Adsorption für P2EHA erfolgt die Elution ausschließlich nach der Kettenlänge der PMA-Blöcke im SEC-Modus. Nach entsprechender Molmassenkalibrierung ließ sich auf diese Weise die Molmassenverteilung des PMA-Blocks in den Blockcopolymeren bestimmen. Dabei zeigte sich, dass die Molmasse des PMA-Blocks während des zweiten Polymerisationsschrittes anwächst. Unter den gewählten Bedingungen konnte auch der Anteil an nicht reaktivem P2EHA-Homopolymer quantifiziert werden. Der Gesamtanteil an 2EHA in den Reaktionsprodukten wurde durch $^{1}$H-NMR bestimmt. Unter Berücksichtigung aller analytischen Daten konnte die Verteilung von 2EHA über alle Produktkomponenten berechnet werden. Dabei ergab sich, dass offensichtlich nach Bildung der Partikel eine Polymerisation im Wesentlichen innerhalb der Partikel stattfindet (Kettenwachstum der PMA-Blöcke). An der Oberfläche der Partikel findet

im Wesentlichen die Rekombination der P2EHA-Ketten statt. Das Komponentenspektrum umfasst daher P2EHA, rekombiniertes P2EHA (doppelte Molmasse), P2EHA-PMA-Blockcopolymer und rekombiniertes P2EHA-PMA-Blockcopolymer (doppelte Molmasse und Anzahl der Blöcke).

7. Für weitere Strukturinformationen wurde eine Methode der direkten Kopplung der SEC mit der $^{1}$H-NMR-Spektroskopie entwickelt. Mit dieser Methode sollte die chemische Zusammensetzung als Funktion der Molmasse direkt und ohne Kalibration bestimmt werden. Die größten Schwierigkeiten bei dieser Methodenkopplung sind die geringen Eluatkonzentrationen, die aus der SEC anfallen, und die Signale des SEC-Eluenten. Nur durch effektive Lösungsmittelunterdrückung war es überhaupt möglich, die relevanten Polymersignale zu detektieren. Anstelle des sonst üblichen THF wurde hier Chloroform als mobile Phase verwendet. Im Ergebnis gelang es, die chemische Zusammensetzung für alle Molmassenfraktionen zu bestimmen. P2EHA-Homopolymer und deren Kupplungsprodukt konnte klar erkannt werden.

Zusammenfassend kann festgestellt werden, dass eine umfassende Beschreibung der molekularen Heterogenität der vorliegenden komplexen Polymerisationsprodukte nur durch Kombination verschiedener Trenn- und Analysenverfahren möglich ist. Die Aussagen aus der SEC, der HPLC, der LC-CC und der 2D-LC kombiniert mit Daten aus der FTIR und NMR geben einen guten Überblick über die vorliegenden Produktzusammensetzungen. Dabei zeigt sich, dass auch Reaktionsprodukte, die durch anscheinend wohldefinierte und kontrollierte Polymerisationsverfahren hergestellt wurden, eine komplexe Zusammensetzung aufweisen.

# II. Introduction

Polymers are present in a large variety of cosmetic formulations and serve diverse purposes. They are used as film-formers in hair fixatives, mascara, nail enamels and transfer-resistant color cosmetics; as thickeners and rheology modifiers in emulsions, gels, hair colorants and hair relaxers; as emulsifiers in lotions, sunscreens and hair colors and as detergents, conditioners, moisturizers, dispersants and waterproofers [1-2]. Such wide range of properties is achieved using a large palette of polymeric products which come from different sources. They are either obtained by extraction from natural sources and used with or without modifications or synthetically produced which is the case for the major part of them. Polymers exhibit different application properties according to their chemical structure (chemical composition, architecture, end-group functionality) and molar masses. Indeed, different from well-defined small molecules, the macromolecular chains which compose a polymer material are usually inhomogeneous, i.e. polydisperse. They are always distributed in terms of molar mass, i.e. chain length, and a fraction of a given molar mass is susceptible to present different chemical structures. Figure 1 shows the possibilities of chain organizations in terms of composition, architecture and functionality. These differences are also the basis of the materials applications.

The relation between the macroscopic properties and the microscopic organization of the repeat units is usually called the structure-property relationship. It is of great interest to precisely establish these relationships to optimize the produced material according to the desired application. As examples of these differences in the cosmetic industry, we can compare two types of polymers which are intended for two specific purposes according to their chemical structure. A high molar mass water soluble polymer would be possibly used as thickener in water-based formulation whereas a water insoluble copolymer would be more indicated for formation of waterproof films. Presence of charges along the chains is also of primary concern in a large numbers of polymers as they favor attachment to the skin or improve cleaning properties.

As a consequence the precise design of the macromolecules is important to finely tune polymer application properties. A control over the synthesis has to be maintained in order to produce (co)polymers with the lowest possible dispersity. Several techniques of controlled polymerization are available using ionic or radical active centers.

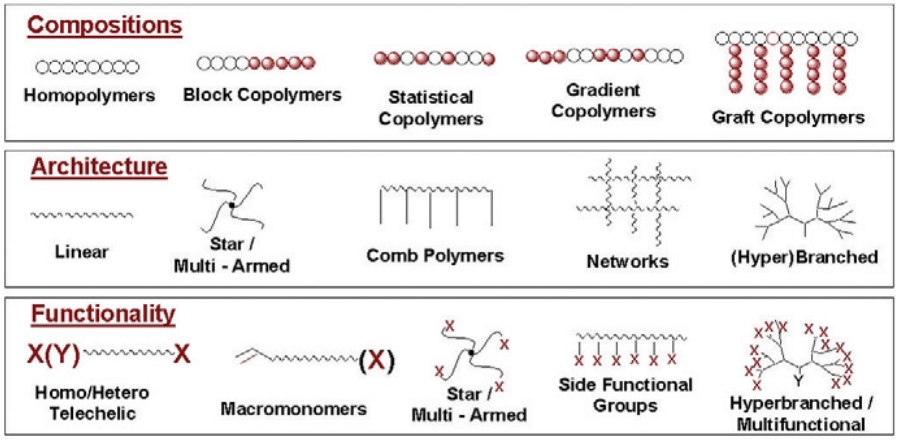


**Figure 1:** Possible molecular structures for polymers in terms of chemical composition, architecture and end-group functionality [15]

To characterize these highly complex (co)polymers it is necessary to determine not only average values of the chemical structure but a precise description of the multiple distributions is required. Separation techniques are for this purpose highly valuable and particularly High-Performance Liquid Chromatography (HPLC). Size Exclusion Chromatography (SEC) is the established method for analyzing polymer molar mass distribution as macromolecules are separated according to their volume in solution (hydrodynamic volume). Chromatographic techniques have also been developed for analyzing chemical heterogeneity. The separation mechanism is based on attractive/repulsive interactions between macromolecules and the chosen chromatographic column (e.g. Liquid Adsorption Chromatography, LAC, or Liquid Chromatography at Critical Conditions, LC-CC) [3,4,5]. Frequently, a mobile phase gradient is used to progressively change the adsorption interactions and thus achieve more selective separations with regard to chemical composition [6,7].

A very peculiar mode of HPLC, specific for polymer analysis, is LC-CC. It is characterized by very narrow chromatographic conditions (stationary phase, mobile phase composition and temperature) which create a specific environment for a given homopolymer. It leads to an elution of this homopolymer as if molar mass distribution was “invisible” for the system. It is very useful for block copolymer analyses since the blocks could be considered as linked homopolymers. In this case, a part of the macromolecule is chromatography “invisible” and the analysis is realized only on the other part of the molecule. It tends to simplify the problem of characterization as it allows to collect information on a selected part of the molecule [8,9].

As previously mentioned, polymers are heterogeneous according to different properties. Therefore, one-dimensional analyses can only partially describe the macromolecular heterogeneity. To get information on all aspects of the macromolecular heterogeneity

coupling of two or more chromatographic techniques have been developed: i.e. multidimensional chromatography and more particularly two-dimensional liquid chromatography (2D-LC). A major advantage of 2D-LC separations is the fact that 2D analyses can differentiate between samples that show identical chromatograms in the first and second dimensions (see Figure 2). A fully automated two-dimensional chromatographic system including two chromatographs was introduced by Kilz et al. 15 years ago [10,11]. In the first step, separation occurred by chemical composition using interaction chromatography and in the second dimension macromolecules were eluted as a function of their decreasing hydrodynamic volumes using SEC. Each fraction collected from the first chromatographic system was automatically transferred into the second separation system for SEC analysis. This system permits a comprehensive analysis of the polymers according to two of their distributions.

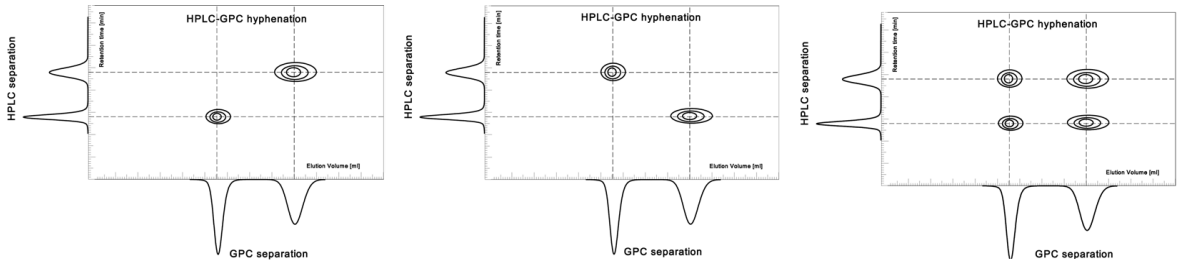


**Figure 2:** Example of possible 2D-LC plots which can be obtained by combining one HPLC chromatogram (separation according to chemical composition) with one SEC chromatogram (separation according to molar mass) [11]

A number of 2D-LC systems have been developed and optimized for a large number of polymer species. This includes the combination of LC-CC and SEC. Such system is well-suited for analyzing functional homopolymers, block copolymers and graft copolymers as reported by Adrian et al. [12,13] or for characterization of linear and star block copolymers synthesized by atom transfer radical polymerization (ATRP) as reported by Gao et al [14].

The aim of the work presented in this thesis was to develop methods to analyze the macromolecular heterogeneity of acrylate and methacrylate ester-based copolymers. These copolymers are produced to be integrated in cosmetic formulations. The document is divided in two main parts. The first one gives an overview of the existing methods to produce and analyze such polymers. The second part is dedicated to the presentation of the results obtained during the thesis.

In the first experimental chapter, method developments for analyzing complex ternary copolymers are given. The samples were produced via a two-step free-radical polymerization

process. Such technique usually leads to the formation of very complex products which exhibit a broad chemical composition distribution. This copolymerization process is thought to produce binary copolymers and homopolymers in addition to the expected terpolymers. For this reason specific chromatographic techniques were developed and coupled to comprehensively characterize the samples. One primary concern was to set up fast separation techniques which nevertheless maintain a high resolution between the analyzed species allowing to be used for quality control. Such techniques should enable us to define the chemical composition of the samples and assign a molar mass to each kind of macromolecule separated. Further investigations were dedicated to couple the developed chromatographic methods to a spectroscopic technique, i.e. Fourier Transform Infra-Red (FTIR) spectroscopy. LC-FTIR off-line hyphenation provided precise information on the chemical composition of the samples. Finally, we were able to measure the percentage of homopolymers and binary copolymers present in the samples by calibrating the detector with standards of these species. As a result we were able to calculate the amount of terpolymer present in the samples.

The second experimental chapter was dedicated to the analysis of diblock copolymers prepared by controlled radical polymerization. A first set of samples was made by ATRP with similar repeat units as those used for polymers analyzed in the first chapter. Samples were then analyzed with the previously developed methods. Differences of the results obtained for these samples were related to the specificities of the polymerization procedure. The diblock copolymers of the second set of samples were prepared by reversible addition-fragmentation chain transfer (RAFT) in dispersed media. These copolymers are supposed to self-assemble in the polymerization solvent. Specific methods for block analysis were developed such as LC-CC in addition to the classical separation techniques. Several 2D-LC coupling methods were set up to achieve a comprehensive characterization of the samples.

# III. Theoretical Considerations

## 1. Polymer synthesis

There are two kinds of reactions for polymer synthesis: step growth polymerization (polyaddition or polycondensation when reaction produces residual small molecules, such as water) and chain growth polymerization (with ionic or radical active centre). In the first case, chains grow by reaction between molecules of different degrees of polymerization (DP). Step-growth polymerization reactions are typical organic condensation reactions (e.g. esterification, amide formation, electrophilic substitution: e.g. Friedel and Crafts reaction, urethane formation…). Chemical initiators of the reaction are usually not required. For chain growth polymerization an initiator is necessary to produce a primary active centre. New monomers add to the growing polymer chain via this active centre to an unsaturated bond (usually vinyl: C=C). The active centre is regenerated at the new added monomer by cleavage of this unsaturated bond. Different kinds of active centers can be used, mainly free radicals, carbocations or carbanions.
The major advantage of chain growth polymerization over step growth is that high molar mass products are produced even at low conversion. Very high conversion percentages (> 95 %) have to be reached with step growth polymerization to obtain high molar masses.

In the present thesis work, we will only deal with products prepared via radical polymerization. A brief overview of the technique will be given with a description of applications using polymers obtained with this method.

### 1.1. Free Radical Polymerization

Free radical polymerization (FRP) is a chain growth reaction which is the major technique to produce polymers industrially. Approximately 50 % of all commercial synthetic polymers are prepared using radical chemistry. Fields of application are very diverse since it is possible to (co)polymerize a wide range of vinyl monomers. Radically produced polymers are found in coatings and adhesives but are also used as detergents, surfactants, lubricants or dispersants in mechanical and engineering as well as in cosmetic and personal care industries. Other

products which can be obtained with polymers prepared by radical polymerization are (polar) thermoplastic elastomers, membranes, (hydro)gels [15].

Free radical copolymerization is the preferred pathway to copolymers [16]. Synthesis conditions are very versatile: limited purification is required (removal of $O_2$) and a large variety of solvents can be used including water, ionic liquids or supercritical $CO_2$. Syntheses can be performed in homogeneous or heterogeneous media (suspension, dispersion, emulsion and mini-emulsion). Reaction temperatures are usually between ambient and 150 °C which are easily implementable. Radical polymerization has a large advantage over ionic polymerization in that ionic, basic and acidic monomers can be (co)polymerized directly.
In the chain reaction mechanism the active center is a highly reactive radical. The first step of the reaction is **the initiation** which corresponds to the production of radicals by degradation of initiator molecules. Usually azo (N=N) or peroxide (O-O) functions are used as radical primers. Formed radicals open the double bond of a vinyl monomer to form a new covalent bond. At the same time a new $C^{\bullet}$ radical is formed at the last added monomer. Further addition of monomers permits to form larger macromolecules. This step is called chain **propagation**. It occurs as long as the radical reacts with other monomers. If it reacts with other species present in the reactor (another radical, a molecule of solvent, another function of the monomer or an already formed polymer) the reaction cannot propagate anymore and the chain "dies" (terminated chains). These side reactions are called **transfer and termination** reactions. A transfer reaction forms a new radical at another molecule which is then able to grow into a macromolecule by adding monomers. Termination reactions occur between two radicals resulting in the formation of inactive species. The reaction process can be summarized as follows:

**Initiation:** $A \rightarrow 2\ R^{\bullet}$ (A containing -O-O- or -N=N- functions)

**Propagation:** $R^{\bullet} + n\ M \rightarrow R\text{-}M_{n-1}\text{-}M^{\bullet}$ (M is a vinyl monomer e.g. $CH_2$=CHX)

**Termination:**

$R\text{-}M_i^{\bullet} + R\text{-}M_j^{\bullet} \rightarrow R\text{-}M_i\text{-}M_j\text{-}R$ Combination

$R\text{-}M_i^{\bullet} + R\text{-}M_j^{\bullet} \rightarrow R\text{-}M_i^{=}\ R\text{-}M_jH$ Disproportionation

**Transfer:** $R\text{-}M^{\bullet} + R'\text{-}X \rightarrow R\text{-}MX + R'^{\bullet}$

with A an initiator molecule giving two R primary radicals. M stands for monomer, R' for any molecule in the polymerization media susceptible to give transfer and X any transferable group (usually X is a proton or a halogen atom).

In FRP, each growing chain is active during a very short time (less than a second) which means that chains are built very fast without control of monomer incorporation. It is very difficult to prepare well-defined homopolymers or copolymers in terms of molar mass and/or chemical composition. For copolymers, the order of monomers in the chain is only directed by kinetic parameters such as reactivity ratios. They describe the reactivity of the active centers and their selectivity related to a given monomer. A description of the monomer distribution in copolymers is given by the Mayo-Lewis equation [17].

## 1.2. Controlled and Living Radical Polymerization

The majority of polymer properties are dramatically improved when polymers are composed of well-defined homogeneous macromolecules. The best example is the self-assembly of diblock copolymers which will result in a narrow monomodal core-shell particle distribution in case of homogeneous macromolecules and in a broadly distributed dispersion if chains are not pure diblocks or if a block length distribution exists for each block [18,19]: higher heterogeneity in the dispersion leads to a higher instability of the dispersion.
The major drawback of free radical polymerization involving extremely reactive species is the lack of control on the synthesis and thus on the produced polymer. For this reason controlled or living radical polymerization (CRP or LRP) processes have been developed to reduce the reactivity of radicals. This research is motivated by the desire of improving materials properties of existing products and furthermore design new polymers in terms of architecture and chemical structure to achieve new properties and open new markets to synthetic polymers [20,21]. The main characteristics of CRP are:

- a linear growth of the degree of polymerization (DP: numbers of repeat units comprised in a chain) with monomer conversion without transfer reaction (constant number of chains) and without termination reaction (constant number of active sites)
- a narrow molar mass distribution with a polydispersity less than 1.5
- a defined and controlled initiation.

The controlled techniques are also called living when it is possible to reactivate a chain after complete consumption of one monomer by introducing a new batch of monomer and eventually also initiator. The necessary condition is the presence of a control agent at the chain. It is for instance possible to polymerize stepwise several monomers to form a multiblock copolymer.

Three main techniques of CRP [22,23] have emerged over the past 15 years, namely Nitroxide-Mediated Polymerization (NMP) [24], Atom Transfer Radical Polymerization (ATRP) [25,26], both based on a reversible activation/deactivation principle and reversible addition-fragmentation chain transfer (RAFT) utilizing a degenerative transfer mechanism mediated by dithioester functions [27,28,29]. One of the most important achievements of these methods is the ability to produce block copolymers and complex architectures such as multi-arm star, hyper-branched, graft and comb polymers, while keeping all the advantages of free-radical polymerization over ionic polymerization, in terms of experimental conditions and process implementation [30,31]. In some cases particularly with ATRP it is possible to perform radical polymerization in the presence of $O_2$ which is usually a radical scavenger [32].Figure 3 gives an overview of the principal CRP mechanism.

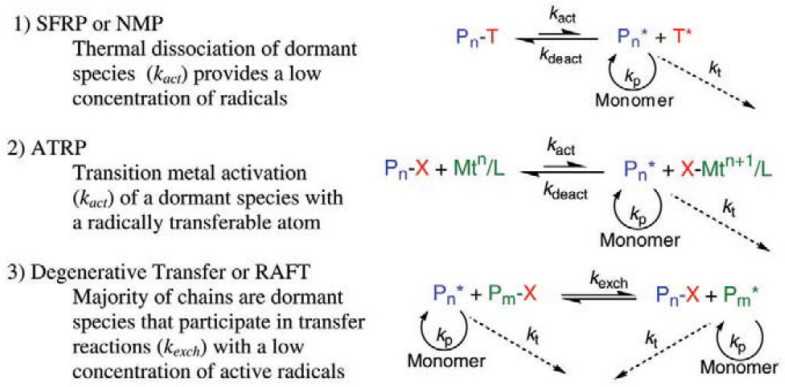


**Figure 3:** Scheme of the main CRP mechanisms taken from [15]

These CRP processes are based on the principle of creating equilibria between a very low amount of active species (from ~ 1 ppm to 1 %) and a majority of dormant species. A molecule or a chemical group is used to "hide" the radical by forming a labile bond with the $C^{\bullet}$. As we can see in Figure 3, for mechanism 1 and 2 the equilibrium favors the dormant form which obviously results in a slow down of the complete polymerization kinetics. On the other hand for RAFT, third example, it appears that when an active chain becomes dormant it directly activates another chain. Accordingly the kinetics of polymerization should not suffer any delay as long as transfer reaction is at least as fast as the propagation speed.

An external activator such as a catalyst (ATRP), temperature (NMP) or transferring radical (RAFT) is required to change the chain status from dormant to active. Thus, the activity period to form a chain (approx. 1 s in FRP) is transformed in thousands of short (ca. 1 ms) activity periods each separated by dormant (i.e. inactive) periods which can last several seconds or minutes. According to these mechanisms, chains are growing stepwise but are statistically regularly reactivated providing finally a relatively "homogenous" polymer sample.

All polymers studied in this work are homopolymers or copolymers synthesized with acrylate or methacrylate monomers which are very good candidates for radical (co)polymerization. Radical polymerization occurs at the vinyl function of these species.
Polymers containing such repeat units are broadly used in all-day life for various applications due to the large scope of functional groups which can be attached to the (meth)acrylic acid function: e.g. molecules that are highly hydrophobic or hydrophilic, polar or non-polar, positive, negative or pH-dependent charged function... With specific functional groups, polymers can be biocompatible and/or biodegradable.

The size of the ester/amide groups of the monomer and their organization along the macromolecules directly influences polymer properties. The architecture of the copolymers plays also a significant role on the properties of the copolymers and has to be carefully designed [33].
Copolymerization is perfectly suited to covalently attach monomers whose homopolymers are habitually incompatible. Such homopolymers usually form macro-phase separation when blended. However, when the monomers are copolymerized, micro-phase separation is generally observed instead with an interpenetration of the phases. Typically monomers are organized in block structure in the copolymers to achieve such micro-phase separation.
The size of the ester/amide group of the monomer also directly influences the polymer glass transition temperature and hence its applicability. If we consider an application at ambient temperature, a polymer with a glass transition temperature ($T_g$) higher than ambient will be rigid whereas a polymer with a $T_g$ lower than ambient will be flexible. It has to be noted that methacrylates have usually a higher $T_g$ than acrylates with similar ester/amide groups. Thus by combining two monomers with very different $T_g$ at application temperature, it is possible to obtain a material with both brittle-plastic and soft-elastomeric behaviors. This is used to produce (polar) thermoplastic elastomers [34] used as sealants and adhesives in a wide range of industries.

Block copolymer structures were extensively studied particularly in medical and pharmaceutical industries for drug-release materials [35,36]. Using stimulus responsive groups, such as pH dependent charged functions, it is possible to modify the supra-molecular organization of polymers in targeted organs. Macromolecules organized in micelles at low pH can be dissociated at higher pH by the appearance of charges and thus release of a drug contained in the micelle occurs in a specific location. Graft copolymers are also considered

for the same properties [37]. Using the possibility to copolymerize hydrophobic with hydrophilic monomers allows for production of a large variety of surfactants to lower the interfacial tension between two liquids [38,39,40]. Such materials are widely used to form emulsions and to disperse components in non-dissolving media. Such application is of great interest when formulating health and cosmetic products. For these purposes biocompatible (meth)acrylate monomers are polymerized. The highest surfactant efficiency is achieved with block copolymers but gradient structures can also be used for such properties [41].

Graft copolymers are often used as polymer blend compatibilizers [42] or surface modifiers by copolymerizing sticky acrylates (low $T_g$) with a rigid second part (high $T_g$) leading to a polymer able to stick to a surface on one side and exhibiting the rigid structure at the new surface [43]. These nano-structured morphologies are extensively studied for microelectronic applications [44].

Other types of architectures achievable with radical polymerization are multi-arm stars, branched and comb-like copolymers. Control of branch lengths and branch numbers via CRP allows producing materials susceptible to finely tune the viscosity of liquids by either increasing it with highly branched polymers or on the contrary playing the role of lubricants. This area is of great interest for the industry considering the number of patents filed in this domain.

Finally a very important aspect of these polymers is their end-group or chain-end functionality. They may have an important effect on polymer organization in solution or at surfaces especially for low molar mass macromolecules. End-group functionality can be very well controlled with CRP as the control agent usually reacts with the chain ends. End functional polyacrylates are used as components of sealants for out-door applications and automotive industry. They are also interesting when polymer post-synthesis modifications by reacting polymer end-groups are envisaged.

New developments have been conducted in this domain. A certain number of reactions called “Click Reactions” attract a growing interest. Click chemistry was defined by Sharpless et al. [45] and covers all chemical reactions forming stable carbon-heteroatom bonds, quantitatively, irreversibly and exothermically. Moreover the reactions should be stereospecific and should give easily removable by-products. A model reaction of this chemistry is the hetero Diels-Alder reaction of an azide function with an alcyne catalyzed by $Cu^I$. Examples of polymer post-treatment using such reaction have been reported: examples of coupling of functionalized poly(methyl methacrylate) (PMMA), poly(ethylene glycol) (PEG) and polystyrene (PS) have been realized to form different copolymers [46] and stepwise growth of

telechelic PS [47]. End-functionalization was achieved thanks to the CRP control agent. A polymer coupling reaction scheme is presented in Figure 4.

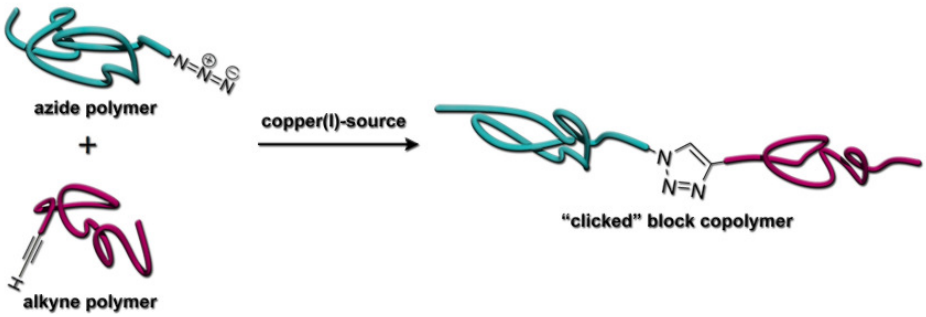


**Figure 4:** Scheme of a hetero Diels-Alder reaction to form block copolymer by post-synthesis treatment [46]

The design of such complex polymer architectures requires a huge effort of analysis and characterization of final products. Investigations are conducted in different areas such as chemistry and/or physics and/or technology in order to determine the chemical structure (molar mass, chemical composition, chemical architecture, end-functionality distribution, charge distribution…), macroscopic properties (crystallinity, film formation, aging process…) for potential applications and mechanical properties as well as processability. The final aim of all these investigations on polymers is the determination of structure-property relationships [48,49]. Establishment of these relationships is a major issue in polymer analyses since they connect microscopic and macroscopic properties.

## 2. Analysis of polymer chemical structure

In this work, we concentrated on the characterization of polymer chemical structures. As previously described, huge efforts are made to synthesize more and more complex (co)polymers. This results in a very challenging work to characterize these products as polymerization gives inhomogeneous products. Indeed, even with controlled living radical polymerization, it is not possible to completely control the synthesis process. (Co)polymers hence are distributed according to several of their features (molar mass as well as chemical composition, endgroup functionality and/or architecture). It is foreseeable that one technique will not be sufficient to comprehensively describe the products but a combination of several methods will be necessary [50]. Two main steps are usually required for the characterization of polymer structures. On one hand separation techniques are applied in order to fractionate the products in more homogeneous parts and thus obtain a distribution profile for the analyzed feature and on the other hand spectroscopic and/or spectrometric techniques are employed to

get precise chemical information on the samples. Of course it is important and beneficial to hyphenate these methods by either combining two separation techniques or a separation technique with a spectroscopic one. In the case of coupling two separation techniques, two parameters may be analyzed simultaneously (e.g. chemical composition and molar mass distributions) and information obtained for each of them can be directly combined. When a separation technique is hyphenated with a spectroscopic technique, qualitative and quantitative chemical composition of the polymer can be determined [51]. It thus gives more precise information on the chemical composition of the sample in comparison with that obtained when measuring the total sample with the same spectroscopic technique directly.

Method developments which have been conducted for this thesis were particularly focused on liquid chromatography in one or more dimensions. In the following part, a description of the principles of liquid chromatography will be given with a special attention to the particularities of the technique when applied to polymer analysis. A presentation of available detectors will be made with their specificities and the kind of information which could be expected from their utilization.
It has to be noticed that liquid chromatography investigations are conducted on diluted polymer solutions while physical and mechanical tests are carried out on bulk samples.

## 2.1. Liquid Chromatography as an efficient separation tool

In following pages a description of HPLC separation principles will be addressed with a particular attention given to specificities of polymer analysis.

### 2.1.1. HPLC: definitions and principle of separation

Guiochon wrote a review article explicating the possibilities but also the limitations of HPLC [52]. HPLC separation is usually achieved by differences of interaction strengths between analytes and the stationary phase of a chromatographic column. These interactions are a function of the mobile phase elution strength and they determine the required volume for elution. These interactions are governed by thermodynamic rules which describe the distribution of analytes between both phases.

A thermodynamic coefficient is defined to describe the affinity of a molecule for both phases and thus help to predict the order of elution of the molecules. This coefficient is called distribution (or partition) coefficient $K_d$ and can be described as follows:

$$K_d = \frac{[analyte]_{SP}}{[analyte]_{MP}} \qquad \text{III-1}$$

where $[analyte]_{SP}$ and $[analyte]_{MP}$ are the concentrations of the analyte in the stationary phase and in the mobile phase, respectively. Such value can be determined for each molecule present in the analyzed solution. According to the definition, the higher the $K_d$ of a molecule the stronger are the interactions and hence its retention.

$K_d$ is related, thermodynamically, to the Gibbs free energy difference, $\Delta G$, of the considered molecule and mobile phase/stationary phase combination. This difference in free energy comprises of enthalpic and entropic contributions [3,4]. The dependence of $K_d$ on these contributions is given by:

$$\ln K_d = -\frac{\Delta G}{RT} = \frac{-\Delta H + T\Delta S}{RT} \qquad \text{III-2}$$

where $R$ is the gas constant, $T$ the absolute temperature, $\Delta H$ and $\Delta S$ are the changes in interaction enthalpy and conformational entropy, respectively. When analyzing small molecules the entropic term does not play a significant role in comparison with the enthalpic one describing adsorbing interactions. However, for polymers, the entropic term has to be carefully taken into account since macromolecules are able to present large conformation variation when in solution or attached to a surface. As it will be described later, the separation mechanism of size exclusion chromatography, SEC, which is the mostly employed chromatographic technique for polymer characterization, is only governed by entropic contributions.

$K_d$ can be experimentally determined from the following equation:

$$K_d = \frac{V_e - V_I}{V_P} \qquad \text{III-3}$$

where $V_e$ is the elution (or retention) volume of the analyte, $V_P$ the pore volume of the stationary phase and $V_I$ the interstitial volume of the column.

### 2.1.2. Determination of the retention factor: k'

A dimensionless factor, the retention factor $k'$, can be calculated from characteristics of the chromatographic system in order to compare different systems. It is directly related to $K_d$:

$$k' = \frac{V_e - V_0}{V_0} = (K_d - 1)\frac{V_P}{V_0} \qquad \text{III-4}$$

where $V_0$ is the hold-up (or void) volume of the system and corresponds to the volume of mobile phase comprised between the injector and the detector. This volume is the sum of $V_P$ and $V_I$. This retention factor can be also used to predict the elution volume of a compound in an already defined system.

It is possible to express the retention in a time scale instead of volume. Retention time: $t_R$ is used instead of elution volume. Both values are related by the mobile phase flow rate value $F$ as shown in equation III-5. It is however more convenient to use elution volume instead of a retention time. It allows comparing results obtained on a similar chromatographic system but with different flow rates. This is particularly true when comparing results of one-dimensional and two-dimensional chromatography.

$$V_e = t_R \times F \qquad \text{III-5}$$

Most interaction chromatography separations are achieved by performing mobile phase gradients: increase of the solvent strength during the experiment. This technique is well suited to separate complex mixtures containing molecules exhibiting various affinities with stationary phase in initial run conditions. Increase of mobile phase elution strength permits a decrease of adsorption interaction and thus elution of molecules as a function of their affinity with the stationary phase.

Calculation of the retention factor at elution has been reported using the initial retention factor value $k'_0$, gradient slope and solvent strength have to be taken into account (see reference [53] for the details of the calculation). Usually, and especially for reverse phase chromatography, the retention factor is an exponential function of the mobile phase composition as defined Snyder et al. [54]. The molar mass has also an influence on the variation of the retention factor: k' increases exponentially with the number of repeat units in a macromolecule as was reported by Martin [55] and later revisited by Skvortsov and Trathnigg [56].

The mobile phase composition at the point of elution can be calculated with the following equation:

$$\Phi = \Phi_0 + GV \qquad \text{III-6}$$

which gives $\Phi_e = \Phi_0 + G(V_e - V_0)$

where $\Phi_e$ and $\Phi_0$ are the mobile phase composition at the point of elution and in initial conditions, respectively and $V_e$ and $V_0$ the elution volume of the considered analyte and the hold-up volume of the system, respectively. $G$ is the mobile phase gradient slope: i.e. the variation of the mobile phase composition divided by the total volume of solvent pumped during the gradient. It should be noted that equation III-6 assumes that there is no system dwell volume $V_{dw}$, i.e. volume between mixer and injector. However, the gradient is programmed and formed at the pump and not at the injector. Using the total system volume ($V_1 = V_0 + V_{dw}$) instead of $V_0$ in equation III-6 permits to take into account the delay of appearance of the gradient in the column caused by the mixing chamber volume and thus gives a more accurate result for $\Phi_e$. Figure 5 shows a scheme of a chromatographic system with an illustration of hold-up volume, dwell volume and total system volume.

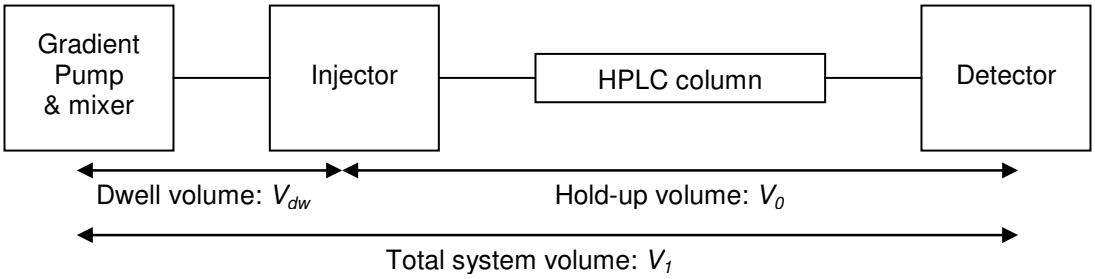


**Figure 5**: Scheme of a chromatographic system with definition of hold-up volume $V_0$, dwell volume $V_{dw}$ and total system volume $V_1$.

## 2.2. Characteristics of HPLC of polymers

### 2.2.1. Peculiarities

As previously described, a chromatographic separation is governed by variations of analyte Gibbs free energy determined as a function of interactions occurring between this analyte and the stationary phase as well as the mobile phase. The distribution between phases is defined by $K_d$.

For small molecules the enthalpic contributions, the affinity and the interactions between the analyte and present phases, is most of the time larger than the entropic contribution which is limited to the entropy of transfer from diluted mobile phase to more condensed stationary phase. A difference of 2 to 3 orders of magnitude between enthalpic and entropic

contributions was found when analyzing polycyclic aromatic hydrocarbons on non-polar C18 bonded column [57].

For macromolecules, the enthalpic contributions are also very important as the chains are made of a large number of repeat units. If one unit has the ability to adsorb, theoretically all similar units contained in the chain are also susceptible to interact with the stationary phase. As a result the retention factor increases dramatically with the number of interacting repeat units, Martin's rule.

However, for polymers, the entropic contributions also play an important role as macromolecules are susceptible to adopt a large number of conformations. The first kind of conformation modification can be found in solution as macromolecules enter stationary phase pores (confinement of the macromolecules). The variation of entropy is a function of the volume of the polymer in solution and of the pore size distribution. The second kind of conformation modifications, which is more dramatic in terms of entropy variation, occurs when a macromolecule changes from a solvated globule to an adsorbed chain on the solid stationary phase surface (see Figure 6).

Taking into account this brief summary of possible thermodynamic contributions which are susceptible to occur when analyzing polymers, it is possible to define three kinds of chromatographic modes for polymer separation:

- adsorption chromatography, where chromatographic conditions are designed such that the polymer interacts with the stationary phase. The strong adsorption of macromolecules usually requires performing a mobile phase gradient to obtain desorption: $K_d >> 1$.
- exclusion chromatography, where macromolecules are repulsed from packing material and thus are separated according to their size in solution (hydrodynamic volume): $0 < K_d < 1$.
- critical condition chromatography, where enthalpic and entropic interactions compensate each other. Polymer chains are neither repulsed nor attracted by the stationary phase. Thus their elution volume is equal to the system hold-up volume: $K_d \approx 1$.

Figure 6 shows a schematic representation of polymer behavior in a HPLC column with either a repulsion from stationary phase surface in case of SEC or an adsorption on pore walls in

case of adsorption chromatography. In first case, penetration of the molecule in the pore depends of its volume in solution (hydrodynamic volume) and of the pore size.

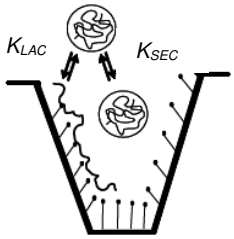


**Figure 6:** Schematic representation of the behavior of a polymer molecule in a pore of a bonded stationary phase: either it adsorbs in LAC or it is repulsed in SEC, from [56]

Usually the three modes of chromatography are represented on the same diagram showing the effect of the molar mass on the distribution coefficient for isocratic chromatography (see Figure 7). Gradient LAC can also be figured on this plot.

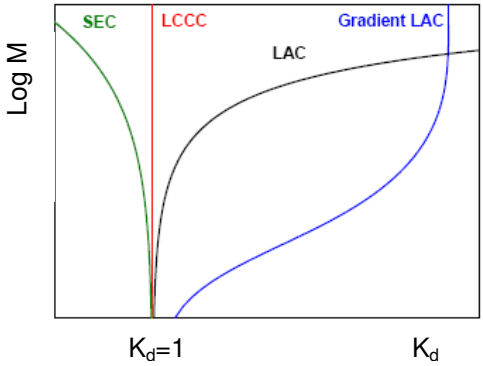


**Figure 7:** Schematic representation of the molar mass dependences of the distribution coefficient in polymer liquid chromatography. SEC, LC-CC, and LAC modes operate under isocratic conditions of eluent while in gradient LAC, the eluent strength is changed (weak to strong) with time [59]

In the following part, a chromatographic model will be described which has been developed to explain the behavior of polymers in the different chromatographic conditions.

### 2.2.2. Polymer Chromatographic Model (PCM)

This model was developed to better understand and predict the behavior of polymers when analyzed by chromatography. It is applicable to all three modes of chromatography described previously. The model is based on the molecular statistical theory of an ideal polymer chain. According to this theory the distribution coefficient of polymer molecules in wide (slit like) pores can be described by the following equation [56,58,59]:

$$K_d = 1 - \frac{4R_g}{D\sqrt{\pi}} + \left[\frac{2R_g}{D}\frac{Y(-cR_g)-1}{cR_g}\right] \qquad \text{III-7}$$

where $R_g$ is the radius of gyration of the polymer molecule, D the diameter of the pore (with $D >> R_g$ ), and $c$ is an interaction parameter defined on the complete range of chromatographic modes. $c$ depends on the nature of the repeat unit, stationary phase, eluent composition (c varies oppositely to mobile phase strength) and temperature. It is, however, independent of the degree of polymerization (DP) and thus of $R_g$.

$Y$ is a mathematical function whose general expression and limiting forms can be formulated as follows:

$$Y(-x) \equiv \exp(x^2)\left[1 - erf(-x)\right]$$

$$Y(-x) \approx \begin{cases} \frac{1}{\sqrt{\pi}}\left(\frac{1}{-x} + \frac{1}{2x^3}\right) & x = cR_g \le -1 \quad SEC \\ 1 + \frac{2x}{\pi} + x^2 & |x| = |cR_g| \le 0.4 \quad LCCC \\ 2\exp(x^2) & x = cR_g \ge 1 \quad LAC \end{cases} \qquad \text{III-8}$$

The first two terms in equation III-7 correspond to size exclusion contribution to $K_d$ ($K_{SEC}$) which was defined by Casassa and Tagami [60], while the last term represents the contribution of adsorption to $K_d$ ($K_{LAC}$).

When no adsorption occurs, the interaction parameter is negative as well as $cR_g$, such that the last term vanishes for large negative values. The ratio $R_g/D$, smaller than unity by definition, then governs retention and $K_d < 1$: i.e. the separation occurs in SEC conditions. The order of elution of macromolecules is also properly described by the model: with increasing $R_g$, $R_g/D$ increases but $K_d$ decreases, i.e. elution volume is smaller with increasing molecule hydrodynamic volume (and molar mass).

The second term of equation III-7 is compensated by the third term at the critical point where c is close to zero, $|cR_g| \le 0.4$. In these conditions, we have $K_d \approx 1$ which means, according to equation III-1, that the analyte is equally distributed in the stationary and mobile phases. It corresponds to the definition of the critical conditions of elution.

Positive values of $cR_g$ (> 1) lead to $K_d > 1$, molecules are preferentially concentrated in the stationary phase (i.e. adsorbed on the stationary phase), as the third term increase exponentially with the value of $cR_g$.

Thus, according to this theory, $K_d$ at a given isocratic mobile phase composition depends on two parameters, $R_g/D$ and $cR_g$.

It is possible to relate the retention factor to the interaction parameter. Replacing $K_d$ given in equation III-7 with LAC approximation of Y(- x) in equation III-4, we obtain:

$$k' \cong \left[ -\frac{4R_g}{D\sqrt{\pi}} + \frac{4R_g}{D} \frac{\exp\left(c^2 R_g^2\right)}{cR_g} \right] \frac{V_P}{V_0} \qquad \text{III-9}$$

As we consider LAC conditions, $cR_g$ is larger than unity and by definition we have $D >> R_g$. Thus equation III-9 can be further simplified by neglecting the first term to give following equation:

$$k' \cong \frac{4R_g}{D} \frac{\exp\left(c^2 R_g^2\right)}{cR_g} \frac{V_P}{V_0} \qquad \text{III-10}$$

According to the definition of the radius of gyration in conformational statistics of polymers in solution, we have $R_g \propto \sqrt{N}$ with N the number of bonds in the polymer chain of course related to the degree of polymerization (DP). Thus, as it was predicted by Martin rule, the exponential relationship between the retention factor and the DP has been established.

As previously mentioned, *k'* decreases exponentially with an increase of good solvent proportion in the mobile phase. The interaction parameter, *c*, also varies with mobile phase composition, $\Phi$ . No exact definition of these variations has been yet made but it can generally be represented by a power series. The development of the function is usually stopped after the first term especially in the vicinity of critical composition. This domain is important in gradient HPLC as it corresponds to the conditions of polymer elution. In this domain, c changes linearly with $\Phi$ [61]. The relation can be written as follows:

$$cR_g = \frac{d\left(cR_g\right)}{d\Phi}\left(\Phi_c - \Phi\right) + \ldots \qquad \text{III-11}$$

where, $dc/d\Phi$ represents the change in interaction parameter per change of mobile phase composition. $\Phi_c$ is the critical mobile phase composition leading to polymer elution and $\Phi$ the mobile phase composition whose variation as a function of the pumped volume is described by equation III-6. Thus equation III-11 gives:

$$cR_g = \frac{d\left(cR_g\right)}{d\Phi}\left(\Phi_c - \Phi_0 - GV\right) \qquad \text{III-12}$$

In equation III-10, the ratio $R_g/D$ may also vary with the thermodynamic quality of the mobile phase composition and thus influence the *k'* value: polymer solvation (i.e. hydrodynamic volume) varies with the quality of the solvent and the stationary phase pore volume might also vary in the case of a polymeric stationary phase (gel swelling) or in the case of a bonded

silica phase depending on the polarity of the solvent. However, the change in $R_g/D$ per change in mobile phase composition is expected to be much smaller than that in $c$, especially when components of mobile phase are solvents for the polymer. Skvortsov and Trathnigg showed that this ratio was only slightly dependent on the mobile phase composition. A light decrease of the ratio was observed when adding methanol to water in the mobile phase for the analysis of poly(ethylene glycol) on a polymeric stationary phase. In comparison the decrease of $cR_g$ product was much more significant [56]. Thus $R_g/D$ is assumed to be independent of the mobile phase composition. As a result, the elution volume of a polymer molecule can be described by the three following parameters $\frac{R_g}{D}$, $\frac{d(cR_g)}{d\Phi}$ and $\Phi_c$ which all have a physical significance. After determination of these three adjustable polymer specific parameters, the elution of a polymer in gradient chromatography can be predicted in various virtual chromatographic conditions. These parameters of PCM can be extracted using non-linear fitting procedures, from the data obtained by at least three isocratic experiments performed at different mobile phase compositions. A procedure to determine these parameters was given by Bashir et al [61].

More detailed characteristics of each chromatographic mode will be now given using mainly the analysis of block copolymers as example.

### 2.2.3. Size exclusion chromatography (SEC)

As shown by the PCM, in SEC the separation depends on the differences of hydrodynamic volumes of the macromolecules, i.e. the size of the molecules in the solvent. The stationary phase is composed of a porous material, usually a swollen gel, with a certain pore size distribution. The mobile phase should dissolve the polymer properly and avoid interactions between the stationary phase and the macromolecules. Thus, the separation is only directed by entropic contributions: a macromolecule which enters a pore cannot anymore occupy all possible conformations. This results in a decrease of its conformational entropy: the bigger the macromolecule, the larger the decrease of the entropy. Thus, molecules with the largest volume in solution are eluted first and elution occurs in the order of decreasing hydrodynamic volume. SEC is not a direct method to obtain the molar mass distribution of the sample, but using a calibration the hydrodynamic volume can be related to the molar mass [62].
Two kinds of average molar masses are typically determined to characterize polymer molar mass distribution: the number average molar mass, $\overline{M_n}$, and the weight average molar mass,

$\overline{M_w}$. The first corresponds to the ordinary arithmetic average molar mass of the chains contained in the sample, whereas the second is the average molar mass of a chain in which a monomer has the highest probability to be found. The molar mass distribution is usually characterized by the polydispersity index, PDI, calculated by dividing $\overline{M_w}$ by $\overline{M_n}$. Since $\overline{M_w}$ is always equal or higher than $\overline{M_n}$ we always have $PDI \geq 1$. PDI is equal to 1 only if all chains of a polymer sample have exactly the same molar mass. The higher is the PDI the broader is the molar mass distribution. Equations to calculate both average molar masses and PDI are:

$$\overline{M_n} = \frac{\sum_i N_i M_i}{\sum_i N_i} \qquad \text{III-13}$$

$$\overline{M_w} = \frac{\sum_i N_i M_i^2}{\sum_i N_i M_i} \qquad \text{III-14}$$

$$PDI = \frac{\overline{M_w}}{\overline{M_n}} \geq 1 \qquad \text{III-15}$$

When analyzing block copolymers SEC allows to determine the molar mass distribution of the total sample. It is usually possible as well to characterize the first block when the synthesis is performed sequentially by taking a sample at the end of the first step. Besides, it is also possible, in particular cases, to get more information on the sample, such as the chemical composition as a function of the molar masses or the conformation of the macromolecules. Examples of characterization of diblock copolymers are reported by Grubisic-Gallot et al. [63]. In the first example, a system was presented in which one block (polydimethylsiloxane) has a refractive index identical to that of the SEC mobile phase (THF). Low angle light scattering detection, in this case, gives the molar mass for the copolymer but allows also the determination of the average molar mass of the scattering part (PS block) of the copolymer chains during the same experiment. In the second example, the authors also used SEC coupled to a viscosimeter to obtain information about the conformation of copolymer chains in dilute solution. Determining intrinsic viscosity for samples of poly(ethyl methacrylate-*block*-deuterated methyl methacrylate) in THF and comparing them with values of the corresponding homopolymers they were able to conclude that the copolymers exhibit very few contact points. This suggests that the blocks are segregated in solution. A segregated conformation was also observed in the solid state for these samples. Finally an example was given showing the possibility to determine the chemical composition of the molecules as a

function of the molar masses for a poly(styrene-*block*-methyl methacrylate) sample. They combined an ultraviolet-detector, PS-sensitive only, and a refractive index detector sensitive for both kinds of repeat units to calculate the percentage of PS repeat units in the chains.

Considering the opportunity to characterize the chemical composition of the samples while analyzing their molar mass distribution, several reports have been made using either Fourier-transform infra-red [51,64] or proton nucleic magnetic resonance [65] as spectroscopic detectors instead of UV. More details will be given in the part III.3 dedicated to the detectors and their possibilities in polymer analysis.

### 2.2.4. Adsorption chromatography (LAC)

In LAC, separation is directed by enthalpic interactions. The entropic term is generally not significant in comparison with the enthalpic one. The principle of polymer adsorption in isocratic chromatography is described as a multiple attachment mechanism. In the given chromatographic conditions, only certain types of monomers are susceptible to be adsorbed on the stationary phase. Each of these monomers, distributed along the chain, becomes a point of attachment for the macromolecule. This approach explains the chemical composition dependence of the separation: a macromolecule rich in adsorbing monomers will be eluted later than a macromolecule containing less of these monomers. The adsorption lasts as long as the adsorption energy is large enough to balance the decrease of entropic energy caused by the polymer deformation due to adsorption. The adsorption is favored by the presence of blocks of adsorbing repeat units, also called "trains" [66]. The retention factor of a "train" $k'_{train}$ composed of *n* identical repeat units with a retention factor $k'_u$ for each unit has been defined as follows:

$$k'_{train} = (k'_u + 1)^n - 1 \qquad \text{III-16}$$

It results from equation III-16 that retention of a block copolymer is always prolonged in comparison to that of a random copolymer with the same chemical composition. This is due to the length of the "trains". Indeed, in random copolymers, the average sequence length of homologous repeat units is small which leads to adsorption of short "trains" on the stationary phase. On the contrary, block copolymers contain long sequences of identical species: *n* and thus the total retention factor takes high values. These long "trains" are responsible for the stronger retention.

This mechanism of adsorption also supposes that the separation is dependent of the number of adsorbing points, i.e. degree of polymerization. Indeed two molecules with the same average chemical composition but with different chain lengths will not be eluted together: it is called the molar mass effect. The molar mass dependence is more pronounced for block or graft than for random copolymers. For the block or graft architectures an increase of the number of adsorbing units generally occurs in the existing "trains" and thus dramatically increase the retention factor value (i.e. increase of the exponent value).
It must also be taken into account that an increase of the length of the non-adsorbing block tends to facilitate the desorption of the copolymer. It has been called the "dragging" effect [67]. It explains why block copolymers elute before the homopolymers of the adsorbing block.

A theoretical study has been conducted to define the separation possibilities of this technique in the case of binary copolymers [68]. Three cases are considered:

- When one of the components is eluted at its critical condition while the second exhibits adsorption, the separation is governed by the molar mass of the latter component regardless of the architecture. Furthermore, it is theoretically possible in these conditions to separate linear diblock, triblock and multi-block copolymer containing similar amounts of adsorbing units.
- A separation of large binary copolymers by chemical composition independently of their architectures is possible when the chromatographic conditions are set up so that one component is slightly adsorbed and the other slightly excluded.
- Finally, it seems possible to separate binary copolymers of similar average molar mass and chemical composition according to their architecture. To achieve such separation, one component must be excluded whereas the second had to be strongly adsorbed.

Despite these various possibilities, the isocratic LAC technique remains marginal and is mostly applied for the analyses of oligomers. Polymers with large adsorbing blocks would be fully retained in the column. An example of efficient oligomer separation according to chemical composition in reasonable experimental time scales was reported by Trathnigg et al [69].

Gradient chromatography was developed to separate polymers according to chemical composition as it reduces the influence of the molar mass on the separation [70]. Thus it is of great value for the analysis of large copolymers which can not be analyzed in LAC. The principle of gradient chromatography is to adsorb the polymer on the stationary phase and to elute polymers of similar chemical composition in the same fraction thanks to a gradual

increase of the mobile phase strength without or with a little influence of macromolecule molar mass. Nevertheless, in gradient HPLC, it is commonly observed that smaller macromolecules elute slightly in advance since they present less adsorbing points. Retention processes have been discussed by Snyder and others and tests have been suggested to identify the actual operative mechanism [71,72].

The macromolecules start eluting when the composition of the mobile phase becomes close to their critical conditions: $\Delta G \approx 0$. This corresponds to the point where adsorptive interactions are dramatically reduced by the proportion of eluting solvent in the mobile phase and they reach the same order of magnitude than entropic contributions. As these desorbing conditions differ according to the chemical composition of the chains (the nature of the repeat unit is responsible for the interaction strength), a chemical composition distribution is determined: similar fractions of macromolecules will elute from the column together independent of the molar mass with a mobile phase composition close to their critical conditions [73].

### 2.2.5. Chromatography at critical conditions (LC-CC)

If conditions can be found where the enthalpic interactions resulting from adsorption and the entropy losses of a macromolecule within a pore exactly compensate each other ($K_{SEC}$ and $K_{LAC}$ from Figure 6), it is possible to elute a homopolymer independent of its molar mass. In this situation the analysis is performed in critical conditions, or conditions for enthalpy-entropy compensation, where $K_d$ value is close to unity. The homopolymer is considered to be chromatographically "invisible" as the macromolecules elute at the void volume of the system being neither excluded from the stationary phase nor adsorbed on it. These conditions are related to the nature and porosity of the stationary phase, the composition of the mobile phase, usually a mixture of solvents, which remains constant (isocratic experiment) and temperature.

The LC-CC technique appears to be a very convenient method to analyze binary copolymers, since it permits to make one of the components "invisible". The retention of the copolymers will only be governed by the other component. Two possibilities occur: either the mobile phase is a good solvent for the "visible" component and the copolymer chains elute in SEC mode or the mobile phase strength is insufficient to provoke elution and the copolymers remain adsorbed on the stationary phase. In this latter case a gradient should be carried out to elute the macromolecules. In the case of SEC elution of the copolymers, the construction of a calibration curve will provide the molar mass distribution of the "visible" block only even if it

is part of a copolymer. Such experiment was carried out to analyze a poly(MMA-*block-tert*-butyl methacrylate) diblock copolymer [74].

Computer simulations of such separation have also been performed and show that a small influence of the "invisible" block always remains on the elution of the "visible" block which tends to decrease when the "visible" block proportion in the copolymer increases and when the size of the pore decreases [75]. The results obtained are in good agreement with the experimental observations.

A theoretical approach of the "invisibility" in LC-CC has been developed by Skvortsov and Gorbunov [76]. They showed that a component is really "invisible" if it forms a block with a free end: e.g. end blocks in a three-block copolymer, side chains in graft copolymers. In all other cases, middle block of a terpolymer, multiblock copolymers or backbone of a graft copolymer, the "invisibility" is possibly achievable by using stationary phases with very narrow pores in order to favor the exclusion of the "visible" part. In this latter case, the conditions for "invisibility" seem to be more difficult to be achieved.

Other computational investigations have been performed to better understand the evolution of interaction between the polymer and the stationary phase in the proximity of critical conditions. Plotting standard deviation of $ln(K_d)$ as a function of surface interaction energy allows determining the critical point of adsorption. It confirms that elution occurs independently of polymer molar mass but it also shows that the results are highly dependant of the pore size and configuration of the packing material [77].

A review has been written detailing the principles of the technique and summarizing critical conditions determined for a large variety of polymers [78]. The determination of the critical conditions of elution for a polymer is frequently a long and difficult experimental process. Indeed these conditions are very narrow and a slight deviation in the mobile phase composition can change the retention mode from SEC to LAC. New approaches are developed with few experiments of gradient elution chromatography and a theoretical treatment to facilitate this determination [79].

## 2.3. Two-Dimensional Liquid Chromatography. 2D-LC

It is very profitable to couple chromatographic techniques to determine and combine information on distributions of various properties in order to better understand structure-

property relationships of polymers. Indeed, treatment of data obtained from 2D-LC allows drawing a map showing the polymer chains dispersion with regard to two different distributions (such as chemical composition and molar mass) simultaneously [80].

Experimentally, the coupling is possible through a specific device, an eight (or ten) port injection valve, which collects a fraction of the first dimension into a storage loop while the content of a second loop, a previous fraction, is injected and analyzed by the second dimension. Figure 8 schematically represents the process of the 2D-LC system. This fully automated two-dimensional chromatographic system including two chromatographs was first developed by Kilz et al. [81]. In the first dimension, gradient LAC separation, governed by enthalpic interactions led to the determination of the polymer chemical composition distribution and in the second dimension macromolecules are eluted as a function of their decreasing hydrodynamic volume using SEC.

Since the second dimension is repeated multiple times on first dimension fractions, the run time for this chromatography has to be as fast as possible but conserving its separation capacities.

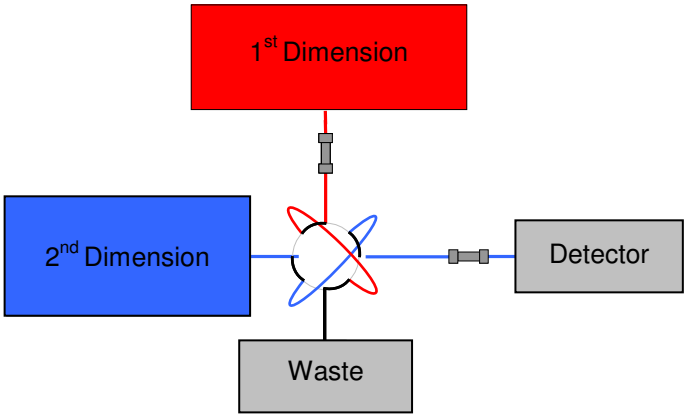


**Figure 8**: Schematic representation of a 2D-LC system coupling, in red the first dimension route, in blue the second dimension route

According to the definition it seems conceivable to couple any kinds of LC technique which each other to obtain a 2D-LC system. However, several couplings are easier to achieve and others are technically not possible or are useless in terms of obtained information. Kilz reviewed the use of 2D-LC giving examples of possible couplings to characterize macromolecular chemical structures [11].

The most often reported system corresponds to coupling of a gradient HPLC system in the first dimension with a SEC separation in the second [82,83,84]. The experimental set up is relatively simple in such case as the second dimension is performed isocratically. Experiments can be repeated directly one after another without column reconditioning delay.

Performing the analysis in reverse order (gradient HPLC in second dimension) is technically much more complicated as a reconditioning period is necessary after each gradient run. Each second dimension run lasts very long and as a result the flow rate in the first dimension is too low to be properly controlled by the pump. This is the principal reason why 2D-LC is carried out according to the first method: gradient HPLC x SEC.

A second technique is of great interest: it is the coupling of LC-CC with SEC especially for block copolymers. LC-CC provides information on the molar mass distribution of the "visible" block. When coupled to SEC it is possible to know the size of macromolecules containing this block. By simple subtraction it is also possible to obtain the molar mass of the "invisible" block in the copolymer. Since both techniques are isocratic it is possible to invert them. It is however advised to perform the technique with the highest resolution in first dimension [14,85].

Different reviews were published to better understand the issues of 2D-LC [86] and also to design such systems by choosing the best suited chromatographic systems according to the desired information [87].

# 3. Detection

After the separation in the column the macromolecules must be detected. Different kinds of instruments can be used to obtain the required information. Detectors can be divided in two main classes: concentration-sensitive or molar mass sensitive detectors. Table 1 contains the most common detectors used on-line or off-line after a liquid chromatography system.

**Table 1:** Classification of LC detectors according to their sensitivity

| Concentration sensitive detectors | | Molar mass sensitive detectors |
|---|---|---|
| **Selective detectors** | **Universal detectors** | Viscometers: *Single capillary, Differential* |
| Ultraviolet (UV) | Refractive Index (RI) | Light scattering: *LALLS, MALLS…* |
| Infrared (FTIR) | Density | MALDI-ToF-MS |
| $^{1}$H-NMR | Evaporative Light Scattering | |
| Fluorescence | | |
| Electrochemical | | |

## 3.1. Selective detectors

Selective detectors are usually spectroscopic detectors which are able to measure specific functional groups present in polymer samples. Their use is of great interest for product quantification and chemical composition determination. Hyphenation of different kinds of detectors gives a maximum of information on the analytes at one time [88]. However two main drawbacks limit their utilization. First, the polymer must entail specific functions for which the detector is sensitive. For example, UV-detectors are of little interest for aliphatic polyacrylates or polymethacrylates which adsorb at 220 nm as this adsorption is very often hidden by adsorption of the mobile phase. Of course if the ester/amide groups contain UV-absorbing functions implementation of such detector is useful. UV detectors are widely used for styrenic and other aromatic polymers. A second limitation of this kind of detector is the fact that chemical functions should be specific for the polymer and solvents should not absorb at the same wavelength.

The IR detector is a very useful specific detector applicable to all kinds of polymers. Used on-line with specific flow-cells, it can give quantitative information on the sample [89]. However solvent adsorption remains the main limitation of this coupling. Off-line coupling is possible through an evaporative interface called LC-Transform. The major advantage of this off-line setup (two-steps: first deposition and then measurement) is that we get rid of the solvent which leaves the complete FTIR measurement window (800 to 4000 $cm^{-1}$) free for analysis [90].

LC-Transform is used to evaporate the mobile phase eluting from the LC column and spray the separated sample fractions on a Germanium plate. It uses high temperature and an inert gas flow to perform evaporation. After deposition, the plate is transferred in a FTIR spectrometer which is able to measure FTIR spectra at regular intervals along the polymer track. The lower face of the plate is coated with aluminum, rendering it reflective. Infrared energy is directed from the FTIR source onto the sample deposit. The laser beam passes through the deposit and the Germanium, to reach the reflective Aluminium surface. It is then reflected from this surface back through the sample, and then to the FTIR detector. The result is a double-pass transmission measurement of the sample. It is possible to define intervals of measurement as a function of the desired measurement precision. Albrecht et al used this technique to determine the chemical composition distribution in poly(ethylene-*co*-methyl acrylate) and poly(ethylene-*co*-butyl acrylate) previously separated by high temperature

HPLC [51]. This LC-Transform technique was efficient to analyze samples with either narrow or broad chemical composition distributions.

Kok et al presented a comparative study of on-line and off-line SEC-FTIR measurements. They found that both systems give comparable results and that the on-line coupling technique is very convenient [64]. They admit that a considerable experience is needed to properly set up the FTIR flow cell detector and that a careful choice of solvent system has to be made in order not to disturb the polymer signal.

NMR is also used now directly on-line after LC separations with a specifically designed probe (LC probe) [91,92]. This hyphenation can provide very important data on polymer structure and/or end groups and/or chemical composition. Hiller et al showed by coupling a LC-CC separation with $^1$H-NMR that it is possible to determine in one experiment the molar mass distribution and the tacticity of a PMMA block together with the total chemical composition of the diblock copolymer (PMMA-*block*-PS) [92]. HPLC–$^1$H-NMR experiments require the use of solvent-suppression techniques. The method used has to be fast in order to operate under on-flow conditions and it must be able to suppress more than one solvent signal easily. Highly selective pulses have to be used. A widely used solvent suppression technique is called WET (Water suppression enhanced through $T_1$ effects) [93].

The lack of sensitivity of NMR spectrometry combined with the low sample concentration used in liquid chromatography limits the development of this coupling. However, off-line NMR on LC fractions obtain after analytical or preparative chromatography is a very valuable combination. Fractionation of the samples after HPLC separation permits to collect more homogeneous parts of the sample. Applying spectroscopic techniques on these fractions gives access to more detailed information on the total sample. In this case, results are more specific and are not an average result on the total sample. Depending on the quantity of sample collected it is possible either to implement $^1$H-NMR for small amounts or $^{13}$C-NMR and correlated techniques when the quantity of the collected fraction is sufficient. These last techniques are very well adapted to analyze and define polymer branching [94].

## 3.2. Universal detectors

These detectors measure changes of physical properties of the mobile phase due to the fact that it contains dissolved macromolecules. For example, refractive index (RI) detectors measure the changes of the refractive index of the mobile phase during experiments. Polymer molecules dissolved in the mobile phase change the refractive index of the solvent which

causes a detector signal. RI detectors are frequently used after SEC separation. It is a valuable and sensitive detector but is not applicable to gradient chromatography. Indeed, the refractive index changes caused by the mobile phase composition changes are usually much greater than those induced by the presence of the polymer.

Another kind of detector widely used in chromatography of polymers is the Evaporative Light Scattering Detector (ELSD). The ELSD is able to detect any non-volatile component present in the mobile phase. The mobile phase leaving the column is nebulized and the solvent is evaporated from formed droplets. When a droplet contains a non-volatile product, it becomes a particle which is driven through a light beam by a carrier gas. Particles scatter the light beam and the intensity of scattered light is the base of the detector signal. Different kinds of interaction between light beam and particles are possible according to the size of particles as shown in Figure 9.

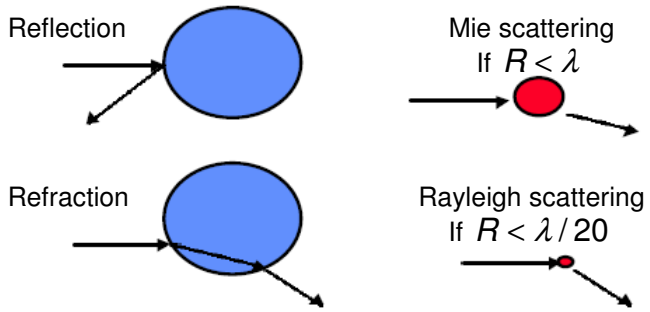


**Figure 9:** Scheme presenting the different possibilities of interactions between ELSD light beam and particles formed after evaporation of the mobile phase

The ELSD is relatively easy to set up and to use even for gradient chromatography. However the response depends on a large number of factors which influence the formation of particles. Analyte concentration in the mobile phase when it reaches the detector is definitely the most important factor as ELSD is a concentration sensitive detector [95]. But it has to be taken into account that a high sample concentration is susceptible to favor formation of larger particles hence giving a more intensive response. This is one of the reasons why the ELSD response as a function of the concentration cannot be linearly fitted when a calibration is performed on a large concentration domain. Other influencing factors are the mobile phase composition and the flow rate which both change the quality of the evaporation. The ELSD signal is also affected by polymer mass, structure and chemical composition which are responsible for the formation of different sizes of droplets even at equivalent concentration.

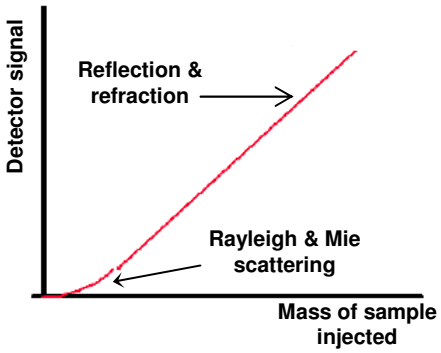


**Figure 10:** Plot of detector response as a function of the mass of polymer injected in the chromatographic system

Calibration of the ELSD should be made very carefully to obtain reliable quantitative results. Usually a second order polynomial function is found as best fit to relate detector signal and injected polymer mass. This second order fit is best suited to describe the Rayleigh and Mie scattering part together with the reflection and refraction part of the detection. Figure 10 shows a plot of detector response as a function of the mass of sample injected.

## 3.3. Molar mass sensitive detectors

On-line molar mass detectors, such as viscometers and light scattering detectors (LALLS and MALLS: Low-Angle and Multi-Angle Laser Light Scattering), are mainly used after SEC because separation is already performed according to molar mass [96]. In the light scattering detector, the laser beam crosses directly the mobile phase and the intensities of light scattered according to different angular positions are measured. The quantity of light scattered is a function of the size of the macromolecules in solution. These detectors are sensitive to concentration as well as molar mass, so they have to be used in combination with a concentration sensitive detector to isolate the information relative to the molecular size. The detector combination consists very frequently of a refractive index detector (concentration sensitive), a light scattering detector (molar mass sensitive) and a viscometer (also molar mass sensitive, added to obtain more accurate values for the low molar masses).

Another type of detection sensitive to molar mass is mass spectrometry (MS) especially Matrix-Assisted Laser Desorption/Ionization Time-of-Flight Mass Spectrometry coupling (MALDI-ToF-MS) [97]. Currently electrospray ionization (ESI) and atmospheric pressure chemical ionization (APCI) are principally available for on-line coupling of LC-MS. However, these interfaces are limited to oligomers with molar masses under approx. 5.000 Da. The main use of MS for polymers is done with the MALDI technique. This is a soft ionization method

allowing the analysis of macromolecules, which tend to be fragmented when ionized by more conventional ionization methods [98].

Analytes are dispersed in a matrix used to protect them from being destroyed by the laser beam used to trigger the ionization. The matrix also plays an important role as it helps the vaporization and the ionization of the sample macromolecules. Laser pulses are directed onto the matrix/sample deposit which cause its desorption and an ionization of some components of the matrix. The ionized gas formed is usually called the MALDI-"plume". The matrix is then thought to transfer part of its charge to the analytes (e.g. polymer), thus ionizing them while still protecting them from the disruptive energy of the laser.

MALDI generally produces singly-charged ions by either attachment of $H^+$, $Li^+$ or $Na^+$ onto the analytes to produce positively charged species (quasimolecular ion, for example $[M+Na]^+$ in the case of a sodium ion adduct) or by extraction of a proton to form negatively charged analytes ($[M-H]^-$).

Usually a ToF-MS is used to analyze the ions formed by the MALDI source for two main reasons. The ToF-MS is able to analyze molecules with very large molar masses which is of great interest for polymers.

ToF-MS consists of an electric field of known strength which accelerates the ions into a drift tube. The velocity for each ion is a function of its mass-to-charge ratio and the value of the electric field. The time needed for the ion to reach the detector at a known distance is measured. From this time and the known experimental parameters one can calculate the mass-to-charge ratio of the ion which usually is equivalent to the mass since ions are singly-charged.

MALDI-ToF-MS instruments are typically equipped with a reflector also called "ion mirror" (electrostatic energy mirror). This reflector deflects ions with a second electric field under a small angle onto the detector. Thereby the ion flight path is increased but the main advantage of this device is that it increases the resolution by focusing ions with same mass-to-charge ratios which were spread in space and time during the ionization process. Figure 11 shows a schematic representation of the MALDI ionization process and a complete MALDI-ToF-MS apparatus.

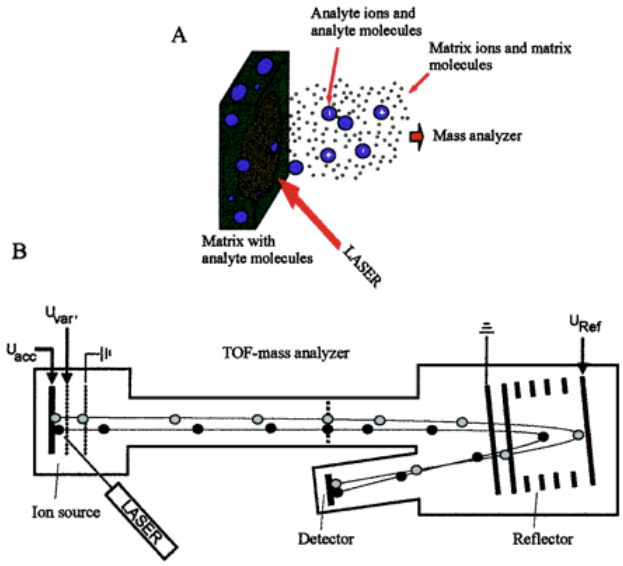


**Figure 11:** Schematic representation of (A) the ionization process in the MALDI source and of (B) a complete MALDI-ToF-MS analyzer [99]

Recent report indicates that it is possible to replace SEC separation in 2D-LC experiments by MALDI-ToF-MS. This hyphenation should provide more precise results in terms of molar mass determination as no calibration standards are required [100]. A procedure for the solvent-free transfer of LC-CC separated polymer fractions onto a MALDI plate has also been described. This technique should allow a fast and automated analysis of the separated samples [101]. These two examples remain however limited by the size of the analyzable polymers. The results are of very high quality only for oligomers or small polymers.

Furthermore, it has been reported that a software was developed to achieve a detailed structural analysis of diblock copolymers from acquired MALDI-ToF-MS spectra [102]. A method was described to achieve a reliable peak assignment. This whole process was used to follow the progress of a multistep anionic copolymerization of α-methyl styrene with 4-vinylpyrydine.

# IV. Results and Discussion

In this part, results of the chromatographic method development for copolymer samples which have been prepared by radical polymerization in L'Oréal research laboratories will be presented. These copolymers are prepared in order to improve the properties of cosmetic formulations. The analyses were mainly conducted in order to obtain structural and compositional information on products with the aim of understanding the copolymerization and by this mean optimizing the reaction parameters.
The results are divided in two main chapters. The first is dedicated to a group of terpolymers synthesized via free-radical polymerization. Several methods were developed to elucidate their chemical structures and to achieve quantification of the constituting species. In the second chapter polymers produced by controlled radical polymerization (ATRP and RAFT techniques) are analyzed. Two different kinds of diblock copolymers are presented.

## 1. Analysis of complex copolymers

The copolymers under investigation are all composed of three different monomers. For this reason they are called terpolymers. They are produced according to a two-step free radical polymerization. The initiator is first added in the solvent with two monomers to form an intermediate random binary copolymer. The second step consists in addition of a new portion of initiator with the third monomer in the solvent containing the preformed copolymer. It results in the formation of a complex segmented terpolymer. Because of the lack of control of free radical polymerization (FRP) over monomer incorporation in both steps, the final polymer is expected to be broadly distributed in molar mass as well as in chemical composition. It is assumed that the complex reaction products contain homopolymer fractions of the third monomer together with binary and ternary copolymer fractions. The segmented copolymers were obtained from different combinations of acrylate and methacrylate esters: isobutyl acrylate (iBuA), isobutyl methacrylate (iBuMA), isobornyl acrylate (iBorA), isobornyl methacrylate (iBorMA), and 2-ethylhexyl acrylate (EHA). Figure 12 shows chemical structure of these five monomers. The copolymer compositions are given in Table 2. The monomers are listed according to the sequence of copolymerization. For example, sample

1 was formed by copolymerizing iBorA and iBorMA in the first step followed by the addition of iBuA.

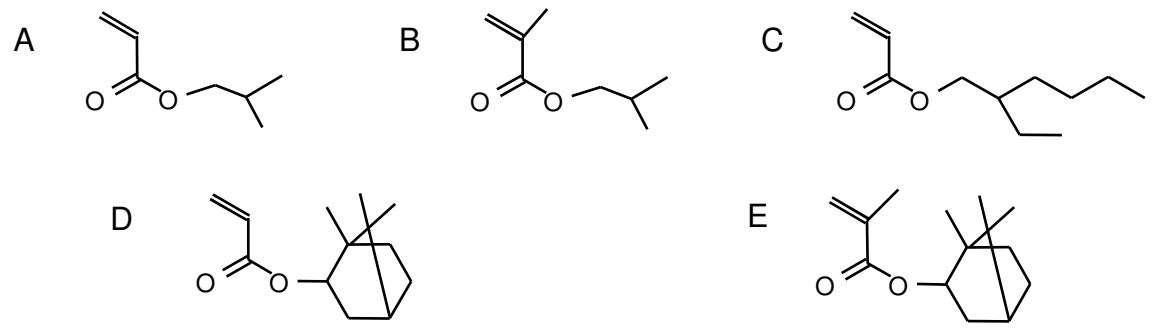


**Figure 12:** Chemical structures of the five monomers used for the synthesis of the terpolymers: (A) isobutyl acrylate (iBuA), (B) isobutyl methacrylate (iBuMA), (C) 2-ethylhexyl acrylate (2EHA), (D) isobornyl acrylate (iBorA) and (E) isobornyl methacrylate (iBorMA)

## 1.1. Development of chromatographic methods

In order to characterize these five copolymers, we developed chromatographic techniques capable of resolving both kinds of distributions. We first started by setting up a SEC separation for elucidating the molar mass distribution and subsequently we optimized gradient HPLC conditions to be able to characterize the chemical composition distribution. The last step was the coupling of these two techniques in a 2D-LC system to correlate information obtained from both separation systems.

### 1.1.1. Analysis of molar mass distribution with SEC

The copolymers were first analyzed by SEC in THF to determine their molar mass distributions. For each copolymer, both average molar masses were determined: $\overline{M_n}$ and $\overline{M_w}$. The SEC analysis of the five copolymers gave in all cases monomodal distributions of molar masses however with a tailing towards higher elution volumes, i.e. towards smaller molecular sizes. The $\overline{M_n}$ values for the five copolymers were found to be between 20 000 - 35 000 g/mol and $\overline{M_w}$ 59 000 -110 000 g/mol. The PDIs varied between 2.9 and 4.0 and were, therefore, higher than one would expect for products of free radical polymerization. One reason for the high polydispersity could be a significant chemical heterogeneity as a result of the two-step polymerization procedure. The molar mass results are reported in Table 2.

**Table 2**: Description of the polymer samples with their average molar masses as determined by SEC using a PMMA calibration

| Sample | Copolymer Composition | $\overline{M_n}$ (g/mol) | $\overline{M_w}$ (g/mol) | PDI |
|---|---|---|---|---|
| 1 | isobornyl methacrylate<br>isobornyl acrylate<br>isobutyl acrylate | 25 600 | 94 000 | 3.7 |
| 2 | isobornyl acrylate<br>isobornyl methacrylate<br>2-ethylhexyl acrylate | 20 200 | 59 000 | 2.9 |
| 3 | isobutyl methacrylate<br>isobornyl acrylate<br>2-ethylhexyl acrylate | 20 700 | 83 000 | 4.0 |
| 4 | isobutyl methacrylate<br>isobornyl acrylate<br>isobutyl acrylate | 33 800 | 109 000 | 3.2 |
| 5 | isobornyl methacrylate<br>isobutyl methacrylate<br>isobutyl acrylate | 34 500 | 100 000 | 2.9 |

The SEC separation of sample 1 is shown in Figure 13 as a triplicate measurement for reproducibility. As can be seen monomodal profiles are obtained with a tailing towards high elution volume which indicates the presence of lower molar mass polymer fractions. Similar profiles were obtained for all samples.

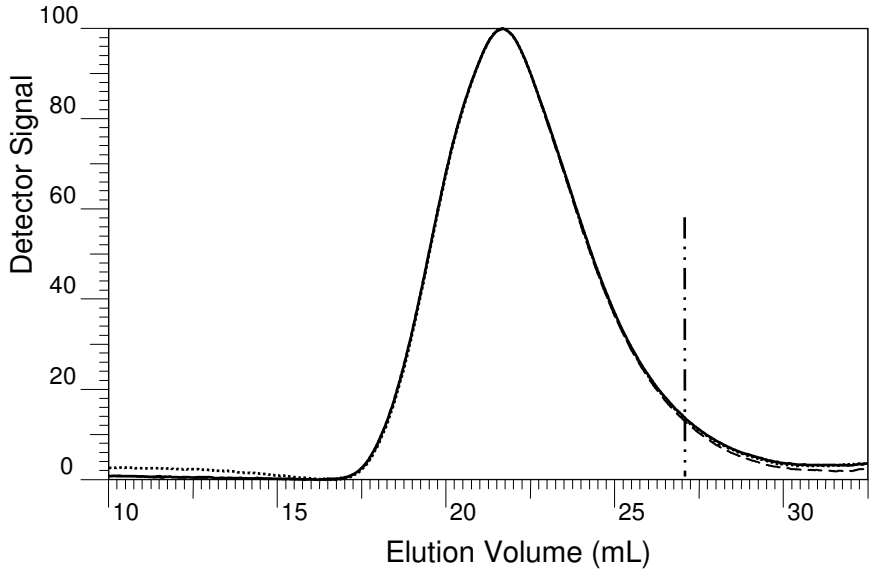


**Figure 13**: SEC chromatograms of sample 1, triplicate measurement, stationary phase: PSS SDV $10^3$, $10^5$, $10^6$ Å (each 300 x 8 mm I.D.), mobile phase: THF, flow rate: 1 mL/min, detection: RI

To analyze the tailing peak of sample 1, the sample was fractionated several times and the tailing part was collected. This part represents nearly 1.2 % of the total peak area. A concentrated polymer solution of 10 mg/mL was used for injection to reduce the number of experiments. After evaporation of the SEC mobile phase, the polymer was redissolved in the MALDI matrix solution (10 mg of dihydroxybenzoic acid in 1 mL of THF). Figure 14 shows the mass spectrum of the low molar mass sample fraction.

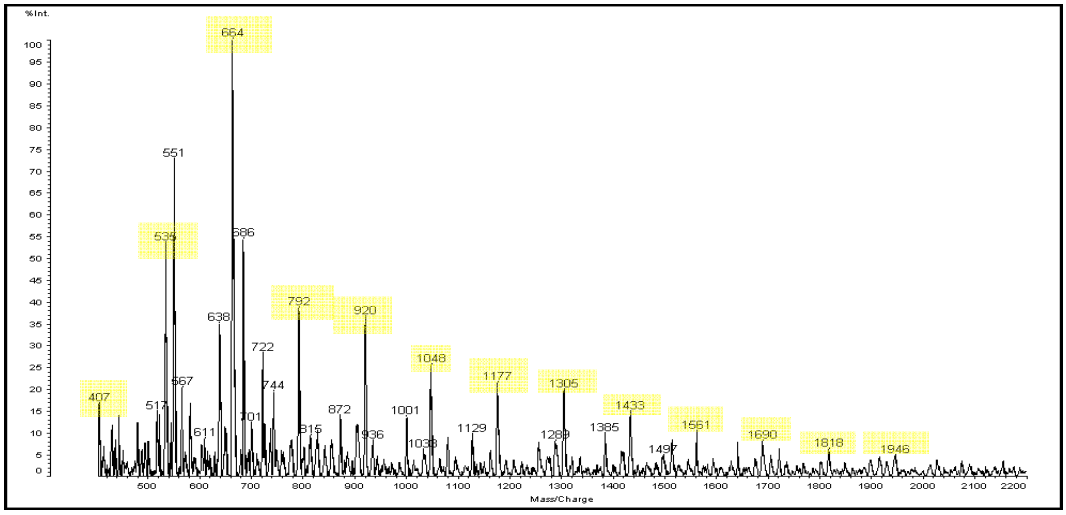


**Figure 14**: Mass spectrum of the low molar mass SEC fraction of sample 1

The average molar mass determined by SEC was 700 g/mol which was in agreement with the result seen in MS. The assignment of the MALDI signals to different kinds of oligomers was done taking into account that ionization took place mainly by attachment of a sodium ion.

All structural formulas given below are hypothetical and, as they are determined from mass spectrometry, no information can be given on the monomer organization. Oligomers should then be considered as randomly organized.

The peak distribution marked in yellow can be attributed to a distribution of poly(isobutyl acrylate) oligomers. Each signal is separated by a m/z value of 128 Da which corresponds to the molar mass value of the isobutyl acrylate monomer. The m/z values seen on Figure 14 correspond to $([iBuA]_n + Na)^+$ ions. For example, the ion with an m/z of 664 Da is a proton-terminated pentamer of isobutyl acrylate (128.17 g/mol) with a sodium ion (23 g/mol) attached:

$$-(CH_2\text{-}CHCOOiBu)_5\text{-} + Na^+$$
$$5 \times 128.17 + 23 = 663.85$$

As expected, the oligomers found in the low molar mass part of the SEC chromatogram are composed of the monomer added in the second step, i.e. iBuA. However, it can be noticed that the majority of the detected oligomers appears to be free of initiator end-groups. This result is surprising but it could be due to an intra-molecular transfer-to-polymer (back-biting) during the polymerization of the acrylates which tends to form cyclic chains [103].

### 1.1.2. Analysis of the chemical composition distribution (CCD) by gradient HPLC

For investigating the chemical composition distribution of the copolymers, a gradient HPLC procedure was developed. It was found previously that polar or non-polar stationary phases could be used for separating binary blends of polymethacrylates, depending on the polarity of the components [73,104].

The most common polar stationary phases used in normal phase chromatography are made of colloidal silica, either as packed spherical particles or as monolithic columns. The surface of these stationary phases is covered with silanol groups, SiOH, which enhance polar interactions with analytes resulting in a separation according to increasing polarity. Other kinds of polar stationary phases could be found such as materials with diol, amino or nitro groups which are grafted onto the silica surface. Hydrophobic and/or non-polar molecules are repulsed from the surface of the silica and remain mainly in the mobile phase. Therefore, they elute before more polar ones which remain adsorbed on the stationary phase. Desorption can

be achieved by modifying the composition of the mobile phase in favor of a more polar solvent (mobile phase gradient). The more polar mobile phase reduces the strength of the interactions between the molecules and the stationary phase and thus allows elution of previously adsorbed molecules. A typical example of this kind of system for (meth)acrylate copolymers is the use of a cyclohexane (cHex, non-polar) and methylethylketone (MEK, more polar) gradient on a bare silica stationary phase. This gradient leads to elution of the polymers regarding decreasing size (i.e. increasing polarity) of the aliphatic ester groups and to elution of polymethacrylates before polyacrylates with the same ester group.

It is possible to completely inverse the chromatographic conditions to perform reversed phase chromatography. In this case, the stationary phase is non-polar. Most frequently the stationary phase is a silica material grafted with large non-polar aliphatic groups such as octadecyl (C18). The polarity of the stationary phase can be tuned by carefully choosing the grafted chain. Stationary phases with different grafted chains are commercialized such as C8, C4, C2 or phenylhexyl to be used in reverse phase chromatography. Another frequently used non-polar stationary phase is made of a synthetic polymer instead of silica gel. Polystyrene cross-linked with divinylbenzene allows doing reversed phase HPLC at extreme pH values. Its major drawback, however, is its swelling in the presence of a good solvent for the polymer which results in large variations of column backpressure during the experiments. In this case the mobile phase consists of a gradient starting with a polar solvent and going to a less polar one which of course leads to a separation according to decreasing polarity of the molecules. The elution order is reversed in comparison with that given for normal phase chromatography. An example of reversed phase HPLC is the separation of poly(meth)acrylate blends on a C18 column with an acetonitrile(ACN)-tetrahydrofuran(THF) gradient.

***a) Gradient HPLC separation of the homopolymers***

To investigate the feasibility of normal and reversed phase separations for analyzing the present copolymers, polar and non-polar stationary phases were tested on a blend of homopolymers: poly(isobutyl acrylate) (PiBuA), poly(isobutyl methacrylate) (PiBuMA), poly(isobornyl acrylate) (PiBorA), poly(isobornyl methacrylate) (PiBorMA), and poly(2-ethylhexyl acrylate) (P2EHA). The average molar masses of the homopolymers are given in Table 3. They were obtained with the SEC system described previously.

**Table 3**: Description of the homopolymers with their average molar masses as determined by SEC using a PS calibration

| Homopolymer of | | $\overline{M_n}$ (g/mol) | $\overline{M_w}$ (g/mol) | DPI |
|---|---|---|---|---|
| Isobornyl acrylate | PiBorA | 8 000 | 37 000 | 4.6 |
| Isobornyl methacrylate | PiBorMA | 14 000 | 41 000 | 2.9 |
| 2-Ethyl hexyl acrylate | P2EHA | 19 000 | 60 000 | 3.2 |
| Isobutyl methacrylate | PiBuMA | 13 000 | 33 000 | 2.5 |
| Isobutyl acrylate | PiBuA | 49 000 | 117 000 | 2.4 |

For HPLC method development a blend was prepared consisting of the five homopolymers. For this blend, test separations using 10 min mobile phase gradients on normal and reversed phase columns were performed in order to determine the most adequate system. Longer gradients (15 or 20 min) giving more time to the molecules to interact with the stationary and mobile phases and should result in better separations. Of course such long gradients are not used for the screening of chromatographic conditions.

Trials on a normal phase silica column were performed using cHex-MEK or toluene-MEK gradients but it was not possible to obtain a sufficient separation. The homopolymers exhibited a weak adsorption on the very polar stationary phase. Homopolymer elution occurred with very low amounts of MEK in all cases. The polarity difference of the monomers was not sufficient for a selective separation since all monomers are acrylate or methacrylate aliphatic esters.

On the contrary, non-polar stationary phases (reversed phases) using a mobile phase of ACN-THF allowed a better separation of the homopolymers. The homopolymers were all strongly adsorbed on the C18 surface and different amounts of THF in the mobile phase were required for polymer elution. This solvent combination gave the best separation in comparison to ACN-chloroform or ACN-ethyl acetate gradients. Therefore, this system was used for the separation process. Figure 15 shows a fast linear gradient from 100 % ACN to 100 % THF to separate the homopolymers on a monolithic C18-modified silica gel. The dotted line represents the mobile phase composition at the detector. As expected, using such chromatographic conditions the homopolymers elute in the direction of increasing hydrophobicity of the ester groups: more polar polymers elute before less polar polymers. For the same reason, acrylates elute before methacrylates having an identical ester group.

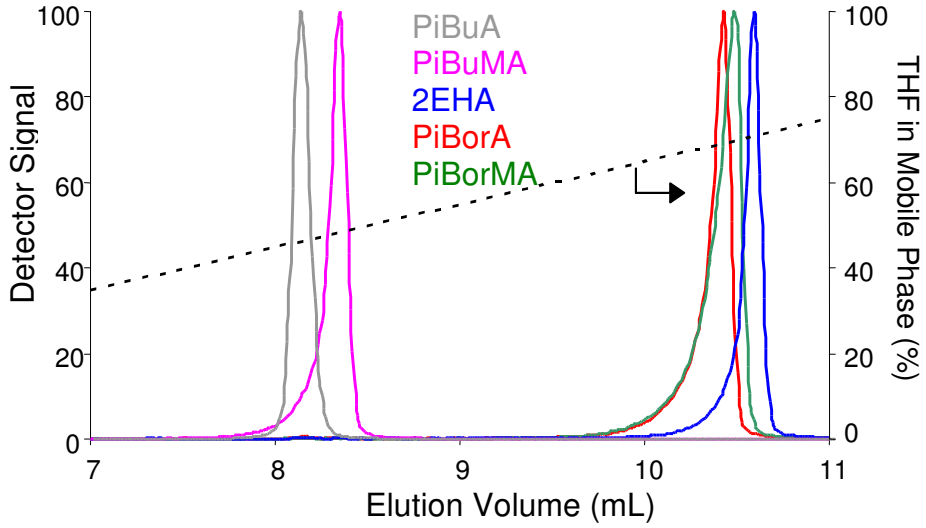


**Figure 15:** Gradient HPLC separation of the homopolymers, stationary phase: Chromolith C18 (100 x 4.6 mm I.D.), mobile phase: 10 min linear gradient ACN-THF 100 to 0 % ACN, flow rate: 1 mL/min, detection: ELSD. Dotted line represents the mobile phase composition at the detector

Using these chromatographic conditions, it was not possible to achieve baseline separation of all components but it was possible to separate them into two groups. The more polar PiBuA and PiBuMA eluted close to each other but still separated, while the less polar PiBorA, PiBorMA, and P2EHA co-eluted. An increase in the gradient time led only to a slightly improved separation with this column.

In order to achieve a better separation, a polymeric stationary phase was tested, i.e. a polystyrene-based cross-linked material of Polymer Laboratories (PLRP-S). Such stationary phase was tested as it is non-polar. On the other hand, it contains phenyl groups which are susceptible to interact with the π-electrons of the carbonyl groups of ester functions. The polymers that were to be separated are only different with regard to the aliphatic group of the ester: the larger the ester group, the less polar it was and, thus, the more the π-electrons were susceptible to interact with the π-electrons of the phenyl groups of the stationary phase.
Different gradients of ACN-THF were evaluated. The first one was a linear gradient from 100 % to 20 % ACN in the mobile phase in 10 min (see Figure 16 showing the separation of a mixture of the five homopolymers). Separation was achieved within 12 min.

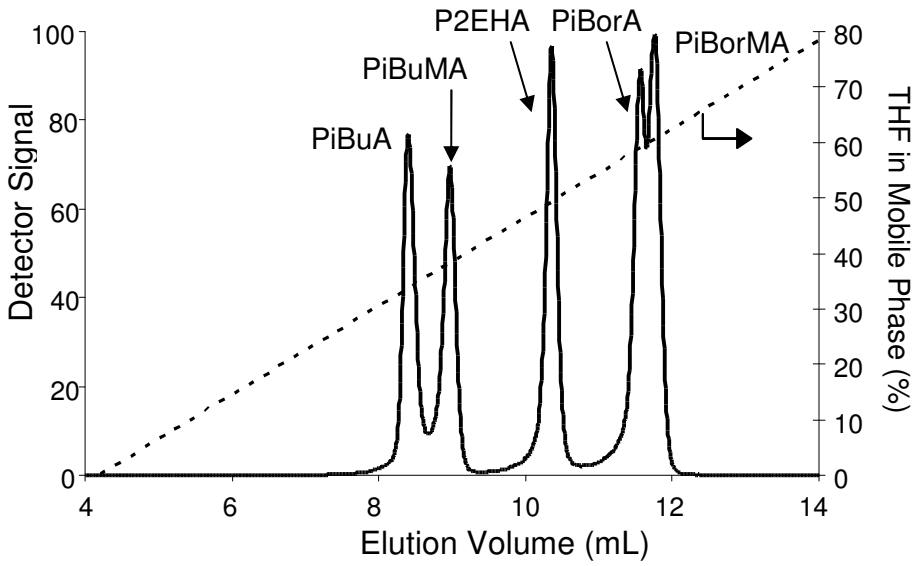


**Figure 16:** Gradient HPLC separation of the homopolymers, stationary phase: PLRP-S (150 x4.6 mm I.D. 5 µm), mobile phase: 10 min linear gradient ACN:THF 100 to 20% of ACN, flow rate: 1 mL/min, detection: ELSD. Dotted line represents the mobile phase composition at the detector

The separation of the component mixture was significantly improved on the polymer-based stationary phase compared to the normal phase. It was now possible to separate PiBuA and PiBuMA from each other. P2EHA was baseline separated from all other components while PiBorA and PiBorMA were not fully separated. Following the procedure described by Bashir et al. [61] using the Polymer Chromatographic Model (PCM), a step gradient for the mobile phase was designed in order to improve the chromatographic separation. The method recommends determining mobile phase compositions at elution for the homopolymers: $\Phi_e$, which should be close to the critical conditions of elution.

$$\Phi_e = G(V_e - V_I - V_P - V_{dw}) + \Phi_0 \qquad \text{IV-1}$$

where $\Phi_e$ and $\Phi_0$ are the mobile phase compositions at elution and at the beginning of the gradient, respectively. $V_e$, $V_i$, $V_p$ and $V_{dw}$ are the analyte elution volume, the system interstitial volume, the column pore volume and the system dwell volume, respectively. For more precise definition of these volumes refer to Figure 5. G is the gradient slope describing the evolution of mobile phase composition as a function of the pumped volume.

Mobile phase compositions at elution for each polymer could be read from Figure 16; they correspond to the Y-values of the dotted line at each peak maximum. These values are given in Table 4.

**Table 4:** Mobile phase composition at elution for the five homopolymers determined from the gradient experiment shown in Figure 16

| Homopolymer | PiBuA | PiBuMA | P2EHA | PiBorA | PiBorMA |
|---|---|---|---|---|---|
| Mobile Phase composition at elution: $\Phi_e$ (% THF) | 33.2 | 37.8 | 48.9 | 58.5 | 60.1 |

Isocratic experiments in SEC and LAC modes were conducted for each sample with mobile phase compositions close to the composition determined. With the equation of PCM model given in bibliographic part (chapter III.2.2.2) and with a non-linear fitting procedure we were able to extract the parameters of the model. Knowing then critical condition of elution, and evolution of the retention with composition of the mobile phase, we designed a gradient with four steps with different gradient slopes to obtain the best resolution. Figure 17 shows the chromatogram of the homopolymer blend. The four-step gradient is presented in dotted-line.

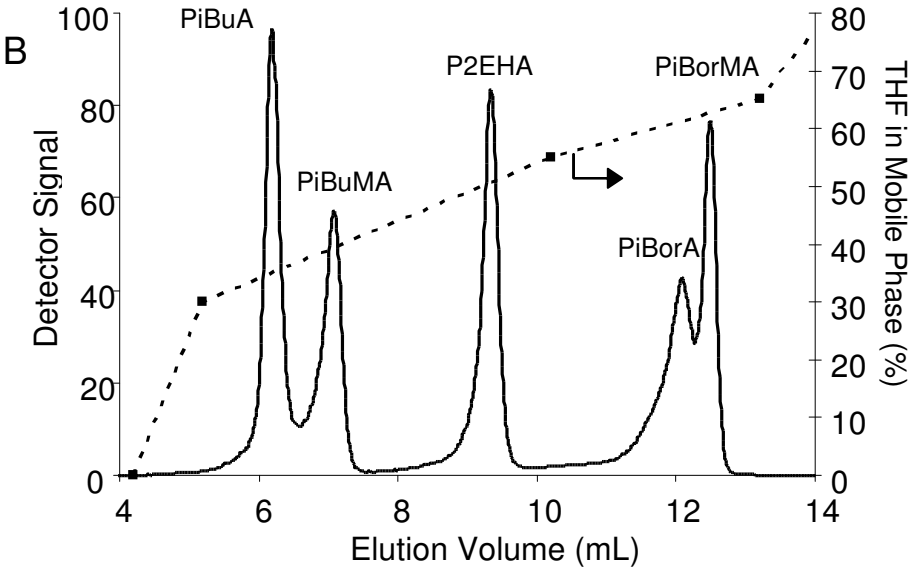


**Figure 17:** HPLC separation of the homopolymer blend, mobile phase: ACN-THF gradient as described, stationary phase: PLRP-S (150 x 4.6 mm I.D. 5 µm) flow rate: 1 mL/min, detection: ELSD. Dotted line represents the mobile phase composition at the detector

A better separation of the five homopolymers was achieved with this step gradient. It involved four steps. The first one from 0 to 30 % of THF was done in one minute to rapidly reach the eluting domain. It was not possible to condition the column directly at 30 % of THF as it gave a large breakthrough peak [105]. This peak appears at void volume of the system and corresponds to macromolecules which remain in the plug of solvent injection. Indeed, the polymer is dissolved in a good solvent for injection but the conditioning solvent of the column is a rather poor solvent for the macromolecules. As a result a part of the injected

sample remains in the injected solvent and elutes through the column without interacting. If the conditioning solvent contains a percentage of a good solvent, it is also possible that interactions between the stationary phase and the macromolecules are impeded. It also leads to formation of a breakthrough peak. This phenomenon is particularly pronounced when large volumes of concentrated polymer solution are injected in a very poor solvent of the sample. A short column favors the appearance of this peak. Usually the peak contains all kinds of macromolecules in approximately the same proportion as in the injected solution [105]. In the present case, macromolecules were dissolved in THF. If injected into a mobile phase comprising 100 % of methanol, nearly all polymer fractions remained adsorbed on the stationary phase. However, when the mobile phase contained 30% of THF, a large part of the sample was not retained and eluted at 1.8 mL, the void volume of the system.

The second gradient step from 30 to 55 % of THF led to the elution of PiBuA, PiBuMA and P2EHA. The slope in this case is more moderate (gradient slope of 5 % of THF/min) than for the linear gradient (gradient slope of 8 % THF/min) which led to a better separation of the peaks.

The third step with the smallest slope changed the mobile phase composition from 55 to 65 % of THF in 3 minutes (i.e. gradient slope of 3.33 % THF/min). It was designed to better separate PiBorA and PiBorMA.

The fourth step was programmed to flush the column and thus ensure complete elution of all injected polymer species.

However, the isobornyl acrylate peak became significantly broader which decreased resolution. This is due to the development of a molar mass dependence of the gradient HPLC separation. At a certain stage of the gradient, elution occurs simultaneously according to chemical composition and molar mass. Here we could see that large PiBorA molecules eluted simultaneously with small PiBorMA molecules.

The polymer chromatographic model does not predict the width of the elution peaks which is mainly due to molar mass distribution of the samples. The homopolymers analyzed here are indeed broadly distributed in molar masses and especially the isobornyl acrylate homopolymer which exhibits a polydispersity index of 4.6. Nevertheless the prediction of the elution volumes for the peak maxima was efficient and improved the separation without increasing time for analysis.

***b) Copolymer analyses***

As shown in Table 1 the copolymers in all cases are formed by copolymerizing three different monomers. As for sample 1, in the first step iBorA and iBorMA are reacted to form a random copolymer followed by the addition of iBuA to form PiBuA sequences. For detailed analysis of the final copolymers, in a first step the intermediate random copolymer was analyzed by gradient HPLC. As shown in Figure 18 (dotted curve), the chromatographic behavior of the copolymer is mainly directed by isobornyl acrylate moieties. Accordingly, the copolymer co-elutes with PiBorA homopolymer (second peak of the dot-dashed curve). In the HPLC elugram there are no indications for the formation of iBorMA homopolymer. NMR analysis of the binary copolymer shows that a random copolymer is formed having a chemical composition close to the composition of the monomer feed.

In the second reaction step the random copolymer is copolymerized with iBuA. As a result PiBuA chains are attached to the preformed random copolymers. From the spectroscopic analysis of the final reaction products the chemical composition, i.e. the amounts of iBorA, iBorMA and iBuA in the samples, can be calculated quantitatively. Information on the presence of homopolymers or the intermediate random copolymer, however, cannot be obtained from spectroscopic analyses.

Figure 18 also presents the chromatogram of sample 1 (solid curve) which shows a trimodal elution profile. The first peak at an elution volume of 5 mL co-elutes with PiBuA. This would confirm the presence of homopolymer of the last added monomer. Similar results have also been obtained by analyzing the other samples.

The second peak elutes between 6 and 9 mL and can be assigned to the ternary copolymer. As can be seen, this peak is particularly broad, which indicates a broad chemical composition distribution of the ternary copolymer. This is in agreement with the synthesis process and suggests that the third monomer is randomly added to the previously formed binary copolymer. This result also corroborates the large values of polydispersity calculated for the ternary copolymers.

A third elution peak is obtained between 9.5 and 12 mL, close to PiBorA and the intermediate random copolymer. According to the elution profile of this peak, it seems as if very few chains remained as binary copolymer. The shift of the peak maximum towards lower elution volume indicates that the macromolecules are more polar than the binary copolymer. This can occur only when the macromolecules contain a more polar monomer, in this case iBuA. In contrast to the second elution peak, the ternary copolymer forming the third elution peak contains a relatively small amount of the third monomer.

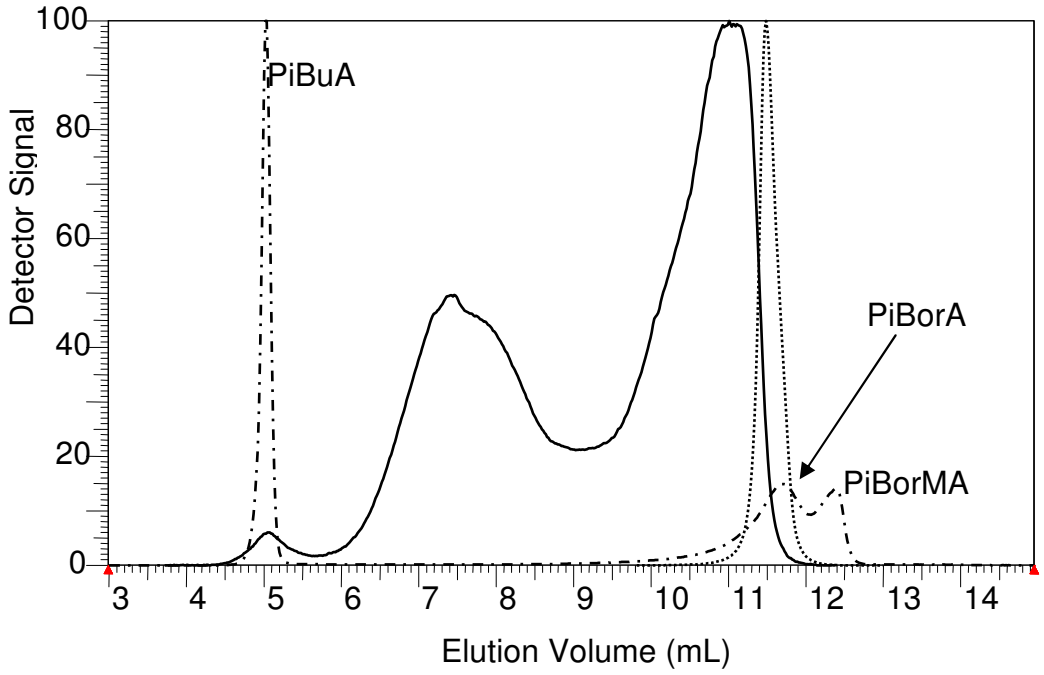


**Figure 18:** Overlay of gradient HPLC curves of three homopolymers (dot-dashed line), the intermediate random copolymer (dotted line), and sample 1 (solid line), stationary phase: PLRP-S (150 x 4.6 mm I.D. 5 µm), mobile phase: step gradient ACN:THF as in Figure 17, flow rate: 1 mL/min, detection: ELSD

### 1.1.3. 2D-LC to combine CCD and MMD information

***a) 2D-LC specificities***

As previously described, more detailed information on the composition of complex copolymers can be obtained by 2D-LC. Coupling the gradient HPLC method to SEC provides simultaneous information on chemical composition and molar mass distribution. The following experimental setup was used:

In the first dimension the PLRP-S column (150 x 4.6 mm I.D., 5 µm) was used. To achieve a complete automation of the system, the mobile phase flow rate was reduced to 0.06 mL/min in order to fill one 100 µL loop in the time needed to perform one SEC (second dimension) experiment. The gradient was then recalculated according to this new value. The total volume of mobile phase pumped to complete the gradient should be identical for one- and two-dimensional experiments. Thus the times corresponding to gradient slope modification should be corrected according to the new mobile phase flow rate.

| T (min) | 0 | 17 | 100 | 150 | 170 | 185 |
|---|---|---|---|---|---|---|
| % THF | 0 | 30 | 55 | 65 | 80 | 0 |

The second dimension separation was performed on a PL Rapide M column (150 x 7.5 mm I.D.). The flow rate in this case was 2 mL/min. ELSD was used to detect the polymer species at the end of the SEC separation.

A calibration curve for the 2nd dimension has been obtained with 8 polystyrene calibration standards at a flow rate of 2.0 mL/min, see Figure 19. This is used to determine the molar mass distribution in the 2D-LC plots.

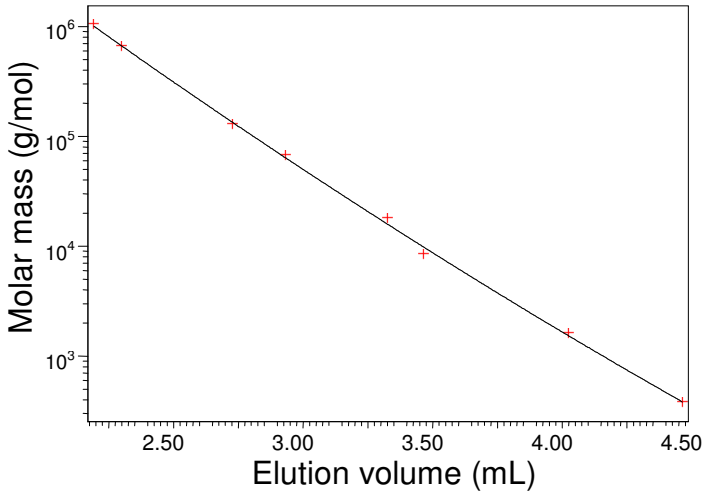


**Figure 19**: Polystyrene calibration curve, stationary phase: PL Rapide M (150 x 7.5 mm I.D.), mobile phase: THF, flow rate: 2.0 mL/min, detection: ELSD

It can be seen that the first calibration standard (1 040 000 g/mol) elutes at an elution volume of 2 mL (i.e. 1 min in the second dimension) and a total SEC experiment requires 5 mL (2.5 min). Complete elution in gradient HPLC is achieved within 13 mL. Each fraction of this LC separation injected into the second dimension contains 100 µL. Consequently, 130 SEC measurements are required for a comprehensive 2D-LC experiment. If we had kept 2.5 min per SEC experiment, total analysis time would have been 325 min for the 2D-LC. Therefore, it is useful in order to speed up the total measurement to inject a sample when the SEC analysis of the previous one is not entirely completed. In the present case, a transfer into the 2nd dimension can be made every 1.7 min instead of 2.5 min (as would be the case when waiting for the full volume of 5 mL of the column). The resulting total separation time for one experiment is then around 220 min.

Detection is realized with an ELSD. As mention before it is a universal detector capable of detecting all non volatile molecules. For this reason, we used its response for approximating the quantity of species present in each sample. For each 2D-LC chromatogram we integrated, when present, the spots corresponding to binary random copolymer, terpolymer and homopolymer of the third added monomer. Since the experiment comprised two LC

separations we obtain a three dimensional spot which corresponds to the peak of one-dimensional chromatography experiments. Its integration gives relative volumes instead of peak areas. The total peak volume was set at 100 %.

It has to be remembered that ELSD sensitivity is dependent on a large number of factors which are e.g. analyte structure (size and architecture) and mobile phase composition. In case of the present 2D-LC system, the detector evaporates always the same mobile phase, i.e. THF, as it is placed after the SEC separation. However the separated spots obtained with 2D-LC are heterogeneous in molar mass and chemical composition. The results of spot quantification must hence be taken carefully. A calibration of the detector with references has to be conducted in order to properly quantify all present species.

***b) Homopolymer analyses***

A first indication of the separation capability of 2D-LC can be obtained from the separation of the homopolymers corresponding to the monomers used to synthesize sample 1, see Figure 20. In this 2D-LC plot, the gradient separation is represented along the Y-axis whereas the SEC is given on the X-axis. As shown in Figure 18, PiBuA elutes first in a baseline separated peak (peak at 5 mL) while PiBorA and PiBorMA are not baseline separated (peaks at 11.7 and 12.4 mL). An improvement in the separation of these two homopolymers is obtained in 2D-LC due to the fact that separation is directed by molar mass in addition to chemical composition. From Figure 20 it is clear that the PiBuA homopolymer spot is very narrow on the Y-axis which marks the absence of chemical composition distribution as expected for a homopolymer. However, PiBorA and PiBorMA are unexpectedly much broader along the Y-axis. Since homopolymers are analyzed, no chemical composition distribution should be seen. The curved signal for these homopolymers is directly related to the molar mass dependence of the step gradient separation: the lower molar mass molecules elute before the larger ones even if they have the same chemical composition. This drawback of the method cannot be overcome at the present chromatographic conditions.

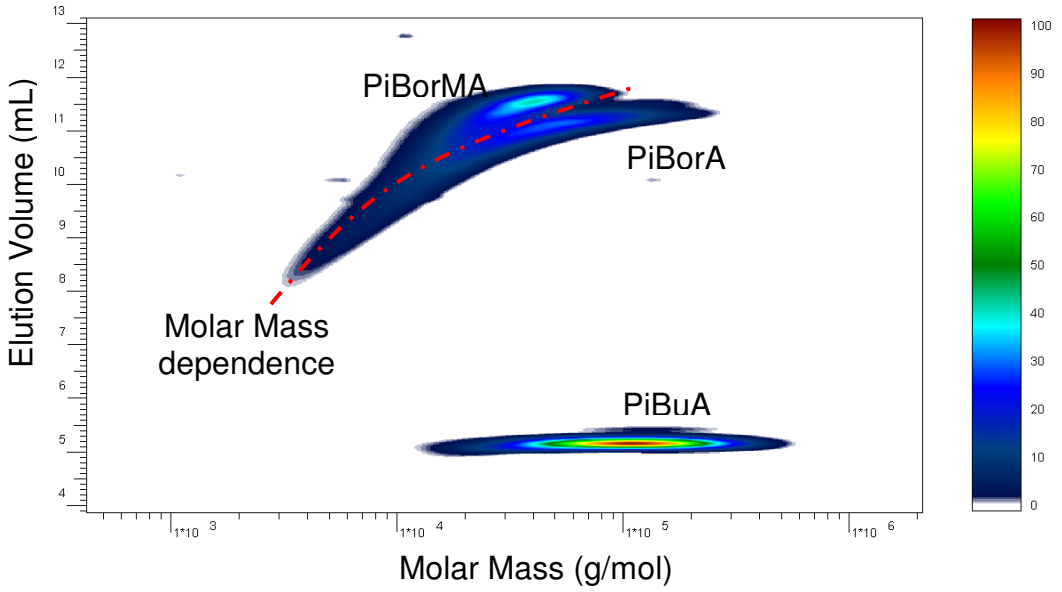


**Figure 20**: 2D-LC separation of the mixture of the three homopolymers PiBuA, PiBorA, and PiBorMA, 1st Dimension: step gradient HPLC ACN:THF at 0.06 mL/min on PLRP-S 5 µm; 2nd Dimension: SEC with THF at 2.0 mL/min on PL Rapide M; Calibration: PS; Detection: ELSD

Using the same experimental conditions, the random copolymer of iBorA and iBorMA was analyzed. The 2D-LC contour diagram given in Figure 21 shows clearly that the copolymer is quite uniformly distributed with regard to molar mass and chemical composition, the weight average molar mass being 97 000 g/mol. As expected, the intermediate polymer elutes at the same elution volume as the iBorA and iBorMA homopolymers.

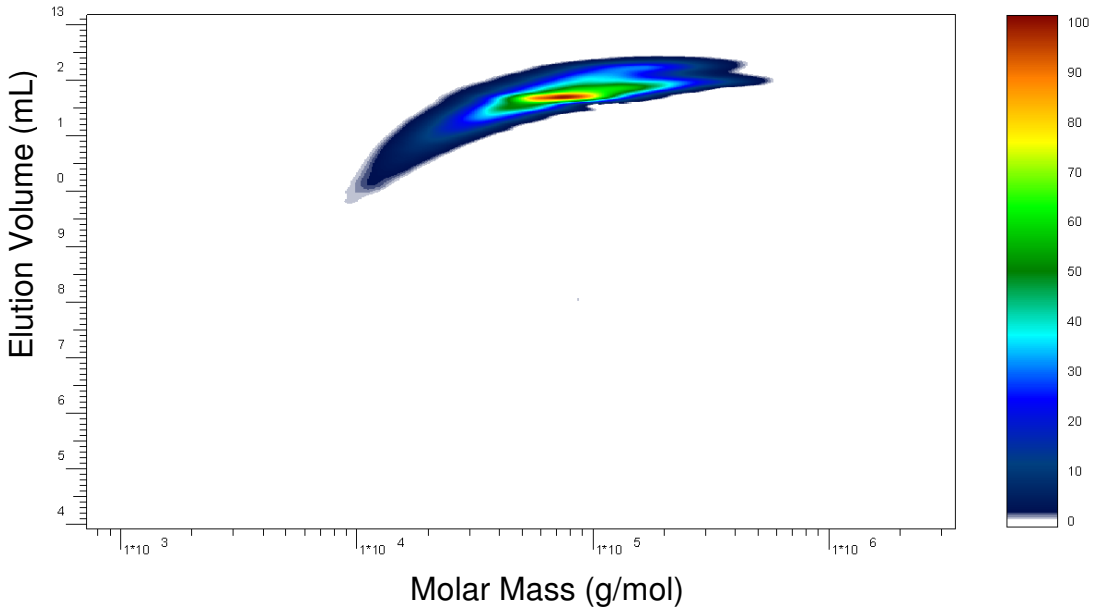


**Figure 21**: 2D-LC separation of the intermediate random copolymer, using experimental conditions as given in Figure 20

This random copolymer was subsequently reacted with iBuA to form the final sample 1. This product was also analyzed by 2D-LC.

### *c) Sample 1*

Due to the fact that the 2D-LC technique is a "dual dilution" technique (one dilution step by injecting in the 1st dimension, second dilution when injecting fractions from 1st dimension into 2nd dimension) a larger sample concentration needs to be used as compared to the gradient HPLC separation. To make sure that different concentrations do not change the separation, experiments were conducted at sample concentrations from 8.4 to 23.7 mg/mL using the same injection volume. Two corresponding 2D-LC plots are given in Figure 22.

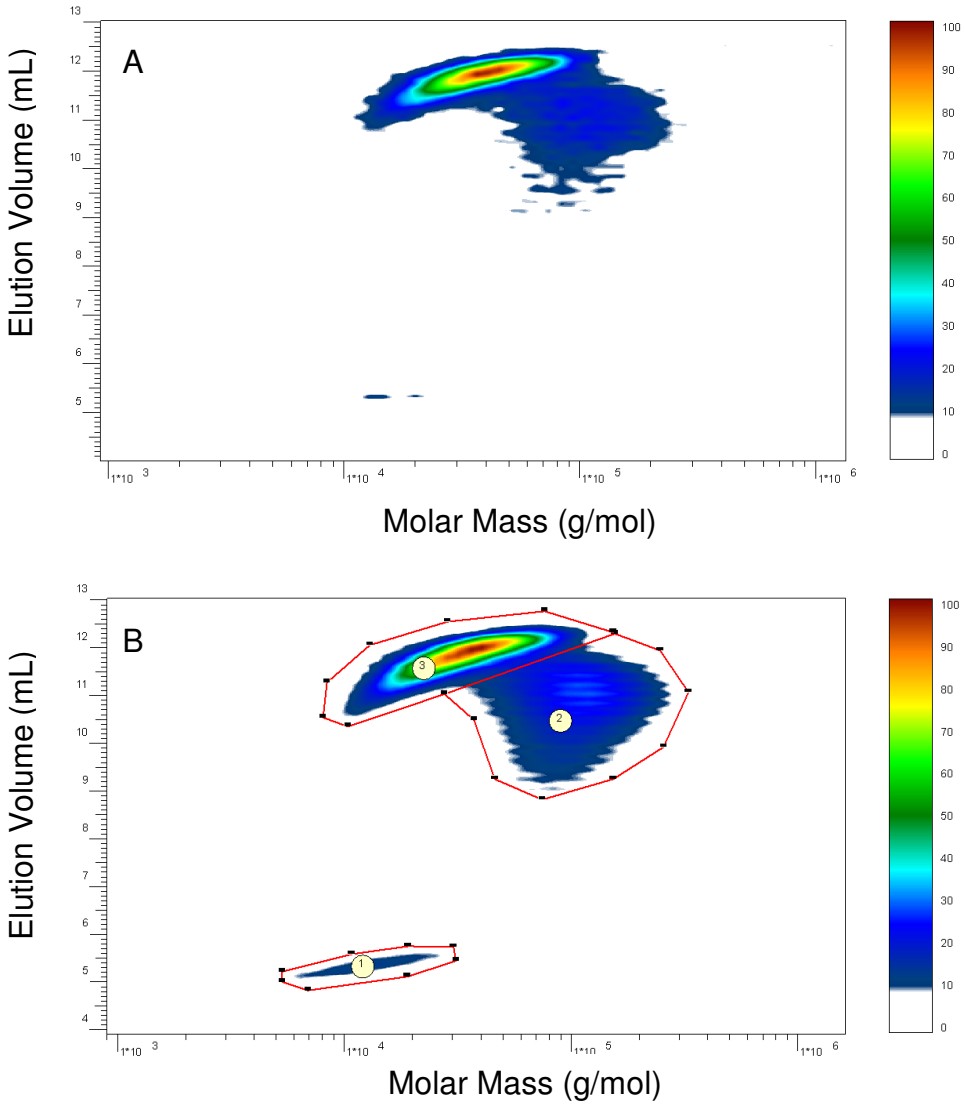


**Figure 22**: 2D-LC contour plots for sample 1 at different concentrations, using experimental conditions as given in Figure 20, concentrations: (A) 8.4 mg/mL (B) 23.7 mg/mL

As can be seen, rather similar contour plots are obtained for the two concentrations. Sample components 2 and 3 are readily detected at both concentrations while component 1 gives a

significant spot only at higher concentration. This indicates that the chromatographic behavior is not influenced by sample concentration. In agreement with the one and two dimensional LC results given in the previous Figures, component 1 can be identified as PiBuA. Accordingly, components 3 and 2 are binary and ternary copolymer species. Taking the shape and position of component 3 into account, it can be assigned to the intermediate random copolymer. Consequently, component 2 must be due to the ternary copolymer. As discussed before, component 3 contains also a part of ternary copolymer, however, with a smaller amount of isobutyl acrylate in the copolymer composition.

As could be expected from dilution effects, low concentrated polymers such as component 1 can only be detected when a high sample amount is injected. The good reproducibility of measurements for four different concentrations is shown in Table 5. The component concentrations as well as the molar masses determined from the contour plots are very similar in all the experiments.

**Table 5:** Quantification of component amounts and molar masses for sample 1 as determined by 2D-LC, molar masses are PS equivalents

| **Sample 1** | **Relative Volume (%)** | | | $\overline{M_w}$ **(g/mol)** | | |
|---|---|---|---|---|---|---|
| | **1st peak** | **2nd peak** | **3rd peak** | **1st peak** | **2nd peak** | **3rd peak** |
| **8.4 mg/mL** | 4 | 45 | 51 | 15 000 | 121 000 | 40 500 |
| **11.7 mg/mL** | 6 | 42 | 52 | 17 300 | 111 000 | 39 600 |
| | 6 | 45 | 49 | 15 900 | 110 800 | 38 000 |
| **18.2 mg/mL** | 5 | 42 | 53 | 14 100 | 119 700 | 38 600 |
| **23.7 mg/mL** | 5 | 44 | 51 | 14 000 | 116 200 | 36 600 |

As shown in Table 5, the weight average molar masses of PiBuA, the ternary copolymer and the binary copolymer are roughly 15 000 g/mol, 116 000 g/mol, and 38 000 g/mol, respectively. Comparing the molar masses of the binary copolymer in Figure 21 and Figure 22 (97 000 and 38 000 g/mol, respectively), it is clear that the copolymerization of isobutyl acrylate with the binary copolymer takes place mainly with the higher molar mass molecules. Apparently, lower molar mass molecules are less likely to add iBuA.

***d) Sample 2***

The random copolymer of iBorA and iBorMA shown in Figure 21 was also reacted with 2EHA to obtain sample 2. The analysis of sample 2 by 2D-LC is shown in Figure 23 overlaid with the intermediate random copolymer of iBorA and iBorMA. The quantification results for this sample are given in Table 6.

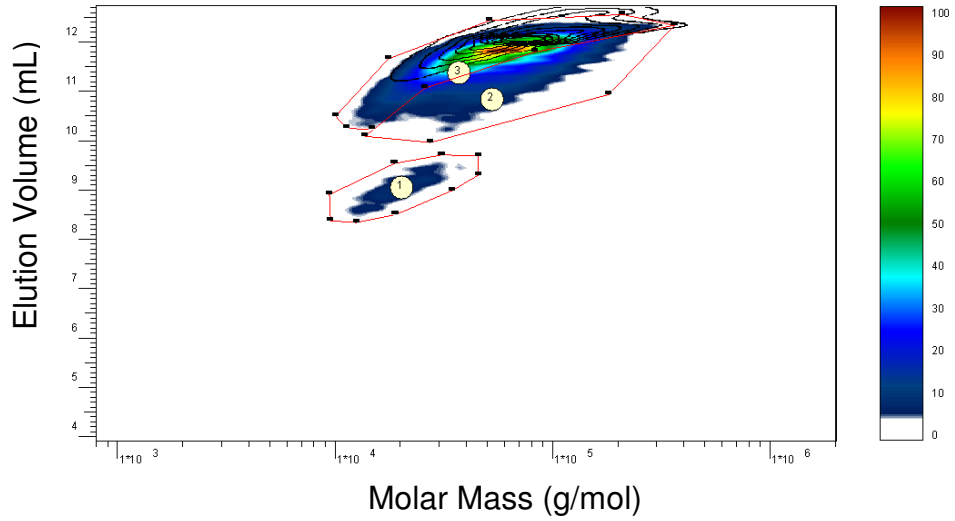


**Figure 23**: 2D-LC contour plot for sample 2 with intermediate copolymer overlaid (black isolines), using experimental conditions as given in Figure 20

**Table 6:** Quantification of component amounts and molar masses for sample 2 as determined by 2D-LC, molar masses are PS equivalents

| **Sample 2** | **Relative Volume (%)** | | | $\overline{M_w}$ **(g/mol)** | | |
|---|---|---|---|---|---|---|
| | **1st peak** | **2nd peak** | **3rd peak** | **1st peak** | **2nd peak** | **3rd peak** |
| **23.5 mg/mL** | 7 | 36 | 57 | 21 000 | 97 000 | 57 000 |

Spot 1 can be attributed to the homopolymer of the third monomer: P2EHA. This spot shows some molar mass dependence as it is not perpendicular to the Y-Axis. The amount of homopolymer of the last added monomer is very comparable to the value found for sample 1. This could indicate that the addition of the third monomer is achieved in a similar proportion as has been obtained in sample 1. However, the relative volume determined for spot 2 in sample 2 is close to 36 %, which is lower than what was found for sample 1.

The quantification was done as follows. Since we had the intermediate random copolymer as reference, we analyzed it at the same 2D-LC conditions in order to determine its elution domain (see Figure 21). It is presented in Figure 23 as black isolines. Then, we considered the part of sample 2 which was not covered by the reference and assigned it to the terpolymer. This part was integrated separately. Unfortunately, the terpolymer appears only as a shoulder of spot 3 and, therefore, quantification is not very reliable. The reason most probably is that

the polarity difference between isobornyl monomers and 2-ethylhexyl acrylate is too low to allow the intermediate binary copolymer and ternary copolymer to be completely separated. As shown in Figure 23, the main part of the spot is overlaid with the signal of the intermediate copolymer. Accordingly, the separation obtained is not complete and the quantification is of low accuracy.

***e) Sample 3***

Sample 3 was prepared by copolymerizing iBuMA and iBorA in the first step and adding 2EHA in the second step to form the ternary copolymer. The 2D-LC plot, obtained under the same conditions as described before, overlaid with the 2D-LC plot of P2EHA (isolines) is given in Figure 24. Quantification of spot 3 in Figure 24 is done after considering the 2D-LC plot overlay of sample 3 and sample 4 given in Figure 26.

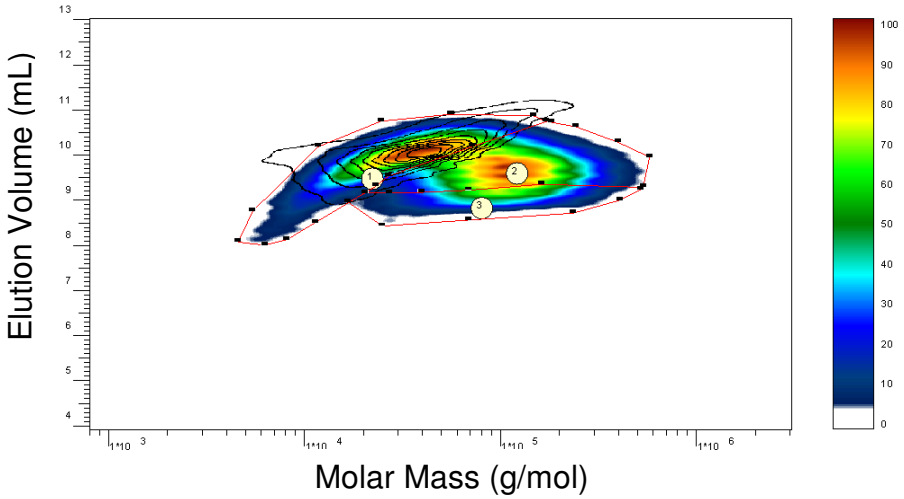


**Figure 24:** 2D-LC contour plot for sample 3 overlaid with the 2D chromatogram of P2EHA (black isolines), using experimental conditions as given in Figure 20

In this 2D-LC plot a large spot representing 2EHA homopolymer (last added monomer) can be seen. It has been identified by comparing it with the 2D-LC plot of the model homopolymer. A curved shape is again found for the homopolymer which characterizes the molar mass dependence of the separation by gradient chromatography.

For this sample, it is also difficult to discriminate between ternary and binary copolymers. Integration limits shown in Figure 24 were confirmed after analyzing sample 4 (see Figure 26). Binary and ternary copolymers elute close to each other and can be separated only by molar mass. Indeed, the terpolymer exhibits a higher molar mass than the binary copolymer and is eluted between the binary copolymer spot and that of P2EHA. Thus, spot 2 is assigned to terpolymer and spot 3 to binary copolymer. As was already shown by SEC experiments, this

sample is the most broadly distributed in molar masses. This is depicted in Figure 24 by a large signal along the X-axis. The spot quantification results are presented in Table 7.

**Table 7**: Quantification of component amounts and molar masses for sample 3 as determined by 2D-LC, molar masses are PS equivalents

| **Sample 3** | **Relative Volume (%)** | | | $\overline{M_w}$ **(g/mol)** | | |
|---|---|---|---|---|---|---|
| | **1st peak** | **2nd peak** | **3rd peak** | **1st peak** | **2nd peak** | **3rd peak** |
| **27.8 mg/mL** | 40 | 47 | 13 | 35 000 | 95 000 | 68 000 |

One can see that the amount of ternary copolymer in sample 3 is comparable to that found in sample 1. Nevertheless the relative volumes of spot 1 and 3 completely differ from the previous ones. The proportion of homopolymer made of the third monomer (spot 1) is in a different range as compared to previous samples. As a consequence the relative volume of binary copolymer is very small but the weight average molar masses remain comparable to the results obtained for samples 1 and 2.

### *f) Sample 4*

To synthesize sample 4, similar to sample 3 iBuMA and iBorA were first copolymerized. This time, the obtained intermediate was reacted with iBuA in the second step. Similar to sample 1, in sample 4 PiBuA is detected as a homopolymer fraction in 2D-LC. It appears as the first eluting spot in the contour diagram shown in Figure 25. The second eluting fraction which shows the highest concentration can be assigned to the ternary copolymer. Accordingly, the latest eluting fraction is due to the binary precursor copolymer, i.e. poly(iBuMA-*co*-iBorA). The results of spot quantification are reported in Table 8.

In sample 4, the proportion of homopolymer (spot 1) and of binary copolymer remains low. This could indicate a better conversion to the ternary copolymer in the second reaction step. This result is corroborated first by the proportion of ternary copolymer detected and second by the average molar masses determined by SEC. Sample 4 exhibits the largest average molar masses (Table 2).

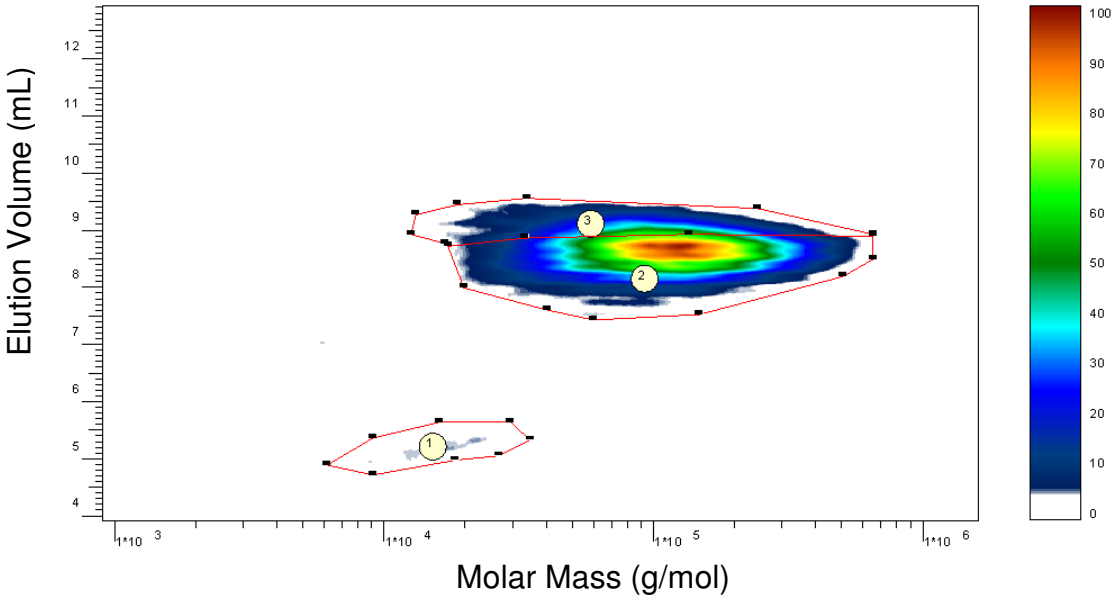


**Figure 25**: 2D-LC contour plot for sample 4, using experimental conditions as given in Figure 20

**Table 8:** Quantification of component amounts and molar masses for sample 4 as determined by 2D-LC, molar masses are PS equivalents

| **Sample 4** | **Relative Volume (%)** | | | $\overline{M_w}$ **(g/mol)** | | |
|---|---|---|---|---|---|---|
| | **1st peak** | **2nd peak** | **3rd peak** | **1st peak** | **2nd peak** | **3rd peak** |
| **23.1 mg/mL** | 1 | 73 | 26 | 11 000 | 128 000 | 55 000 |

As sample 3 and 4 are made of the same intermediate random copolymer (iBuMA and iBorA), we have overlaid the two 2D-LC plots for these polymers to verify that they were properly integrated. As shown in Figure 26, only one part of the plots is overlaid which should correspond to the intermediate binary copolymer.

In sample 4 (plain 2D-LC contour plot Figure 26), the main part of the polymer is eluted before, due to the addition of more polar iBuA as third monomer. On the contrary in sample 3 (isolines 2D-LC contour plot Figure 26), the major part of the spot is eluted later as 2EHA monomer is less polar than the intermediate copolymer. But once again a baseline separation between binary and ternary copolymers couldn't be achieved. The overlay indicates ways for a proper quantification but these results should be considered with care since the amount for all three species are very different to that determined for all other samples.

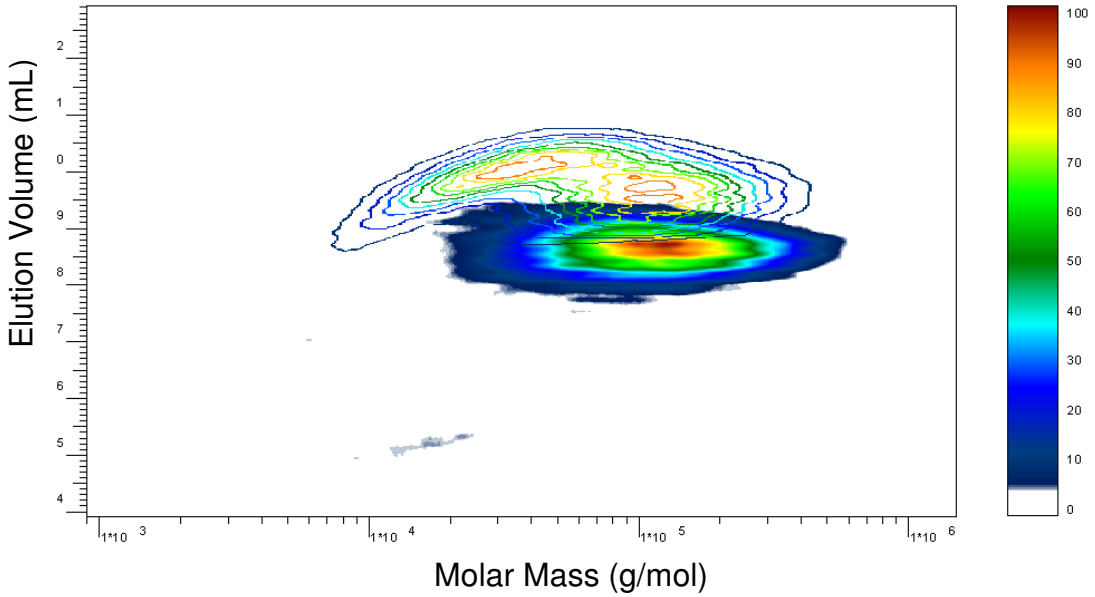


**Figure 26**: 2D-LC contour plot for sample 4 (plain) overlaid with 2D-LC plot of sample 3 (isolines), using experimental conditions as given in Figure 20

### *g) Sample 5*

Finally, sample 5 is synthesized by first polymerizing iBuMA and iBorMA and by adding iBuA in the second step. This sample is the only one with an intermediate copolymer composed of two methacrylates. The 2D-LC plot for this sample is given in Figure 27. The results of the spot quantification are given in Table 9.

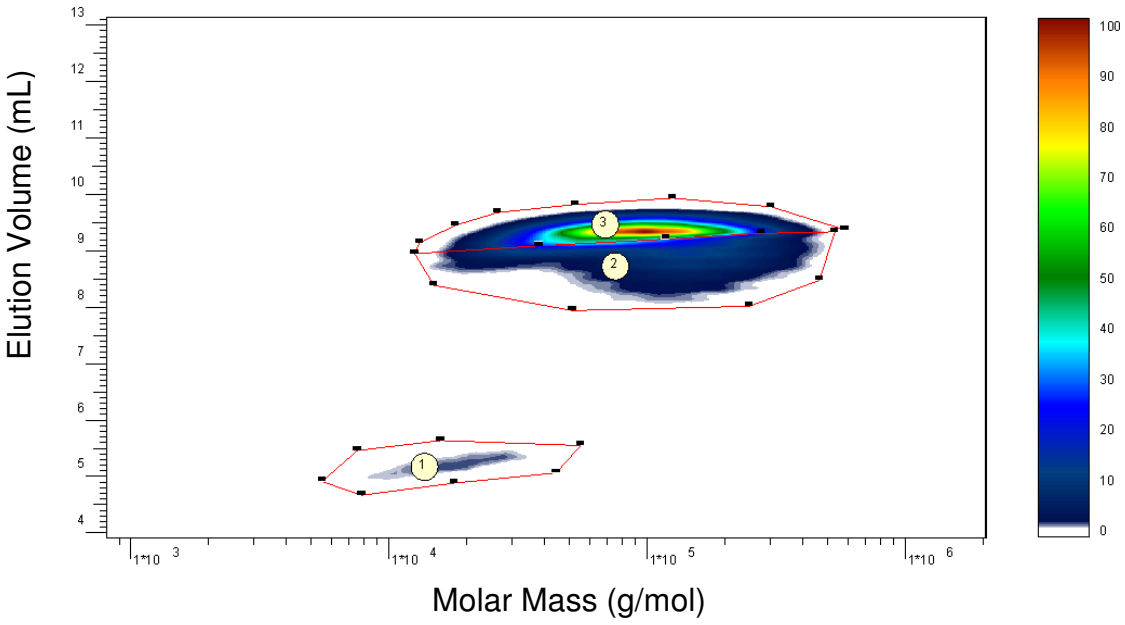


**Figure 27:** 2D-LC contour plot for sample 5, using experimental conditions as given in Figure 20

**Table 9:** Quantification of component amounts and molar masses for sample 5 as determined by 2D-LC, molar masses are PS equivalents

| Sample 5 | Relative Volume (%) | | | $\overline{M_w}$ (g/mol) | | |
|---|---|---|---|---|---|---|
| | 1st peak | 2nd peak | 3rd peak | 1st peak | 2nd peak | 3rd peak |
| **25.7 mg/mL** | 3 | 32 | 65 | 20 000 | 135 000 | 102 000 |

This copolymerization gives the largest intermediate copolymer (spot 3) in terms of weight average molar mass, i.e. approximately 100 000 g/mol. However, according to 2D-LC results, the lowest relative volume for the terpolymer (spot 2) of the five samples is detected here. Both methacrylates seem to copolymerize easily forming long random copolymers, but these intermediate chains give little copolymerization with the third monomer.

In the 2D-LC plot of sample 5, a spot for the homopolymer of the third monomer (iBuA) is also detected. Its relative volume and molar mass is similar to the values previously found for the other samples.

### 1.1.4. Conclusions

The methods developed based on the chromatographic behavior of the five homopolymers allow us to characterize the complex mixtures of macromolecules obtained via a two step free radical polymerization. We have shown that a two-step free radical copolymerization with three monomers can lead to very different polymers. The amounts of homopolymers, binary and ternary copolymers are very different depending on the monomers used.

2D-LC experiments are best suited to elucidate polymer sample composition as it couples both chemical composition and molar mass distribution. Sample fingerprinting has then been achieved and can be implemented for the characterization of the polymerization products.

A first attempt of quantification has been made by integrating the relative peak volumes. A calibration of the ELSD detector will be necessary for more precise results. It has nevertheless been shown that neither separation nor relative volumes depend on polymer concentration in the 2D-LC experiments.

The results of quantification together with the determined average molar masses for the five samples are summarized in Table 10. As can be seen large differences exist between the samples particularly in terms of relative volumes of the separated components. It seems that the terpolymerization is favored in the case of sample 4 over the homopolymerization of the last added monomer. However, it appears that the results in terms of average molar masses

are relatively similar for different samples. The only significant deviation is found for the binary random copolymers of sample 5 which are nearly two times larger than in the other samples.

**Table 10:** Summary of the relative volumes and the average molar masses determined for the three species of the five samples

| | **Relative Volume (%)** | | | $\overline{M_w}$ **(g/mol)** | | |
|---|---|---|---|---|---|---|
| | Homopolymers of the 2nd step monomer | Terpolymers | Binary random copolymers | Homopolymers of the 2nd step monomer | Terpolymers | Binary random copolymers |
| **Sample 1** | 5 | 44 | 51 | 15 500 | 115 500 | 38 500 |
| **Sample 2** | 7 | 36 | 57 | 21 000 | 97 000 | 57 000 |
| **Sample 3** | 40 | 47 | 13 | 35 000 | 95 000 | 68 000 |
| **Sample 4** | 1 | 73 | 26 | 11 000 | 128 000 | 55 000 |
| **Sample 5** | 3 | 32 | 65 | 20 000 | 135 000 | 102 000 |

## 1.2. Development of spectroscopic detection methods for CCD quantification

In order to better characterize the polymer samples, we wanted to quantify more precisely their chemical composition distributions (CCD). Direct spectroscopic measurements with Proton Nuclear Magnetic Resonance ($^1$H-NMR) or Fourier Transform Infra Red (FTIR) spectroscopy on total samples gave average chemical compositions of the samples but no information on the chemical composition distributions. Liquid chromatographic separation of the samples as shown in Part IV.1.1.2 is a powerful tool to obtain qualitative information on CCD. However, it was not possible to determine the copolymer composition quantitatively using ELSD detection. A direct way to quantitative composition would be of course the direct coupling of the LC system with a spectroscopic detector like $^1$H-NMR or FTIR. Unfortunately, such couplings are not straightforward and require method development. For method development, we concentrated our efforts on sample 1 and other samples containing the same monomers (iBuA, iBorA and iBorMA) but in various proportions.

Recent developments in LC-$^1$H-NMR allow to obtain on-line $^1$H-NMR spectra from LC separations. LC-NMR coupling is most common in the pharmaceutical industry but is gaining increasing importance for polymer analysis [91,106,107]. It permits the direct analysis of the chemical composition at each elution volume of the chromatogram. The most important problems related to direct LC-NMR coupling are the intrinsically low sensitivity of NMR and the fact that the analyte is a very dilute polymer solution. Solvent suppression techniques exist [93] to reduce solvent signals and hence make sample signals visible. These techniques are well suited for isocratic LC separations (e.g. SEC separations) but remain difficult to implement for solvent gradient chromatography. The major problem in the latter case is the drift in the solvent signal with gradient evolution: the variation of the mobile phase composition with time makes the solvent signal to shift which causes problems with solvent suppression.

Another limitation is the position of the solvent signals relative to the polymer signals. When solvent and polymer signals overlap then these would be suppressed with those of the solvent. Unfortunately, such overlap occurs with the present chromatographic system. In the present case, monomers added in step one (iBorA and iBorMA) must be differentiated from the monomer added in step two (iBuA) using the signals of the ester protons O-C<u>H</u> (4.6 ppm for iBorA and iBorMA) and O-C<u>H$_2$</u> (3.8 ppm for iBuA), respectively. The intensity ratio of these signals gives the chemical composition provided that deuterated chloroform is used as the solvent. In the present chromatographic system, the O-$CH_2$ proton signal of iBuA exactly overlaps with the O-$CH_2$ signal of THF used in the mobile phase for the gradient HPLC separation. Thus, LC-$^1$H-NMR on-line coupling was not directly applicable to the present polymer systems. It was therefore decided to consider the possibility of coupling LC with FTIR detection.

An on-line coupling of LC with FTIR would have led to the same problems as LC-$^1$H-NMR in terms of solvent/sample signals overlap. To avoid the problems an off-line coupling was used that permits the chromatographic mobile phase to be evaporated prior to the FTIR measurements (LC-Transform interface approach).

To be able to quantify the CCD of the polymers, specific absorption bands of the different monomer units had to be found and a calibration curve connecting chemical composition and FTIR data had to be constructed.

In this part, we investigated sample 1 (see Table 2) and derivative samples 6, 7, 8, 9 and 10 (with different iBuA content). Sample 6 is a random copolymer prepared with iBorA, iBorMA and iBuA in the same proportions as those of sample 1. Samples 7 to 10 were also prepared with these three monomers and with the same two-step synthesis procedure as that used for the polymerization of sample 1 but with different proportions of the monomer feed. Polymer 7 is synthesized with a large excess of iBor(M)A monomers whereas sample 10 contains mainly the third added monomer (isobutyl acrylate). The following diagram shows the distribution of the copolymers according to the proportion of iBuA used for the synthesis:

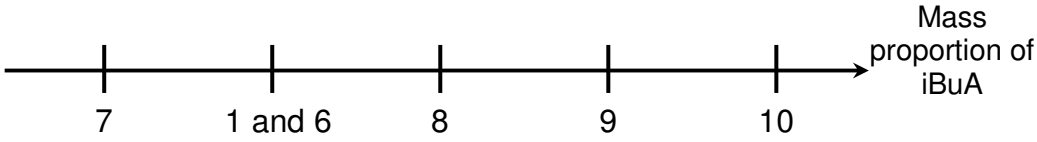


**Figure 28:** Classification of polymer samples according to the mass proportion of iBuA monomer

### 1.2.1. FTIR Calibration by drop deposition

A comparison of the FTIR spectrum of P(iBorMA-*stat*-iBorA) and PiBuA shows a specific absorption band for the copolymer at 1051 $cm^{-1}$ (Figure 29). However, no specific band was found for the homopolymer.

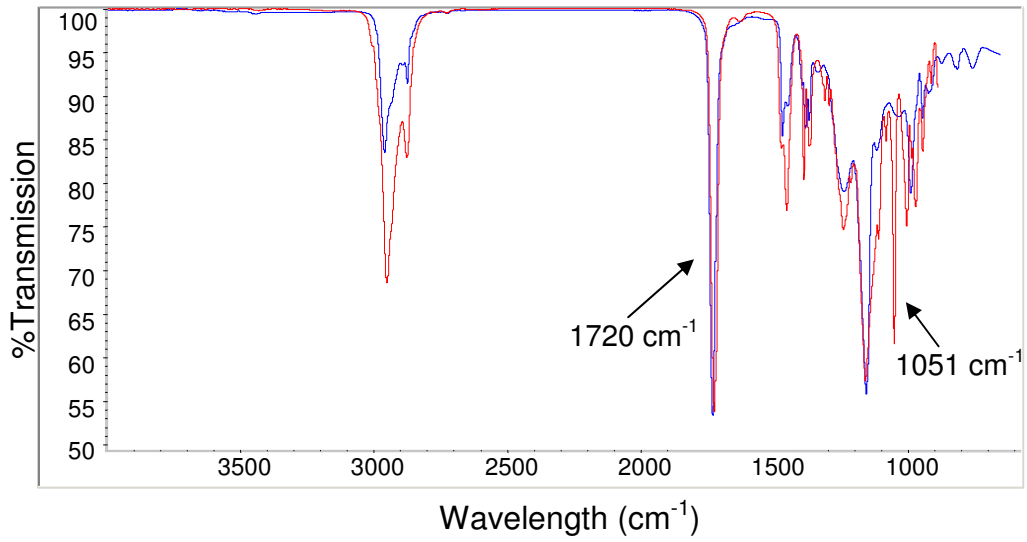


**Figure 29:** Overlay of FTIR spectra of binary random copolymer (red) and poly(isobutyl acrylate) (blue). A specific absorption band for P(iBorMA-*stat*-iBorA) appears at 1051 $cm^{-1}$

To be able to use the iBor(M)A specific band we had to correlate it to the total sample absorption. Since all monomers are esters (iBor(M)A and iBuA) they all absorb in IR at a

wavelength of 1720 $cm^{-1}$, the adsorption of the carbonyl group. The area of this absorption band in IR was used as normalizing factor for the isobornyl specific absorption band. We have assumed that the extinction coefficient is equal for all monomers at this wavelength.

In FTIR, absorption is defined by the formula given below, when we consider two components (e.g. P(iBorMA-*stat*-iBorA) and poly(isobutyl acrylate)):

$$A = d.C\left[\varepsilon_1 \times \omega_1 + \varepsilon_2 (1 - \omega_1)\right] \qquad \text{IV-2}$$

where A is the absorption at the given wavelength, C the sample concentration, $\varepsilon_i$ the extinction coefficient for each component, $\omega_1$ the molar fraction of component 1 and *d* is the distance that the irradiation travels through the material (the path length).

We consider now a ratio of absorption bands which leads to the following equation:

$$\frac{A_1}{A_2} = \frac{d.C\left[\varepsilon_{1,1} \times \omega_1 + \varepsilon_{2,1} (1 - \omega_1)\right]}{d.C\left[\varepsilon_{1,2} \times \omega_1 + \varepsilon_{2,2} (1 - \omega_1)\right]} \qquad \text{IV-3}$$

where $\varepsilon_{i,j}$ is the extinction coefficient for product i at wavelength j.

From our hypotheses, $\varepsilon_{1,2}$ and $\varepsilon_{2,2}$ are equal: the absorption of all monomers for the C=O band (1720 $cm^{-1}$) is similar. The second assumption is that $\varepsilon_{2,1}$ = 0: no absorption of isobutyl acrylate monomer at 1051 $cm^{-1}$. With these assumptions this equation can be simplified to:

$$\frac{A_1}{A_2} = \frac{\varepsilon_{1,1} \times \omega_1}{\varepsilon_{2,2}} = cst \times \omega_1 \qquad \text{cst is a constant} \qquad \text{IV-4}$$

To verify the feasibility of the approach, first a calibration was made by dropping polymer solutions on the Germanium plate. LC fractionation was not utilized in this case. Different mixtures of P(iBorMA-*stat*-iBorA) and PiBuA were prepared and dissolved in THF (~ 1 mg/mL). A few drops of these solutions were deposited on a Germanium plate and the FTIR spectra recorded after evaporation of the solvent.

The calibration curve is given in Figure 30.

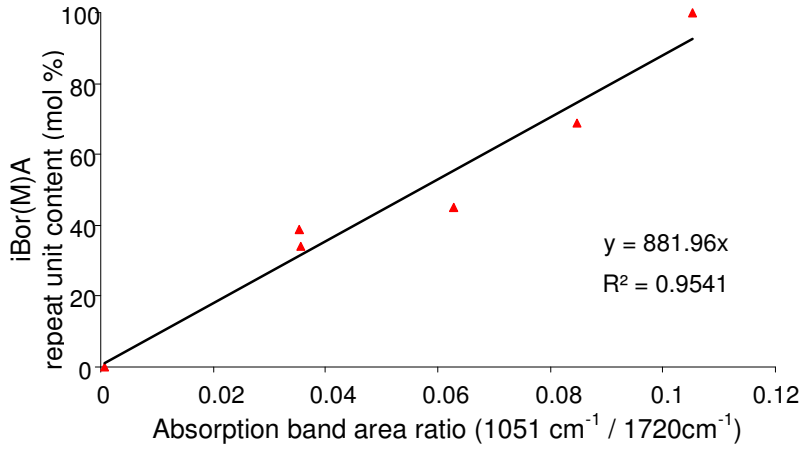


**Figure 30**: FTIR calibration curve: P(iBorMA-*stat*-iBorA) content in molar percent vs. the ratio of adsorption bands area of 1051 $cm^{-1}$ (specific of binary random copolymer) divided by the area of 1721 $cm^{-1}$ (total carbonyl equal total concentration)

One can see that the fit is not perfect, $R^2$ =0.9542, but the tendency is obvious. We used this calibration to quantify the chemical composition of samples 1, 6, 7 and 8.

The results of the chemical composition determination are given in Table 11. Chemical composition of these four copolymers was also determined by $^1$H-NMR to be used as reference values.

**Table 11:** Determination of the chemical composition of four terpolymers by FTIR analysis

| | Chemical Composition: iBorMA and iBorA repeat unit content | | |
|---|---|---|---|
| Sample name | mol % measured with $^1$H-NMR | **mol % measured with FTIR** | Standard deviation (%) |
| Sample 1 | 58 | **57** | 0.9 |
| Sample 6 | 48 | **37** | 23 |
| Sample 7 | 71 | **71** | 0.2 |
| Sample 8 | 46 | **52** | 14 |

As shown in Table 11, the agreement between FTIR and $^1$H-NMR measurements is good for copolymers synthesized with the two step process (samples 1, 7 and 8). The largest relative error (~ 14 %) is found for the product which contains the lowest amount of binary copolymer. It has to be reminded that chemical composition is calculated from the absorption band area of the binary random copolymer and thus the lower its amount the higher the relative error. The calibration curve should also be constructed with more standard mixtures.

The determination of the chemical composition is much less accurate for the random copolymer (sample 6). The relative error is calculated at approximately 23 %. This result confirms the fact that IR absorption depends also on the polymer structure. For the two step

procedure, the resulting polymers could be considered as copolymers with two "blocks": one is the binary random copolymer and the second block is PiBuA. These can be correlated to the chemical structures of the calibration standards. On the other hand sample 6 is not similar to the calibration standards as all monomers are randomly integrated into the polymer chains. For this reason an estimation of the chemical composition is poorly reliable. In this case calibration should have been performed with random copolymers having different compositions.

These results were only preliminary results but seem to be promising. In the next step the LC column was connected to the LC-Transform interface in order to obtain quantitative CCD for these polymers.

### 1.2.2. FTIR calibration using the spraying device

To couple LC and FTIR we have used the LC-Transform 600XY (LabConnections, Carrboro, USA). This device sprays the mobile phase coming from the column on a rotating Germanium plate. A gas flow (compressed air) and high temperature are necessary to completely evaporate the solvent. For the THF and ACN-THF mobile phases the parameters were set on 30 psi for the gas flow and 165 °C for the nozzle temperature. We tested different evaporation conditions to find the best temperature and gas flow rate to obtain uniform and useful deposits. Deposits can be schematically presented as follows depending on the evaporation conditions (Figure 31).

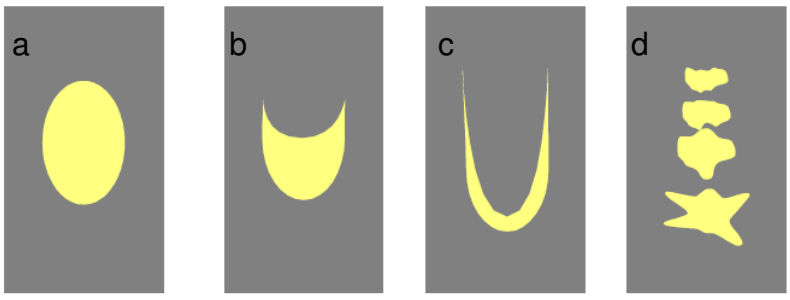


**Figure 31:** Examples of polymer deposit on the Germanium plate according to LC-transform set-up

The deposit shape given in Figure 31a is ideal. The solute peak deposited as a compact symmetric circle or oval on the Germanium plate. The deposit is 1–2 mm in width and should yield a good spectrum even at sub-microgram levels.

In Figure 31b a slightly crescent shape on the tailing edge of the deposit is presented. This is quite typical. The semi-circular form results from the mobile phase not completely evaporated which re-dissolves some of the previously deposited solute as the plate moves under the

nozzle. Such deposit is still quite compact and will produce a good IR spectrum. It is the most commonly observed shape of deposit. In Figure 31c there is extensive redissolution of the deposited spot. The solvent spray has continued to cut into the deposit and moves material on sides of the elution track. Spectra will have lower intensity. A higher nozzle temperature and/or a faster plate movement should be used to reduce this re-dissolution of the solute deposit. Finally, Figure 31d depicts a deposit that results from too high nozzle temperature. In this condition the solute is (partially) precipitating within the nozzle capillary and is ejected as little clots of solid. Some spattering may be evident, or the deposit may appear as a series of deposit spots and not as a track in response to the slight variation in delivered mobile phase flow from the HPLC pump.

The first measurements were carried out with an evaporation temperature of 125 °C, as recommended. At this temperature too much solvent remained in the spray and the deposit looked similar to Figure 31c. The separation that was achieved by LC was lost as the sprayed solvent redissolved the already deposited polymer. An increase of the temperature to 145 °C allowed for a better evaporation but yet too much solvent was contained in the spray. It was possible to overcome the redissolution by increasing the plate movement speed. This resulted in longer and thinner tracks of polymer films which were hard to analyze with FTIR. Finally, optimum conditions for the THF and ACN-THF system, with a mobile phase flow rate of 1 mL/min, were found at a nozzle temperature of 165 °C, a gas pressure of 30 psi and plate speed of 20 mm/min for the formation of a film thick enough for FTIR measurements while conserving the polymer separation.

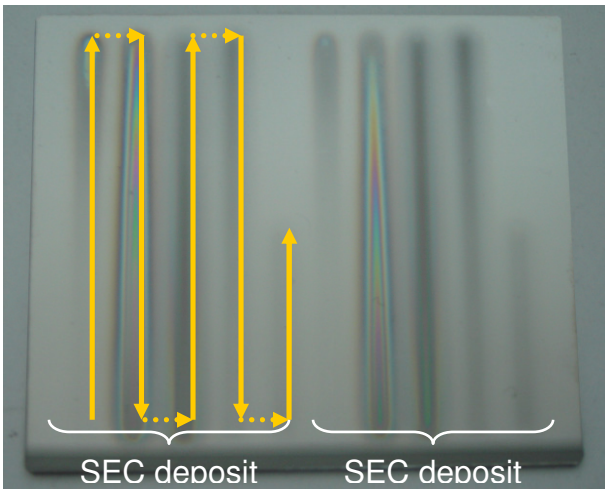


**Figure 32**: Example of a Germanium plate with two deposited polymer tracks. Yellow arrows show deposition of the spray on the plate

FTIR spectra are taken at regular intervals along the polymer film. Separated polymers are sprayed on the upper face of the plate (Germanium) so that chromatograms appear as

serpentine as shown in Figure 32. The lower face of the plate is coated with aluminum, rendering it reflective. Infrared energy is directed from the FTIR source onto the sample deposit. The FTIR beam passes through the deposit and the Germanium to the reflective surface. The laser beam is reflected from this surface back through the sample, and then to the FTIR detector. The result is a dual-pass transmission measurement of the sample. A FTIR spectrum is taken every 2 mm.

To construct the calibration curve we prepared different mixtures of a binary random copolymer and poly(isobutyl acrylate) and dissolved them in THF (~ 1.5 mg/mL). In comparison with the previous approach, the calibration curve was obtained by spraying these mixtures instead of depositing them (Table 12).

**Table 12:** Binary random copolymer and PiBuA mixtures used to build the calibration curve

| Polymer mixtures | P(iBorMA-*stat*-iBorA) copolymer | |
|---|---|---|
| | (mass %) | (mol %) |
| A | 14 | 8.8 |
| B | 30 | 20.3 |
| C | 46 | 33.6 |
| D | 53 | 40.1 |
| E | 61 | 48.2 |
| F | 71 | 59.3 |
| G | 85 | 77.1 |

For the calibration, samples were directly sprayed without separation (no column) in order to obtain the same mixture on the plate. The injection volume was 50 µL. Each point was measured three times to ensure the accuracy of the result. The calibration curve is presented on Figure 33.

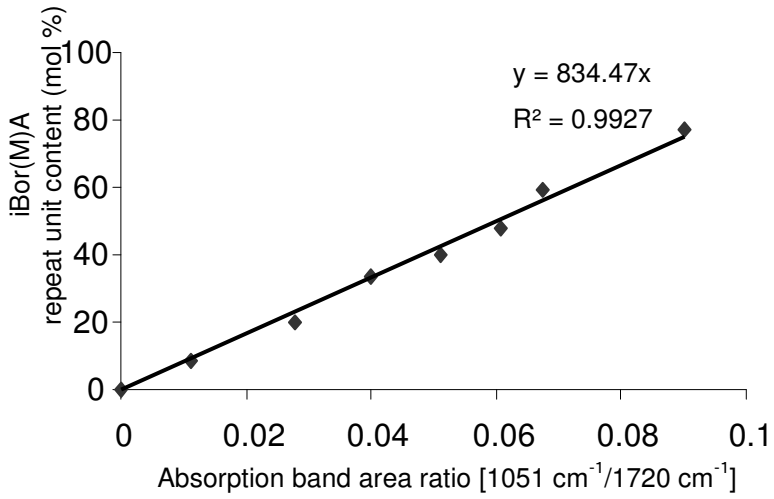


**Figure 33**: FTIR calibration curve: the ratio of adsorption band area at 1051 $cm^{-1}$ (specific for iBorA and iBorMA) divided by the area of 1720 $cm^{-1}$ (total carbonyl equal total concentration)

The calibration gives a linear relation between the absorption band ratio and the molar percentage of isobornyl repeat units in the polymer. The linear fit is relevant if we consider the $R^2$ value: 0.9927. Both slopes for the calibration curves by drop spotting or spraying are very similar, 881.96 and 834.47 respectively. It seems that the deposition method has only a small influence on the FTIR measurement.

After this first result, we investigated sample 1 and its derivative samples 7, 8, 9 and 10 using the complete LC-FTIR system.

### 1.2.3. 2D-LC of the five terpolymer samples

To understand the LC-FTIR results which will be presented, in this part we briefly describe the characteristics of the samples through their 2D-LC analyses. Set-up is slightly different from that previously described (Part IV..1.1.3) but the separation is based on the same principle of coupling gradient HPLC in the first dimension with SEC in the second dimension.

Experimental conditions used for the 2D-LC chromatography are as follows:

| | | |
|---|---|---|
| 1st Dimension: | Column: | PLRP-S (150 x 4.6 mm I.D. 5 µm) |
| | Injected volume: | 50 µL |
| | Flow rate: | 0.143 mL/min |
| | Mobile phase: | ACN → THF gradient |

The gradient profile is described as follows:

| T (min) | 0 | 1 | 50 | 56 | 60 |
|---|---|---|---|---|---|
| % THF | 0 | 30 | 85 | 85 | 0 |

| | | |
|---|---|---|
| 2nd Dimension: | Column: | PL Rapide M (150 x 7.5 mm I.D.) |
| | Loop size: | 100 µL |
| | Flow rate: | 5 mL/min |
| | Mobile phase: | THF |
| | Detection: | ELSD |

The Y-axis of the contour plot corresponds to the first dimension (gradient LC) which separates according to chemical composition. The X-axis corresponds to the SEC measurements and gives the molar mass distribution in polystyrene equivalent of each slice transferred into the 2nd dimension.

A similar distribution is obtained as compared to that presented in Figure 20. In Figure 34 we can see poly(isobutyl acrylate) eluting at 4.4 mL and the two peaks of poly(isobornyl acrylate) and poly(isobornyl methacrylate) between 7.5 and 8.5 mL. It is clearly seen that for poly(isobutyl acrylate) the gradient chromatography elution is not affected by the molar mass distribution. For poly(isobornyl acrylate) and poly(isobornyl methacrylate), however, there is a molar mass effect on elution (curved shape of the spots).

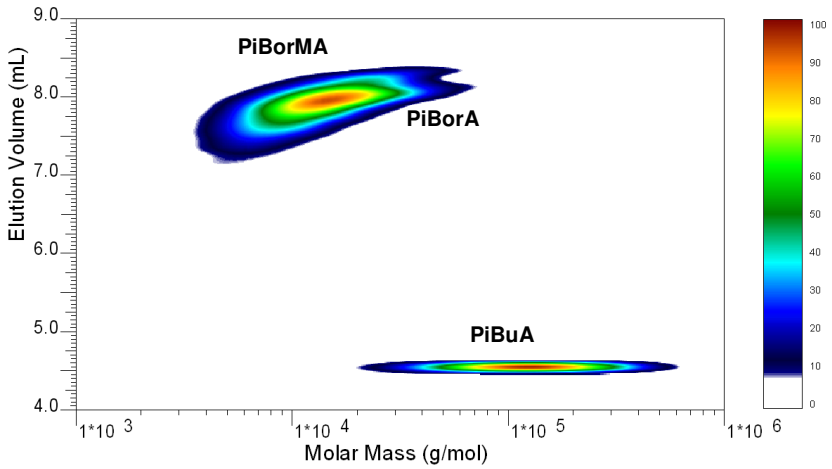


**Figure 34:** 2D-LC contour plot for the mixture of the three homopolymers poly(isobutyl acrylate), poly(isobornyl acrylate) and poly(isobornyl methacrylate); 1st Dimension: step gradient HPLC ACN:THF at 0.143 mL/min on PLRP-S 5 µm; 2nd Dimension: SEC with THF at 5.0 mL/min on PL Rapide M; Calibration: PMMA; Detection: ELSD

Figure 35 to Figure 39 present 2D-LC contour plots of the five copolymers. From these 2D-LC contour plots we can see large differences between the investigated samples in terms of chemical composition distribution, intensities as well as molar mass distribution of present species.

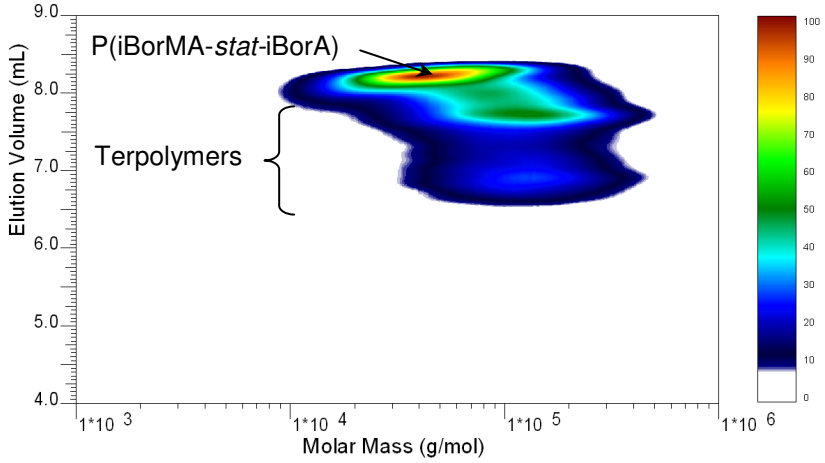


**Figure 35:** 2D-LC contour plot sample 7; conditions as described in Figure 34

For sample 7, the total amount of polymer is detected after 6 mL (Figure 35). This means that all macromolecules are rich in iBor(M)A monomers. The last peak of these three elutes at 8.2 mL and presents the lowest average molar mass: $\overline{M_w}$ ~ 50 000 g/mol. It can be assumed to correspond to residual P(iBorMA-*stat*-iBorA). Two other peaks are eluted before, at 6.5 and 7.5 mL, and have larger average molar masses. They are assumed to be terpolymers with different chemical compositions: the elution volumes are between those of the homopolymers and the increased molar masses indicate the addition of repeat units in comparison with the intermediate copolymer. All peaks are broad in molar mass direction. Such result was also found for sample 1 and was expected for a two step free-radical polymerization.

In the 2D-LC contour plot of sample 1 (see Figure 36) we find indications of homopolymer of isobutyl acrylate. P(iBorMA-*stat*-iBorA) remains the main component of this sample. Terpolymers are eluted in the area between the homopolymer elution volumes. Comparison of sample 1 and 7 shows that an increase of isobutyl acrylate in the polymerization reactor causes iBuA homopolymers to appear. Unexpectedly the terpolymer seems to be more "homogeneous" as only one spot is detected ($V_e$= 7.5 mL) while two spots were detected for sample 7 (see Figure 35). This spot is nevertheless broad along the Y-axis indicating that the ternary copolymers are significantly heterogeneous regarding chemical composition.

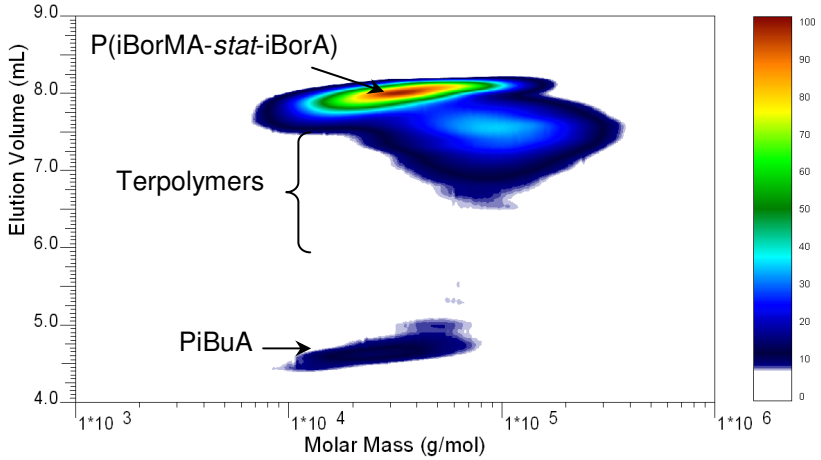


**Figure 36:** 2D-LC contour plot sample 1; conditions as described in Figure 34

The contour plot for sample 8 (Figure 37) shows some similarities with the previous one: presence of residual intermediate copolymer in large proportions, free PiBuA and a terpolymer with the largest average molar mass. However, a major difference to sample 1 is the terpolymer peak eluted at 7.2 mL: it is much more intense (nearly 70 % of the total spots volume) and broader than the previous one. Furthermore, its maximum is shifted in the direction of lower elution volumes and is nearly completely separated from the spot of the intermediate copolymer. It tends to indicate that terpolymer chains in sample 8 contain more iBuA repeat units than those in sample 1. This is of course in agreement with the fact that sample 8 was synthesized with a larger amount of this monomer.

The amount of PiBuA seems also to have increased from the synthesis of sample 1 to that of sample 8. Homopolymerization of this monomer is favored by its higher relative concentration in the reactor with respect to intermediate chains concentration.

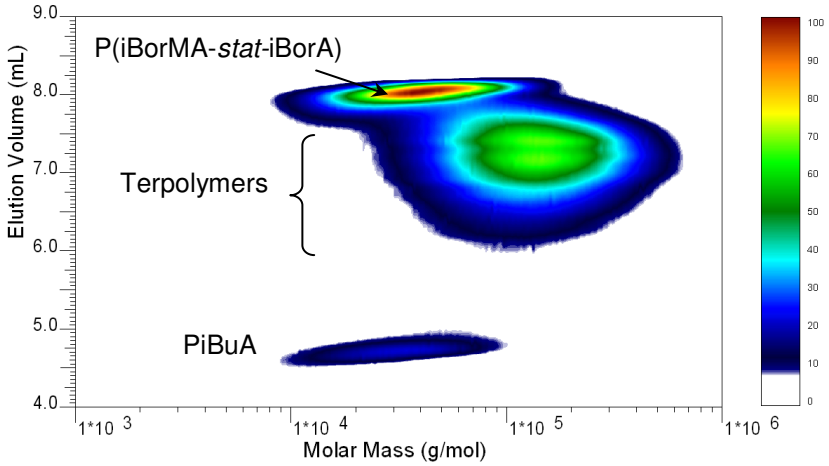


**Figure 37:** 2D-LC contour plot sample 8; conditions as described in Figure 34

Figure 38 presents the 2D-LC plot of sample 9. This 2D-LC plot is very similar to that of sample 8 in terms of spot positions and forms but their relative volumes are considerably different. The spot of the intermediate random copolymer ($V_e$ = 8.2 mL) is still the most intense but it became much narrower. Terpolymer spot ($V_e$ = 7.2 mL) is not as intense as previously for sample 8 but the average molar mass is similar, once more the largest in terms of relative volume with a relative volume of approximately 60 %. PiBuA homopolymer ($V_e$ = 4.5 mL) appears with a very high intensity compared to the contour plots of the preceding samples. It changes from 6 to 22 % relative spot volume from sample 8 to 9. The average molar mass for this peak is $\overline{M_w}$ ~ 50 000 g/mol.

According to these results, it seems that an increase of the proportion of iBuA monomer during the second step of the synthesis leads to an increase of its homopolymerization rather than an increase of its attachment to the preformed random copolymer.

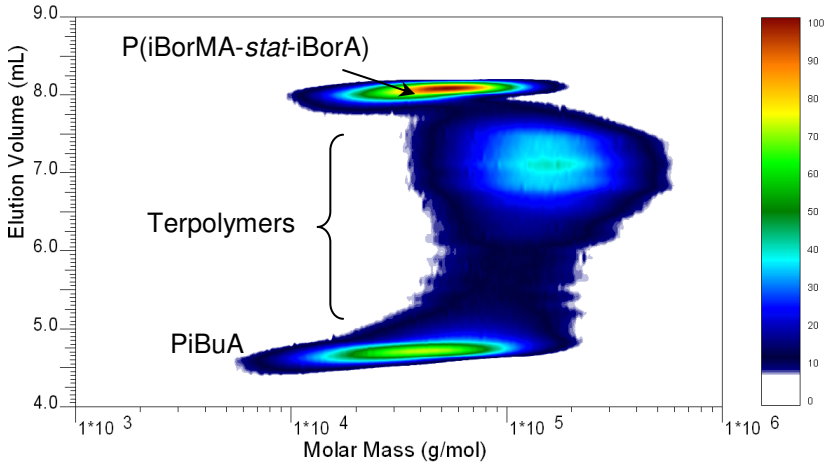


**Figure 38:** 2D-LC contour plot sample 9; conditions as described in Figure 34

The contour plot of sample 10 is presented in Figure 39 and is very different from the previous ones. The spot attributed to P(iBorMA-*stat*-iBorA) ($V_e$ = 8.2 mL) has nearly disappeared. The spot of ternary copolymers previously described in samples 8 and 9 still exists but corresponds to a minority. It seems that the ternary copolymer fractions are yet much richer in iBuA as they were in previous samples (maximum intensity at Ve = 5.2 mL). For sample 10 it is impossible to separate them from PiBuA homopolymers. Terpolymerization seems not to be anymore the principal reaction which is apparently now the isobutyl acrylate homopolymerization. This confirms our previous conclusion that an increase of iBuA in the feed favors homopolymerization during the second step of the synthesis.

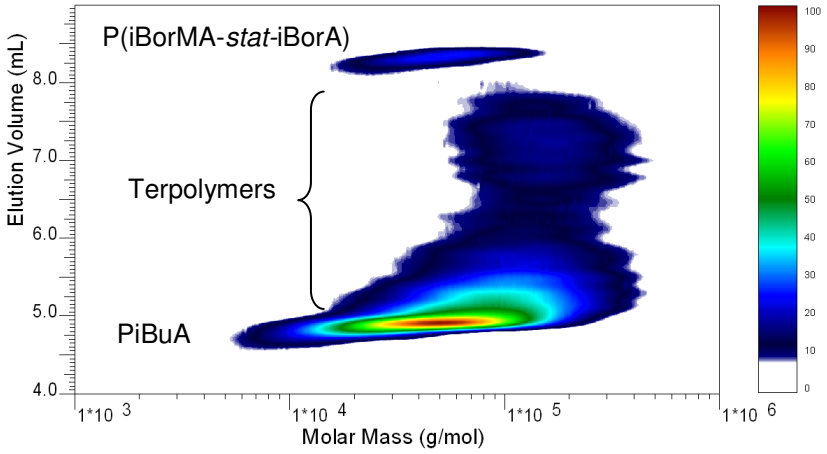


**Figure 39:** 2D-LC contour plot sample 10; conditions as described in Figure 34**.**

As shown by these 2D-LC analyses, all five samples are composed of three different kinds of chains. Their analysis with LC-FTIR will allow us to have more information on the chemical composition of the terpolymers.

### 1.2.4. SEC-FTIR experiments and results

In a first set of experiments the chemical composition of the five copolymers after SEC separation was analyzed. It was performed on a PLgel HTS-C column (150 x 7.5 mm I.D.) with THF as mobile phase at a flow rate of 1 mL/min. Figure 40 shows an overlay of the ELSD chromatogram (red curve), the Gram-Schmidt (blue curve) (reconstruction of the total intensity of the IR spectra to represent the elution profile) and the content of isobornyl monomers determined from the calibration (black points).

The results of the molar mass analysis for the five copolymers are given in Table 13.

**Table 13**: Average molar masses of copolymers obtained after calibration of the system with PMMA standards

| Polymer | $\overline{M_n}$ | $\overline{M_w}$ | PDI |
|---|---|---|---|
| Sample 1 | 16 700 | 89 900 | 5.4 |
| Sample 7 | 19 900 | 117 800 | 5.9 |
| Sample 8 | 21 600 | 138 500 | 6.4 |
| Sample 9 | 22 200 | 158 000 | 7.1 |
| Sample 10 | 22 400 | 158 500 | 7.1 |

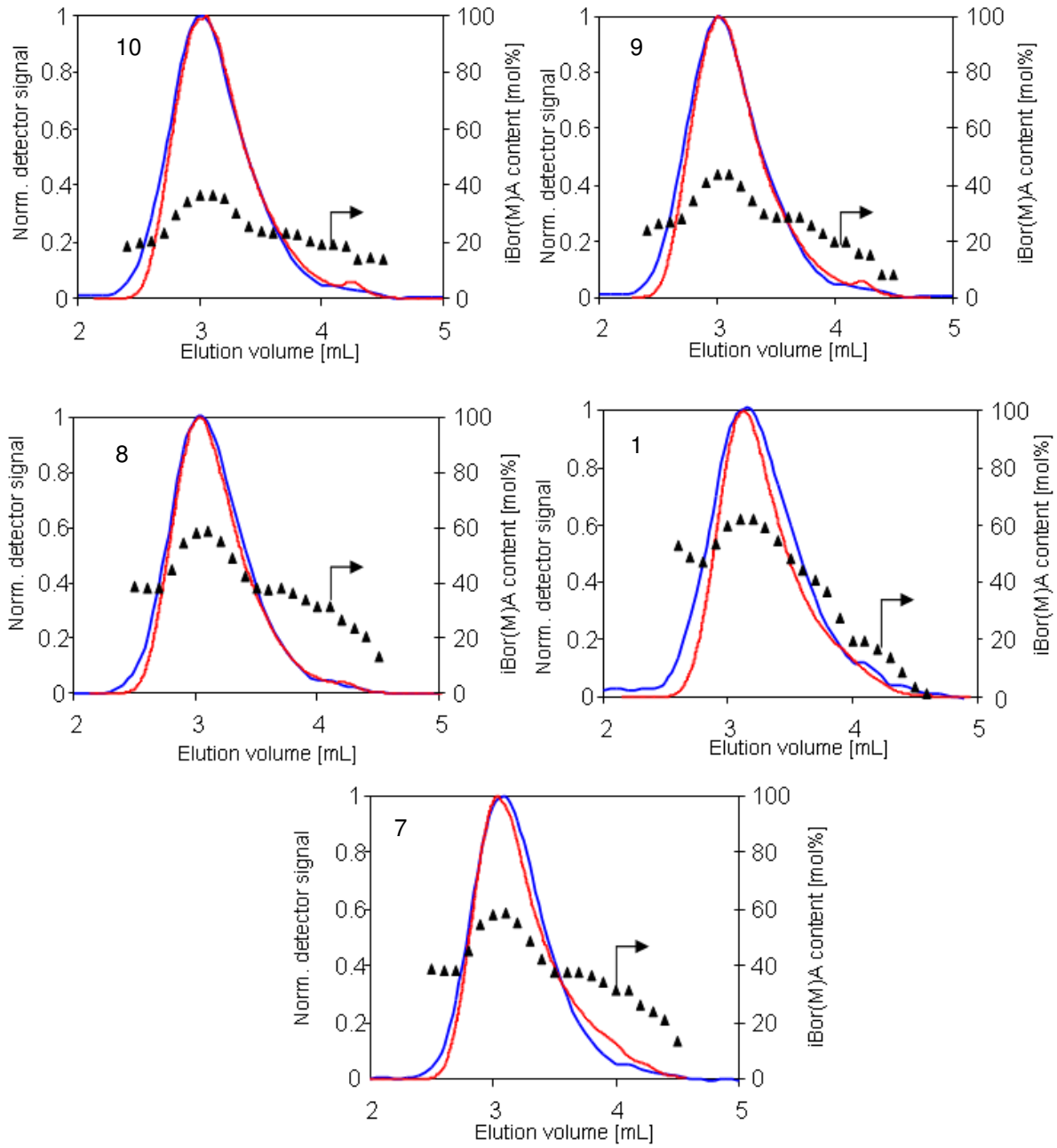


**Figure 40:** Overlay of ELSD signal (red), Gram-Schmidt (blue) and isobornyl repeat unit content (black) of the SEC analyses of five copolymer samples. Column: PLgel HTS-C (150 x 7.5 mm I.D.), Mobile phase: THF at 1 mL/min, Detector: ELSD or FTIR

The SEC traces obtained with the ELSD or with the Gram-Schmidt reconstruction reveal no significant differences between the samples except for sample 1. This sample exhibits a distinctively lower molar mass than the other copolymers. For the four other polymers the average molar masses are quite similar and the polydispersity is large in all cases. As polymerization is composed of two steps, the presence of intermediate binary copolymers and PiBuA is possible which explains why PDI values are so high.

The average values of chemical composition as a function of molar mass are figured by the black points. If all macromolecules would have had the same chemical composition, all points would have formed a horizontal line signifying that the chemical composition is independent of the molar mass. But as can be seen an increase of the isobornyl content occurs in the center of the elution peak followed by a slow decrease towards higher elution volumes. As mentioned above (part IV.1.1.2) binary intermediate copolymer and PiBuA macromolecules are present in the polymer and are most probably responsible for these deviations.

Therefore, the increase of the isobornyl monomers content at approx. 3 mL can most probably be attributed to the presence of P(iBorA-*stat*-iBorMA), which co-elutes with terpolymer. This increase in the center of the elution profile is consistent with the $\overline{M_w}$ value determined for the first block at approx. 90 000 g/mol. This indicates that the larger molecules (the first eluting part) are predominantly ternary copolymers. For the later eluting macromolecules a decrease in the isobornyl monomer content is observed. This could be explained by the presence of PiBuA. This homopolymer fraction assumingly is lower in molar mass because the most part of the third monomer is consumed for the formation of the ternary copolymers. These chains apparently co-elute with P(iBorMA-*stat*-iBorA) and/or with ternary copolymers because there is still some isobornyl content detected. These results confirm the previously reported ones obtained by MALDI-ToF measurements where it was shown that the smallest molecules in the samples are usually small homopolymers of the last added monomers, in the present case PiBuA.

If we now consider the isobornyl content for each sample, we found that, as expected, the values increase with the proportion of isobornyl acrylate and methacrylate used for the synthesis. The isobornyl content at the beginning of the chromatogram is an example of this evolution and we can notice that it increases from sample 10 to sample 7.

A reproducibility test has been performed to verify the validity of the method. Figure 41 shows the overlay of the results obtained by analyzing sample 1 for three times by SEC-FTIR.

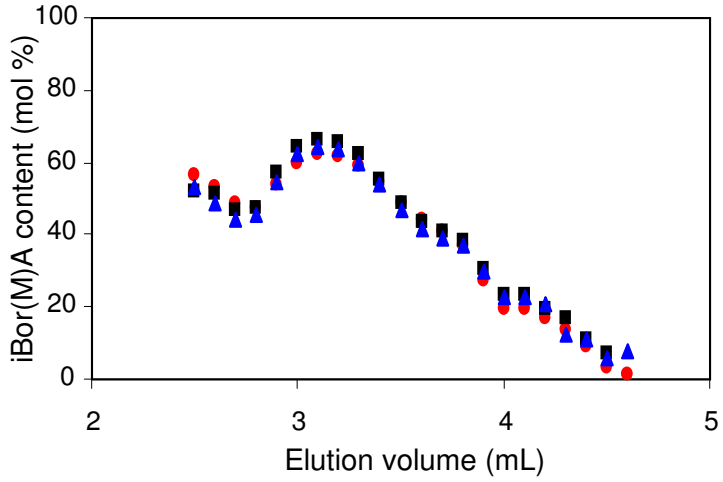


**Figure 41**: Reproducibility measurement of sample 1 by SEC-FTIR; Column: PLgel HTS-C, mobile phase: THF 1 mL/min, LC-Transform gas flow 30 psi, T = 165 °C

The three measurements show a non-significant point to point deviation which indicates that the results presented above are reliable.

### 1.2.5. Gradient HPLC-FTIR experiments and results

With these encouraging results, the technique was used to analyze the five samples by gradient HPLC as a next experimental step. The separation was performed on a PLRP-S 8 µm (150 x 4.6 mm I.D.) column. A first set of experiments was performed with a linear gradient from 100 % of acetonitrile to 100 % of THF in 5 min and a flow rate of 1 mL/min. A second set of analyses was conducted using a step gradient to improve the separation of the polymers. Optimum working conditions for the LC-Transform were found to be exactly the same as described before which could have been expected as the boiling point of acetonitrile is close to that of THF.

***a) Linear gradient HPLC-FTIR***

Figure 42 presents the chromatograms of the three homopolymers synthesized with the monomers constituting sample 1 analyzed with the linear gradient. The more polar PiBuA elutes first (red 5.6 mL) followed by the PiBorA (blue 7.4 mL) and finally the less polar PiBorMA (green 7.6 mL). As discussed in part IV..1.1.2, baseline separation of PiBorMA and PiBorA is not necessary for sample 1 as these monomers are copolymerized in equal proportions in a first step to produce a random copolymer.

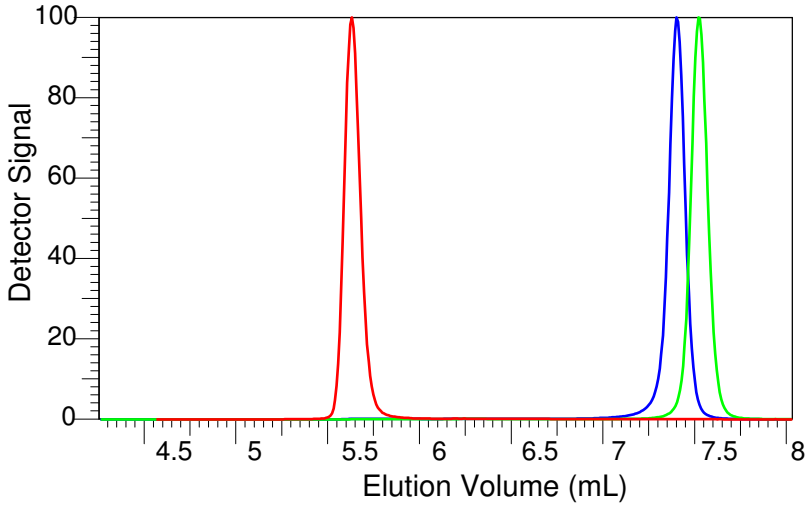


**Figure 42**: Chromatogram overlay of poly(isobutyl acrylate) (red), poly(isobornyl acrylate) (blue) and poly(isobornyl methacrylate) (green), Column: PLRP-S (150 x 4.6 mm I.D. 8 µm), Mobile Phase: linear gradient ACN:THF in 5min, flow rate: 1 mL/min, Detector: ELSD

Figure 43 shows an overlay of the ELSD chromatograms (red curve), the Gram-Schmidt (blue curve) and the isobornyl monomers amounts (black points) determined from the calibration for the five copolymer samples.

The copolymers (binary and ternary) elute as expected between the homopolymers and there is a profile similarity between the ELSD and the Gram-Schmidt traces. However, a difference can be seen if we look at the terpolymer region (5.5 to 7.5 mL) more carefully. Indeed, the intensity of this region detected by ELSD is always lower than for the Gram-Schmidt reconstruction. It is well known that the ELSD detection depends on the polymer structure. Here, it is obvious that the ELSD response is stronger for the binary copolymer than for the terpolymers. It appears that the proportion of ternary copolymers in the samples is much higher than the proportion which can be determined via the integration of the ELSD traces (relative areas). This refers to the general comment we formulated in part IV.1.1.3 about the dependence of ELSD sensitivity on the nature of the analyte (structure, size and architecture). Another quantification method of the different polymer populations will be presented in part IV.1.3.

Regarding the chemical composition analysis (isobornyl content), the profiles show a large and continuous variation of the chemical composition along the elution profile. The chemical composition reading never starts at 0 % of isobornyl monomer, which tends to indicate that either there is no isobutyl acrylate homopolymer or that the small amount of this homopolymer is not completely separated from the ternary copolymers rich in isobutyl acrylate. The second hypothesis is more likely to be true as iBuA homopolymers have already

been isolated in previous analyses. Nevertheless the isobornyl content at the beginning of the chromatogram decreases from sample 7 to 10 which is consistent with the fact that the isobutyl acrylate content increases from polymer 7 to 10.

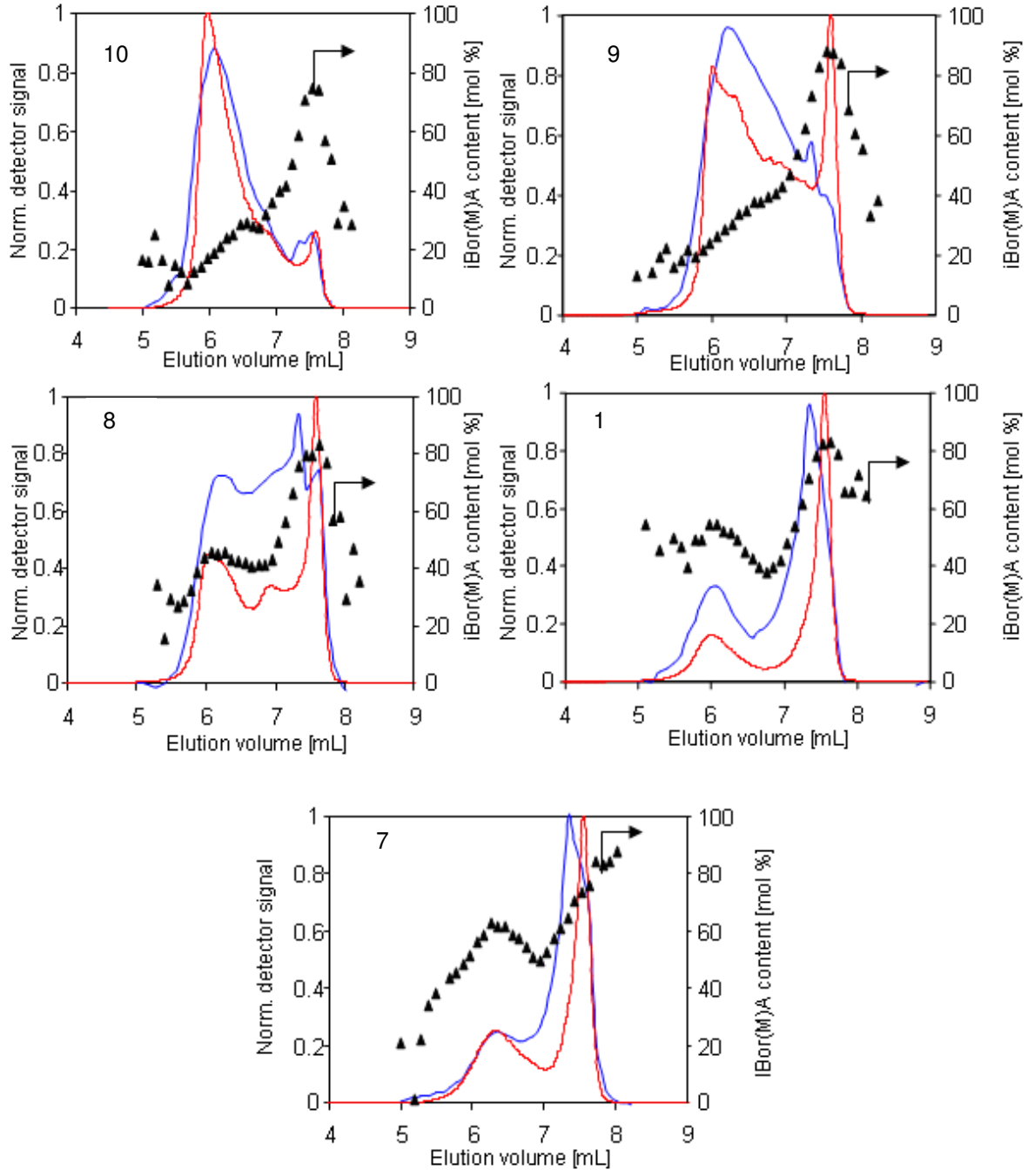


**Figure 43**: Overlay of ELSD signal (red), Gram-Schmidt (blue) and isobornyl monomer content (black points) of the gradient HPLC analyses of five copolymer samples. Column: PLRP-S (150 x 4.6 mm I.D. 8 µm), Mobile phase: 5 min linear gradient acetonitrile to THF at 1 mL/min, Detector: ELSD or FTIR

The peak maximum for the ternary copolymers in the Gram-Schmidt moves from sample 10 to 7 towards the larger elution volumes (5.8 to 6.2 mL) whereas its height decreases (from 1 to 0.2 of the normalized detector scale): the total amount of ternary copolymer is the lowest for sample 7 (smaller peak) and the quantity of isobutyl acrylate attached is also the lowest for sample 7 (shift to the right). This is consistent with the fact that this polymer is made with the lowest amount of isobutyl acrylate.

As expected, the isobornyl content increases with elution volume but in different ways for different samples. For the samples 9 and 10, the increase is relatively linear till 7 mL and then increases dramatically when the binary copolymer peak appears. The isobornyl content does not reach 100 mol % at the end of the chromatogram, as what would be expected, but reaches only 80 or 85 mol %. This is most probably due to an overlapping of the terpolymer peak with the binary random copolymer peak as these two peaks are not completely separated. It has also to be considered that the polymers partially remix when they are sprayed on the Germanium plate.

For polymer 8, a steady state (~ 45-50 mol % of isobornyl monomers) can be seen between 6 and 7 mL after the first increase of the iBor(M)A content and before the peak of P(iBorMA-*stat*-iBorA). This composition corresponds to the expected composition of the ternary copolymers. Moreover, for this sample, a peak appears in the Gram-Schmidt at 7.5 mL which is not detected by the ELSD. The corresponding isobornyl content for this peak is roughly 70 mol %. This peak is also present in samples 1 and 7 with the same chemical composition but with a growing relative intensity. This peak was also detected in samples 9 and 10 but with a much smaller peak area.

For sample 1 and 7, a decrease in the isobornyl monomer content is detected at around 7 mL. This drop in the isobornyl content was unlikely to appear as the separation occurs in the direction of increasing polarity; a decrease of the isobornyl content means an increase of more polar isobutyl acrylate content in the macromolecules which is very improbable. An explanation for this phenomenon is probably that the polymer deposit on the Germanium plate is not thick enough to give a sufficient signal for quantification. That is in agreement with the drop in the Gram-Schmidt construction (blue curve) at approximately 7 mL where fewer polymers are sprayed. For these two samples the isobornyl monomer content does not reach the 100 mol %; it remains between 80 and 90 mol %. Again overlapping of the ternary copolymer with few attached units of isobutyl acrylate and binary random copolymer causes this deviation.

A last and general comment must be made: it appears that the isobornyl monomer content (i.e. the chemical composition) is not identical at a given elution volume from one sample to the other. One would have anticipated that macromolecules with a specific chemical composition will always elute at the same volume. According to the results, there is a large difference of chemical composition for similar elution volumes, e.g. for an elution volume of 6 mL the composition changes from more than 50 mol % for sample 7 to less than 20 mol % for sample 10. This is most probably due to the different amounts of each type of macromolecules present in the analyzed samples which overlaps on the Germanium plate. Because monomer feeds are different, the final products do not contain the same amount of each type of macromolecules: for example sample 10 contains much more iBuA homopolymer than sample 7 and inversely sample 7 is composed of a larger amount of binary random copolymer than sample 10. At the same elution volume it is likely that deposited terpolymers from both samples have the same chemical composition but an overlap with other species (PiBuA for sample 10 or P(iBorMA-*stat*-iBorA) for sample 7) most probably occurs. The chemical composition determined by FTIR is an average value of different deposited polymer species. Thus it is possible to obtain different values of chemical composition for an identical elution volume.

The molar mass effect observed during gradient HPLC separation should also not be neglected and could be also a factor influencing the overlapping of inhomogeneous species.

***b) Step gradient HPLC-FTIR***

Since the gradient slope for the linear gradient was very steep, i.e. an increase of 20 % of THF in mobile phase per minute (i.e. the mobile phase strength increases too fast), in a modified experiment a step gradient was used to obtain a better separation according to chemical composition where the increase of the THF content in the mobile phase was slower. This attempt was made in order to define more precisely the chemical composition especially at the maximum of the terpolymer peak.

The gradient for the next set of experiments is described in Table 14 .The slope in elution range of the terpolymer was 11 % THF/min.

**Table 14:** Description of mobile phase composition for the step gradient

| Time (min) | THF-proportion in mobile phase (%) |
|---|---|
| 0 | 0 |
| 1 | 30 |
| 5 | 85 |
| 6 → 12 | 0 |

Figure 44 shows an overlay of the ELSD chromatograms (red), the Gram-Schmidt (blue) and the isobornyl content (black) for the five ternary copolymers. The separation was obtained via HPLC using the step gradient described in Table 14.

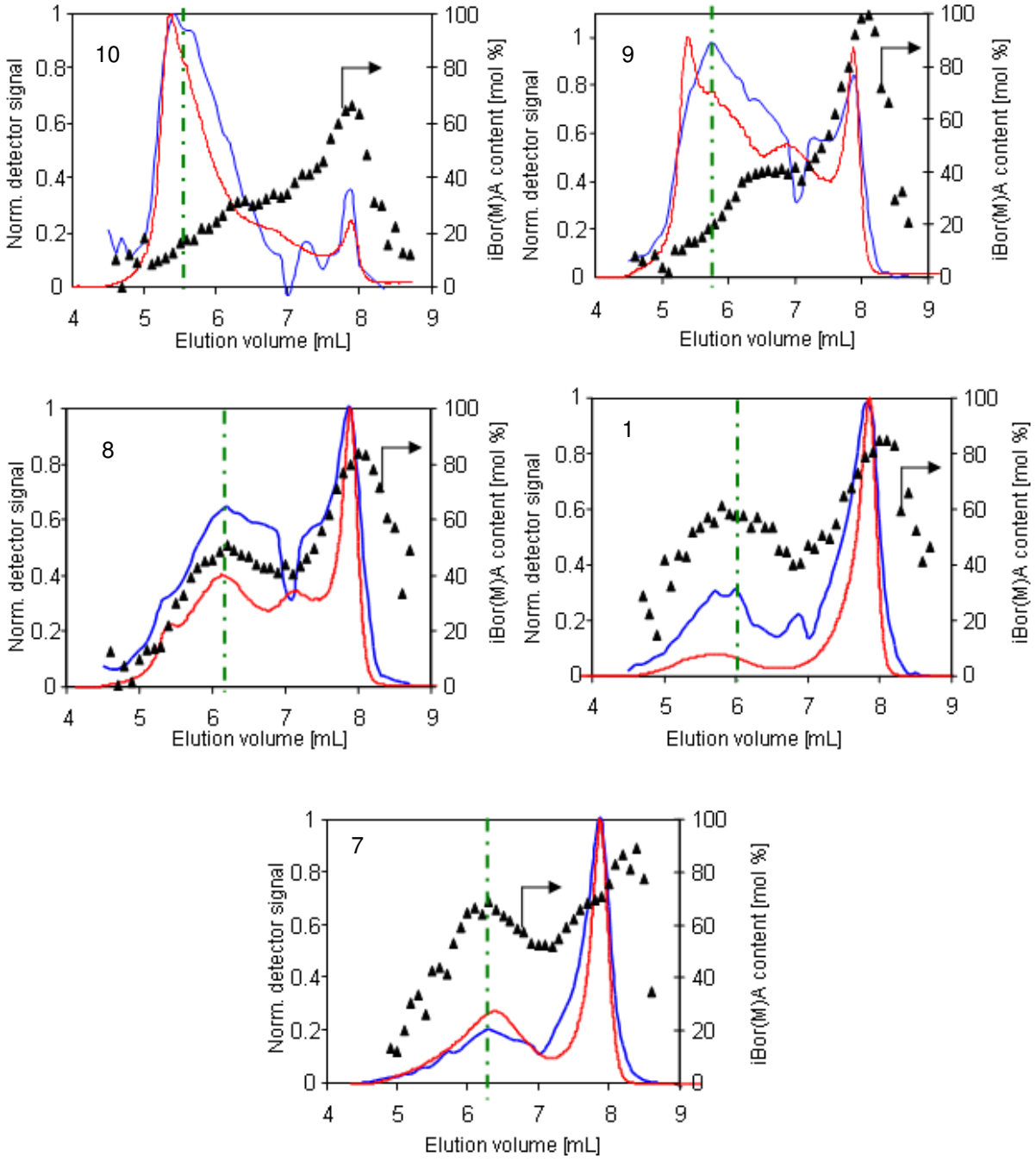


**Figure 44:** Overlay of ELSD signal (red), Gram-Schmidt (blue) and isobornyl monomer content (black) of the step gradient HPLC analyses of five copolymer samples. Column: PLRP-S (150 x 4.6 mm I.D. 8 µm), Mobile phase: step gradient (as described in Table 14) acetonitrile to THF at 1 mL/min, Detector: ELSD or FTIR. The green line indicates the terpolymer peak maximum taken for the quantification

The elution volume range is larger than with the linear gradient. Different from the previous results the isobornyl monomer content starts at 0 mol % which means that the isobutyl acrylate homopolymers are separated from the terpolymers. They eluted between 4.7 and 5.0 mL. From 5.0 to 7.5 mL the elution of the ternary copolymer fractions takes place and finally the binary copolymer peak has its maximum at 8.0 mL. The isobornyl content only reaches 100 mol % for sample 9. This is most probably due to the fact that in this case the amount of ternary copolymer with few isobutyl units is small enough to avoid the overlap with the pure binary copolymer and sufficient amounts of binary copolymer are sprayed to form a readily analyzable film. Terpolymers of sample 9 are mainly rich in iBuA. For sample 10, both ELSD and Gram-Schmidt reconstruction show a small peak for the binary copolymer. In this case the amount of these chains is relatively small and the majority of the macromolecules are rich in iBuA units. For samples 1, 7 and 8 the amount of terpolymers containing few units of iBuA is much higher and they most probably elute with binary copolymers which artificially decreases the isobornyl monomer content maximum.

With these new results the chemical composition at the maximum of the ternary copolymer peak in the Gram-Schmidt curve (blue) has been determined. The quantification points are indicated by green lines in Figure 44. The results of this quantification are given in Table 15.

**Table 15:** Comparison of the expected and the determined isobornyl contents in the five polymer samples, analysis by step gradient HPLC-FTIR

| Sample | Isobornyl monomer content from $^{1}$H-NMR (mol %) | Isobornyl monomer content from FTIR (mol %) |
|---|---|---|
| Sample 1 | 58 | 57 |
| Sample 7 | 71 | 67 |
| Sample 8 | 46 | 50 |
| Sample 9 | 34 | 20 |
| Sample 10 | 26 | 18 |

According to the results of Table 15 there is a very good agreement between the expected and the determined values for polymers 1, 7 and 8. However for polymer 9 and 10, a large difference appears as we detect only half of the isobornyl monomer expected. Two reasons could be mentioned for this deviation. The first one would be the presence of isobutyl acrylate homopolymer in a large quantity which would overlap chromatographically with the terpolymers. This is indeed only possible for polymers 9 and 10 which are made with the largest amount of isobutyl acrylate.

The second reason is based on the quantifying technique itself. The relative error in CCD determination increases with decreasing iBor(M)A content as quantification is based on

intensity of iBor(M)A absorption band: i.e. the lower the amount of iBor(M)A, the smaller the 1051 $cm^{-1}$ band area and thus the larger the error in band ratio calculation.

For samples 1, 7 and 8, it has to be kept in mind that even if the quantification gives accurate results at the peak maximum the chemical composition distribution remains very broad for all samples and the proportion of polymers with the expected chemical composition is rather small.

Finally, a reproducibility test has also been performed for the gradient HPLC-FTIR. Figure 45 shows an overlay of three measurements made for sample 1 with the linear gradient. The polymer was dissolved in THF at the concentration of 1.5 mg/mL.

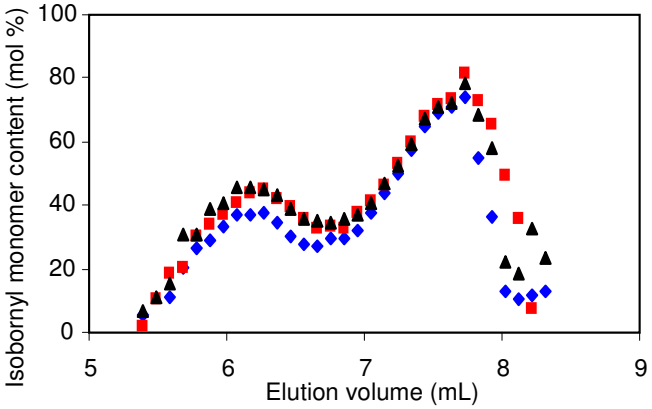


**Figure 45**: Reproducibility measurement of sample 1 by gradient HPLC-FTIR; Column: PLRP-S (150 x 4.6 mm I.D. 8 µm), mobile phase: linear gradient ACN to THF in 5 min, 1 mL/min, LC-Transform gas flow 30 psi, T = 165 °C

The reproducibility of the measurements was very good. An error of approximately 5 % was observed between different measurements.

## 1.3. Intermediate binary random copolymer quantification

### 1.3.1. Development of a normal phase separation to isolate P(iBorA-*stat*-iBorMA)

It has been shown previously, that it was not possible to isolate and precisely quantify the amount of binary random copolymer. As the ternary copolymer has a broad CCD, it was not possible to completely separate the binary from the ternary copolymer even with a reversed phase gradient HPLC. Indeed, it is not always possible to discriminate polymers with slightly different chemical compositions, in particular for high molar masses. In the present case, the

molar masses are close to 100 000 g/mol and the differences in polarity brought about by addition of few repeat units of iBuA is not sufficient to separate these terpolymers from binary copolymers of iBorA and iBorMA. Further, it can be assumed that a simple polarity (i.e. phase) inversion would lead to a similar overlap of the binary and ternary copolymers.
Thus, to achieve baseline separation of the sample components, LC conditions must be found in which one kind of molecules is excluded whereas the other kind is adsorbed. For the present samples, the binary copolymer has to be excluded and the only adsorbing part should be the iBuA repeat units. In the other case, if iBuA were excluded and iBor(M)A adsorbed, both binary and ternary copolymer fractions would exhibit adsorption due to the presence of iBor(M)A repeat units in both species. In a normal phase system assumingly the less polar P(iBorA-*stat*-iBorMA) elutes first in the exclusion mode, while the more polar part (PiBuA) will be adsorbed. Only after increasing the mobile phase strength the ternary copolymer fractions and PiBuA would elute. This corresponds to an inversion of the elution order of the molecules in comparison with previous results.

To enhance the adsorption of the iBuA repeat units in comparison to that of iBor(M)A, a moderately polar stationary phase had to be used. Indeed, a too polar stationary phase would not be selective for our samples as they all exhibit a low polarity. Adsorption of the samples will be possible using a strongly non-polar solvent in initial conditions, such as toluene or cyclohexane. But elution of all kinds of chains will occur with a very small amount of eluting solvent in the mobile phase without any selectivity.
For these reasons, bare silica, alcohol (diol) or amino functionalized columns were not best suited. Two kinds of bonded silica stationary phases corresponding to our criteria were tested: a cyano (CN) functionalized (Luna® CN) and a Synergi® Polar RP (ether-linked phenyl groups with polar end-capping of the silica base). Both stationary phases were only slightly polar and supposed to fulfill our requirements.

The second part of the method development was to find a suitable mobile phase. To achieve a selective exclusion of the less polar binary copolymer, the mobile phase had to be a good solvent for PiBor(M)A in order to avoid precipitation/redissolution. It also had to be as non-polar as possible to preferably solubilize P(iBorA-*stat*-iBorMA) in comparison to PiBuA. Four solvents were tested which are known to be good solvents for the samples: toluene, chloroform, THF and ethyl acetate. They are named in order of increasing polarity. Each solvent was tested with both stationary phases to observe the chromatographic behavior of the

binary random copolymer and PiBuA. For each experiment, the same solvent was used to dissolve the polymer and condition the column.

Chloroform and THF were too good solvents for both kinds of macromolecules. They led to exclusion of the polymers from the stationary phase whichever column was used. When testing the stationary phases, the Synergy® polar RP column (250 x 4.6 mm I.D., 4 µm) showed to be too non-polar to produce a complete exclusion of the binary copolymer using ethyl acetate or toluene. In such conditions, the polymer was partially excluded. The retained part gave two peaks as it was eluted in two different modes.

Finally, we focused our efforts on the CN phase (Luna® CN 30 x 4.6 mm I.D. 3 µm). Such stationary phase can be used in normal or reversed phase chromatography as it exhibits a medium polarity. Since the stationary phase surface is end-capped, residual silanol groups do not play a role. Using ethyl acetate as conditioning solvent led to the exclusion of the binary random copolymer as well as PiBuA. As this solvent is a good solvent for the polymers but also relatively polar, it impeded polar interactions between the cyano groups and the iBuA units.

The expected separation was achieved with toluene as the conditioning solvent for the cyano stationary phase. This very non-polar solvent tended to enhance the interaction between the iBuA units and the stationary phase whereas the less polar iBor(M)A units with larger aliphatic ester groups remained in the mobile phase. This resulted in an exclusion mode for the binary random copolymer and an adsorption mode for PiBuA and more particularly for the ternary copolymer. A more polar but still good solvent had to be used to elute the adsorbed molecules. We used THF to ensure elution of all chains. Surprisingly, the same result could be achieved by using acetonitrile or acetone which are known to be poor solvents for the polymers. A very small amount (e.g. 4 % of THF) of one of these solvents was required to induce desorption. This confirms that separation was only governed by an adsorption/desorption mechanism. Apparently no precipitation/redissolution occurred.

Another parameter had to be considered: the temperature of the column. It has to be as low as possible to enhance adsorption of the iBuA repeat units at the stationary phase. Adsorption is governed by enthalpic interactions. When adsorption occurs, enthalpic interactions between polymers and stationary phase are larger than entropic variations and for this reason $K_d$ and $K_{LAC}$ values are considered to be equivalent ( $K_d \approx K_{LAC}$ ). A decreasing temperature would

increase the gain of enthalpy and hence favor adsorption. The usual temperature for HPLC is 25 °C. In present case the temperature was set at 15 °C.

Figure 46 shows overlay chromatograms of P(iBorA-*stat*-iBorMA) (red), isobutyl acrylate homopolymer (blue) and sample 1 (green) separated under normal phase conditions.

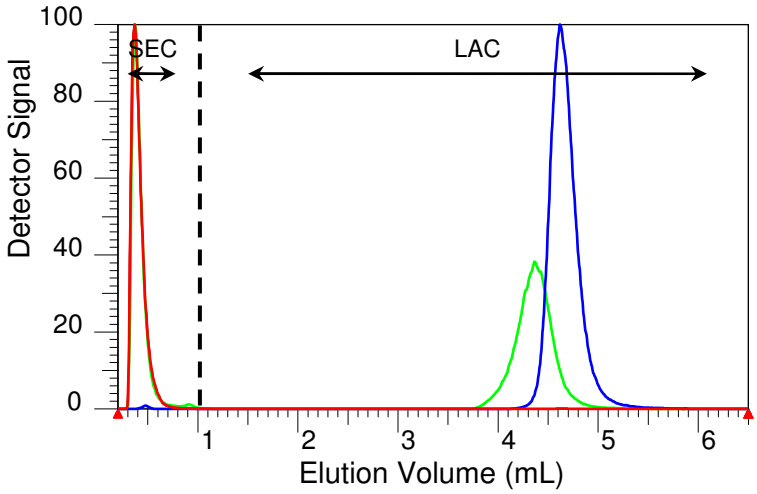


**Figure 46**: Overlay chromatogram of P(iBorA-*stat*-iBorMA) (red), poly(isobutyl acrylate) (blue) and sample 1 (green). Column: Luna® CN (30 x 4.6 mm I.D.), Mobile phase: toluene-THF linear gradient from 0 to 4 % of THF in 8 min at 0.5 mL/min, temperature: 15 °C; detection ELSD

As shown in Figure 46, the binary copolymer (red) and PiBuA (blue) are baseline separated. The first one is eluted in the exclusion mode (SEC) and a similar peak appears when analyzing sample 1 (green) which perfectly overlaps. The second peak of sample 1 (elution volume 4.4 mL) can be attributed to the terpolymer fraction as it elutes before PiBuA. Terpolymers contain iBorA and iBorMA repeat units and for this reason are less polar than PiBuA. This order of elution confirms the normal phase mechanism of the separation. This second peak overlaps with the PiBuA peak. A baseline separation cannot be achieved between ternary copolymers and PiBuA on the normal phase for the same reasons that the terpolymer and the binary copolymer could not be separated in reversed phase chromatography: the smaller molecules of polar PiBuA overlay with the largest terpolymer chains containing a large amount of iBuA. It has to be reminded that peak areas in Figure 46 are normalized. Sample 1 contains between 3 and 5 % of PiBuA (values determined in reverse phase gradient HPLC after calibrating the ELSD detector, results not presented in this document). In fact, these homopolymers represent only the tail of the terpolymer peak in the chromatogram of sample 1.

### 1.3.2. ELSD calibration for P(iBorMA-*stat*-iBorA)

For the quantitative determination of the amount of random copolymer in the samples the ELSD detector was calibrated with standards of P(iBorA-*stat*-iBorMA). Four solutions of P(iBorMA-*stat*-iBorA) were prepared at different concentrations in toluene: 0.48, 0.82, 1.23 and 2.05 mg/mL. Four injection volumes (5, 10, 15 and 20 µL for the three first solutions and 5, 7, 10 and 12 µL for the last one) were defined for each solution to obtain a calibration curve covering a large mass range of injected polymer. Each injected mass was measured three times. Figure 47 shows the calibration curve obtained for the P(iBorMA-*stat*-iBorA) solutions with the ELSD. The covered mass range is from 0 to 25 µg of injected polymer.

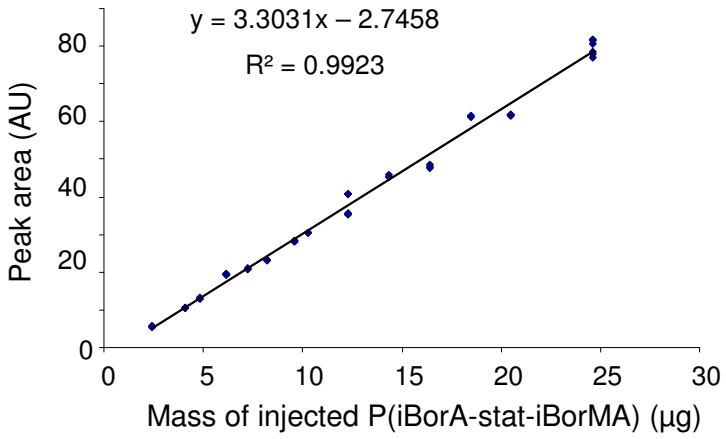


**Figure 47:** Calibration curve of the ELSD for P(iBorMA-*stat*-iBorA). The curve represents the mass of polymer injected versus peak area detected. Column: Luna® CN 30 x 4.6 mm I.D., Mobile phase: toluene-THF linear gradient from 0 to 4 % of THF in 8 min at 0.5 mL/min, Temperature: 15 °C. Detector: PL-ELSD 1000 (Neb T 75 °C, Evap T 110 °C, gas flow 1 L/min)

The linear regression seems to be adequate to fit the data points ($R^2$ = 0.9925). A good repeatability is also found for the three identical measurements. This calibration was then tested by doing a repeatability essay by injecting different volumes of various concentrations of sample 1 solutions. Then, the calibration allowed us determining the residual amount of P(iBorMA-*stat*-iBorA) in the five polymer samples described in Part IV..1.2.

***a) Validation of the calibration curve***

We first analyzed three solutions (0.94, 1.47, 2.05 g/L) of sample 1 dissolved in toluene with three different injection volumes (10, 15 and 20 µL) to test the repeatability of P(iBorMA-*stat*-iBorA) analysis when analysis parameters vary. Each injection was repeated three times. The results are summarized in Table 16.

The results presented in Table 16 show a good repeatability with very low deviation for the quantification of the mass proportion of binary copolymer in sample 1 even when experimental parameters were modified. The determined average mass content is close to 43 %. As previously mentioned, the amount of PiBuA was always found between 3 and 5 % in reversed phase gradient HPLC experiments. This means that at least 50 mass % of sample 1 are composed of terpolymer molecules. It has to be reminded that the terpolymer is very polydisperse in molar mass and in chemical composition, i.e. the addition of iBuA is not homogeneous on the already very complex intermediate P(iBorMA-*stat*-iBorA).

**Table 16:** Results of the repeatability study of the binary random copolymer quantification for sample 1

| Sample 1 concentration (g/L) | 0.94 | | | 1.47 | | | 2.11 | | |
|---|---|---|---|---|---|---|---|---|---|
| Injected volume (µL) | 10 | 15 | 20 | 10 | 15 | 20 | 10 | 15 | 20 |
| Polymer Mass injected (µg) | 9.4 | 14.1 | 18.8 | 14.7 | 22.1 | 29.4 | 21.1 | 31.7 | 42.2 |
| Average P(iBorMA-*stat*-iBorA) mass (% of mass injected) on three injections | 41.7 | 43.1 | 43.4 | 43.0 | 44.8 | 44.7 | 42.5 | 43.3 | 42.7 |
| Standard deviation of measurements | 0.19 | 0.14 | 0.09 | 0.51 | 0.08 | 0.16 | 0.15 | 0.14 | 0.14 |
| Average result for all measurements (mass %) | **43.2** | | | | | | | | |

The value of 43 mass % of binary copolymer in the polymers is much lower than the value found when quantifying in the reversed phase separation (between 60 and 75 %). In this case quantification was done via peak area percentage (which relies on peak integration) and without calibration of the detector. The large deviation which appears here can be the result of two effects. Firstly, the ELSD is a very useful universal detector but one of its major drawbacks is its response dependence on many factors such as polymer structure, polymer size and mobile phase composition. This means that for the same injected mass the response will be in no doubt different for iBuA and for the binary copolymer. Therefore, the peak area percentage is a quantification method with a low reliability. The second point is that with reversed phase chromatography a complete separation of terpolymer and binary copolymer was not achieved. In this case peak integration was always very inaccurate which could lead to a large error in the quantification results. These two reasons and the good quantification repeatability shown in the present part let us prefer the normal phase system to quantify the P(iBorMA-*stat*-iBorA) polymer.

***b) Determination of the amount of iBor(M)A repeat units in samples 1 and 7 to 10***

We finally quantified the amount of P(iBorMA-*stat*-iBorA) present in the five copolymers already analyzed in Part IV.1.2. These copolymers were made with the same monomers as sample 1 but with different percentages. We determined the percentage of iBor(M)A repeat units present in the terpolymers by combining the present LC quantification results giving residual binary copolymer with that obtained by $^{1}$H-NMR giving the total amount of iBor(M)A in the samples. To properly calculate these values we converted all percentages values in mass percentages.

Table 17 gives the chemical composition determined by 1H-NMR and the mass percentage of intermediate binary copolymer found for each of the five samples. From these values we calculated the percentage of iBor(M)A comprised in the terpolymers. Values are given in last column of Table 17.

**Table 17:** Estimated values of the amount of iBor(M)A present in terpolymers from 1H-NMR measurement and mass percentages of intermediate random copolymer determined by LC

| Sample | Total iBor(M)A content from $^{1}$H-NMR (mol %) | Total iBor(M)A content (mass %) | P(iBorMA-*stat*-iBorA) (mass %) from HPLC | **Amount of iBor(M)A in terpolymers (mass %)** |
|---|---|---|---|---|
| Sample 1 | 58 | 70 | 43 | **38** |
| Sample 7 | 71 | 80 | 47 | **42** |
| Sample 8 | 46 | 59 | 32 | **45** |
| Sample 9 | 34 | 47 | 21 | **55** |
| Sample 10 | 26 | 37 | 18 | **51** |

The percentages of iBor(M)A in the terpolymer tend to increase with increase of iBuA content in the samples: the larger the amount of third monomer added in the second step, the higher the percentage of intermediate binary random copolymers which become terpolymers. Nevertheless the percentage of iBor(M)A engaged in the terpolymers is hardly larger than 50 % for samples 9 and 10 and it is close to 40 % for samples 1 and 7.

The present results tend to indicate that the attachment reaction of iBuA onto the binary random copolymer is not a favored reaction in comparison to the homopolymerization of iBuA. Indeed, considering samples 9 and 10, produced with a large excess of iBuA over iBor(M)A monomers, a large amount of iBuA homopolymers is detected while unmodified P(iBorMA-*stat*-iBorA) is still present. If the terpolymerization reaction would have occurred preferentially then no intermediate copolymer should have been detected at the end of the synthesis.

In the particular case of sample 8, which approximately contains as much iBuA as iBor(M)A, only a small amount of PiBuA is detected but more than half of the intermediate chains remain unmodified at the end of the polymerization. This suggests, at least for this sample, that terpolymer molecules contain more iBuA repeat units than iBor(M)A.

Considering the monomer molar ratio (1:1 iBor(M)A-iBuA) in terpolymer of sample 8, two hypotheses for iBuA organization in terpolymers can be given: either iBuA repeat units form large "blocks" which are attached to P(iBorMA-*stat*-iBorA) forming segmented copolymers or several small "blocks" are attached onto one binary intermediate chain.

## 1.4. Conclusions

As a conclusion of the analyses performed on the five terpolymer samples, all the information collected with the different analytical techniques were summarized in Table 18.

The SEC measurements did not show any significant differences between the five samples. Nevertheless the amounts of each monomer (iBorA, iBorMA and iBuA) were different in the five samples. This was confirmed by the total chemical composition determination by $^{1}$H-NMR. Thus gradient HPLC and of course 2D-LC (coupling gradient HPLC and SEC) gave different chromatograms for the five samples. From these separation results, the amounts and the weight average molar masses of the species present in the total samples were determined. The five copolymers were all composed of three different species: binary intermediate copolymers (P(iBorMA-*stat*-iBorA)), homopolymer of iBuA (PiBuA) and ternary copolymers. The amounts and average molar masses of these species vary according to the quantity of each monomer used for the synthesis as shown in Table 18. For example the amount of PiBuA dramatically increased when the amount of iBuA introduced in the reactor increases (from sample 7 to sample 10). In the same time, the amount of P(iBorMA-*stat*-iBorA) decreases and that of ternary copolymers remain constant between 60 and 70 %.

**Table 18:** Summary of the information collected on the five terpolymer samples.

| | Sample 7 | Sample 1 | Sample 8 | Sample 9 | Sample 10 |
|---|---|---|---|---|---|
| iBor(M)A content in total sample (%) from $^1$H-NMR | 71 | 58 | 46 | 34 | 26 |
| $\overline{M_n}$ (g/mol) from SEC | 19 900 | 16 700 | 21 600 | 22 200 | 22 400 |
| $\overline{M_w}$ (g/mol) from SEC | 117 800 | 89 900 | 138 500 | 158 000 | 158 500 |
| PDI | 5.9 | 5.4 | 6.4 | 7.1 | 7.1 |
| PiBuA relative volume (%) 2D-LC | 1 | 10 | 6 | 22 | 32 |
| $\overline{M_w}$ (g/mol) | 20 500 | 36 800 | 35 500 | 50 000 | 55 000 |
| Binary copolymer relative volume (%) 2D-LC | 32 | 33 | 24 | 18 | 6 |
| $\overline{M_w}$ (g/mol) | 50 000 | 42 000 | 45 500 | 50 000 | 52 500 |
| Ternary copolymer relative volume (%) 2D-LC | 67 | 57 | 70 | 60 | 62 |
| $\overline{M_w}$ (g/mol) | 144 500 | 112 000 | 158 500 | 151 500 | 156 000 |
| iBor(M)A content in ternary copolymers (%) from LC | 51 | 55 | 45 | 38 | 42 |

Using 2D-LC it was possible to determine the average molar masses of all these species. Average molar masses of binary and ternary copolymers are similar for all samples except sample 1. However, weight average molar mass of PiBuA increases from sample 7 (20 500 g/mol) to sample 10 (55 000 g/mol).

The calibration of the detector used after the gradient HPLC separation combined with $^1$H-NMR enabled us to determine the amount of iBor(M)A repeat units in the ternary copolymers. Finally, LC-FTIR hyphenation gave very interesting results since it showed the average chemical composition as a function of the molar masses or the elution volume in gradient HPLC of the macromolecules.

# 2. Analysis of controlled block copolymers synthesized by CRP

In this chapter, two kinds of polymers will be presented, the first synthesized with the Atom Transfer Radical Polymerization (ATRP) technique whereas the second was produce using the Reversible Addition Fragmentation Chain Transfer (RAFT) technique. Both types of samples are diblock copolymers prepared in two steps using the living character of CRP.

The first set of samples was prepared with isobutyl acrylate polymerized in a first step to form functionalized PiBuA under ATRP conditions. These macromolecules were used as macromonomer for the synthesis of the second block composed of isobornyl acrylate and methacrylate repeat units. Thus monomers are similar to those used for the previously described samples. The proportion of monomers is close to that used for the synthesis of sample 1.

The second set of samples consists in diblock copolymers made of 2-ethyl-hexyl acrylate (2EHA) and methyl acrylate (MA). First 2EHA is polymerized to form a macro-RAFT agent. It was then used to polymerize MA in a dispersed medium. These copolymers have the property to self-assemble during the synthesis. This peculiarity is usually responsible for a loss of the control over the polymerization. Analyses are conducted to generate information on the synthesis process.

## 2.1. Analysis of ATRP synthesized diblock copolymers containing iBuA, iBorA and iBorMA

The ATRP technique was used in order to produce diblock copolymers. The reaction was performed in the presence of $Cu^{I}Br$ (polymerization catalyst), N,N,N',N'',N''-pentamethyldiethylenetriamine (PMDETA) (metal ligand) and ethyl α-bromoisobutyrate (ATRP initiator). The reaction was carried out at 90 °C in butyl acetate for the first one or in bulk conditions for the second. Darvaux et al reported the synthesis of block copolymers containing isobornyl acrylate in ATRP conditions using comparable operating conditions [108]. A good control over the polymerization was achieved and different experimental conditions were tested (solvent, catalyst-ligand concentration ratios…). A post treatment of the obtained copolymer was performed to produce an amphiphilic copolymer of isobornyl acrylate with acrylic acid.

In the present synthesis, the first block was made of PiBuA whereas the second block was a copolymer with equal amounts of iBorMA and iBorA in order to form a polymer of the

following structure: P(iBuA-*block*-(iBorMA-*co*-iBorA)). If this synthesis is compared to that of sample 1 one can notice that the two polymerization steps were performed in an opposite order but the monomer ratio of the feed was maintained. Using the previously developed chromatographic system the PiBuA precursor and the kinetic samples taken from the synthesis as given below were analyzed:

Block 1: formation of poly(isobutyl acrylate) macromonomer in butyl acetate

1st copolymer: synthesis of Block 2 by addition of isobornyl acrylate and isobornyl methacrylate to block 1 in butyl acetate
ATRP-1 T1 = 2h40
ATRP-1 T2 = 4h05
ATRP-1 T4 = 22h40
ATRP-1 Final (52h30)

2nd copolymer: synthesis of Block 2 by addition of isobornyl acrylate and isobornyl methacrylate to block 1 without solvent at the beginning to speed up the reaction. Butyl acetate was added at a later stage
ATRP-2 T1 = 1h20
ATRP-2 T2 = 3h20 (after addition of solvent)
ATRP-2 Final (7h)

The final products were precipitated with a water/methanol solution and redissolved in THF in order to purify the copolymers by removing residual monomers and small oligomers.

### 2.1.1. SEC analyses

The analyses were conducted on a set of three columns: PSS SDV $10^3$, $10^5$, $10^6$ Å (300 x 8 mm I.D.). Mobile phase was THF at a flow rate of 1 mL/min. The chromatogram of block 1 (blue curve in Figure 48 and Figure 49) shows a uniform symmetrical peak. Average molar mass values are $\overline{M_n}$ = 49 200 g/mol and $\overline{M_w}$ = 54 200 g/mol. Polydispersity index is then 1.10 which indicates a good control of the polymerization. However, for the final products (in black: ATRP-1 in Figure 48 and ATRP-2 in Figure 49) a broad and asymmetric peak at high molar mass is detected. The average molar mass values are given in Table 19. These results tend to indicate a loss of the polymerization control during the second reaction step.

**Table 19:** Average molar masses and polydispersity indices for ATRP-1 and ATRP-2 final products, detection: RI, calibration was performed with PS standards

| Samples | $\overline{M_n}$ (g/mol) | $\overline{M_w}$ (g/mol) | PDI |
|---|---|---|---|
| block 1 | 49 200 | 54 200 | 1.10 |
| ATRP-1 | 86 600 | 113 800 | 1.31 |
| ATRP-2 | 120 600 | 187 800 | 1.55 |

The chromatograms of the kinetic samples also show a peak at high molar mass (the average molar masses increase with synthesis time) but in addition they show a large distribution of molecules in the low molar mass part of the chromatogram. This most probably indicates the presence of oligomers of different orders.

Oligomers are necessarily composed of isobornyl acrylate and methacrylate since these are the only monomer species present in the reactor. Nevertheless to produce new chains it is necessary during an ATRP process to produce new radicals. The most probable reactions which lead to the formation of these chains are transfer reactions. As oligomers are detected in both syntheses (with and without solvent) it is assumed that butyl acetate is not the principal cause of the transfer reactions even if such ester solvents are know to be responsible for transfer reaction during radical polymerization [109]. In the present syntheses the transfer reactions most probably occurs on the molecules of ligand. Indeed, PMDETA has already been described as a transfer agent in ATRP synthesis [110]. For the bulk ATRP of n-butyl acrylate with a high target molar mass polymer, polymerization is better controlled at lower ratio of $[PMDETA]_0/[Cu^IBr]_0$ (<1). Chain transfer became more significant for polymerization targeting higher molar mass conducted using an excess of PMDETA. The maximum polymerization rate was obtained at a 0.5:1 ratio of $[PMDETA]_0/[Cu^IBr]_0$ for bulk ATRP. In present syntheses the ratio of $[PMDETA]_0/[Cu^IBr]_0$ is set at 1:1 which would favor the transfer reaction and thus the production of new chains.

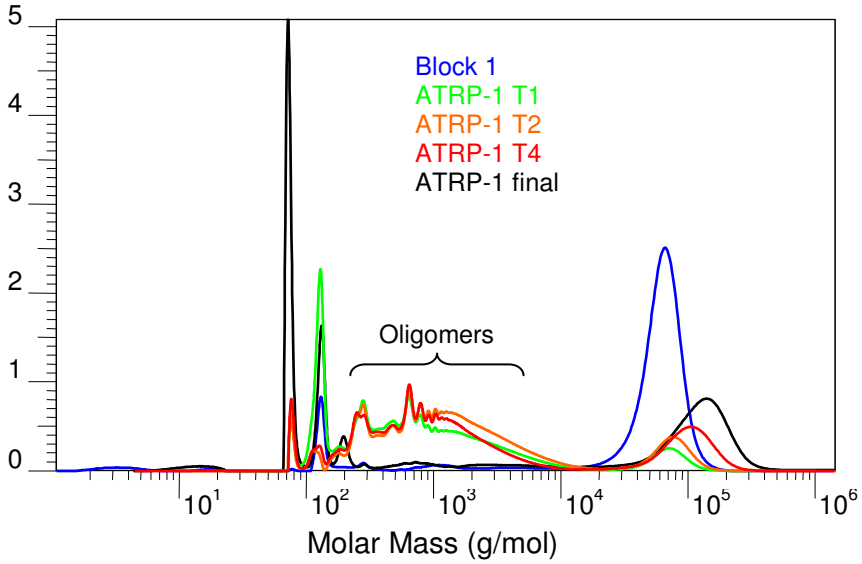


**Figure 48**: Overlay SEC chromatograms of block 1 in blue, terpolymer ATRP-1 kinetic T1 in green, T2 in orange, T4 in red and terpolymer final product in black. Polymer analyzed in THF, stationary phase PSS SDV $10^3$, $10^5$, $10^6$ Å (300 x 8 mm I.D.), flow rate 1 mL/min, detection: RI, calibration PS

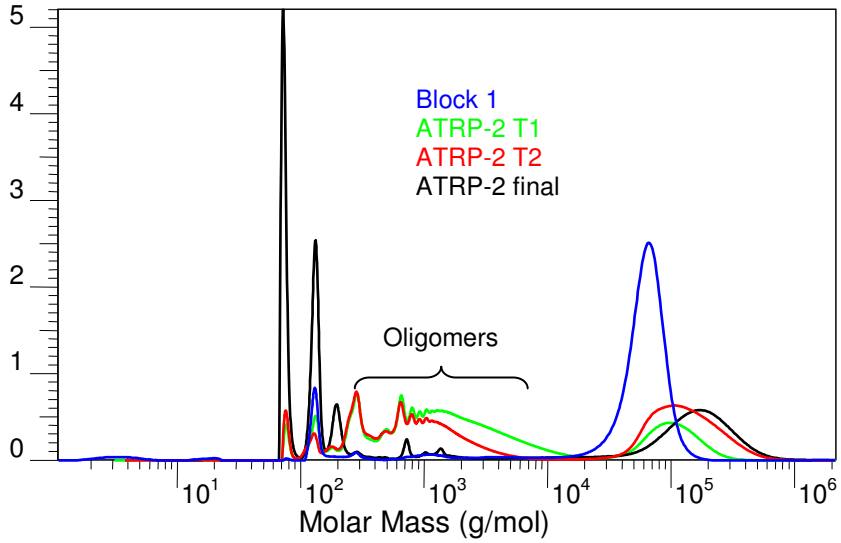


**Figure 49**: Overlay SEC chromatograms of block 1 in blue, terpolymer ATRP-2 kinetic T1 in green, T2 in red and final product in black. Polymer analyzed in THF, stationary phase PSS SDV $10^3$, $10^5$, $10^6$ Å (300 x 8 mm I.D.), flow rate 1 mL/min, detection: RI, calibration PS

According to the SEC traces, it appears that the amount of oligomers decreases with reaction time relatively to the amount of high molar mass polymers. It can be assumed that the oligomers formed during the synthesis acquire the living character lost by the Block 1 molecules. In other terms, the Brome atom can be attached to the oligomer ends which will be then able to grow following the ATRP process. It has to be considered that the binary copolymer of iBorMA and iBorA could grow enough to form large macromolecules: P(iBorMA-*stat*-iBorA), pure block 2. This would be a first hypothesis to explain the loss of symmetry of the high molar mass peak.

### 2.1.2. Gradient HPLC

The separations are performed on a PLRP-S (150 x 4.6 mm I.D., 5 µm) column. The mobile phase flow rate is 1 mL/min and detection is done using an ELSD. The mobile phase step gradient is described in Table 20.

**Table 20**: description of the mobile phase step gradient. Initial conditions 100% of methanol

| Volume (mL) | 0 | 1 | 6 | 9 | 10 | 11 |
|---|---|---|---|---|---|---|
| THF content in mobile phase (%) | 0 | 30 | 55 | 65 | 80 | 0 |

***a) Polymer ATRP-1***

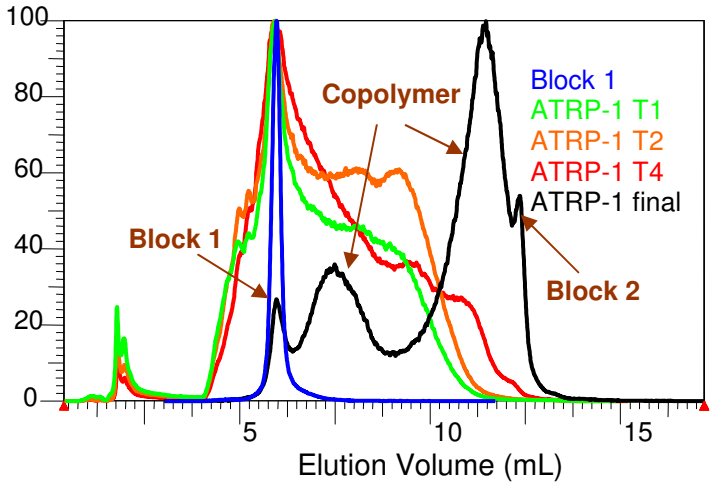


**Figure 50:** Overlay chromatograms of gradient chromatography experiments for polymer ATRP-1. Kinetic samples of copolymer ATRP-1 with block 1 and the final product. Stationary phase: PLRP-S (150 x 4.6 mm I.D., 5 µm); mobile phase: step gradient from methanol to THF as described. Flow rate 1 mL/min; detection: ELSD

In Figure 50 the narrow peak of the first block 1 indicates once again that the control of the polymerization was achieved: i.e. no chemical heterogeneity can be detected. In contrast, four peaks are detected in the final copolymer chromatogram at elution volumes of 5.9 mL, 7.5 mL, 11.5 mL and 12.3mL. As the first peak overlaps with the peak of block 1, it could be attributed to isobutyl acrylate homopolymer. Apparently, this part of block 1 was not re-activated during the second step. The last eluting peak eluted at the elution volume of poly(isobornyl acrylate-*co*-isobornyl methacrylate). This peak clearly indicates the presence of macromolecules only synthesized during the second step of the process: pure block 2. These macromolecules are most probably formed by ATRP by extension of the oligomers. Finally, the two peaks at 7.5 and 11.5 mL are due to ternary copolymers. The difference in

elution volume is due to the different chemical compositions of the two peaks: the first eluting peak contains more isobutyl acrylate whereas the second is richer in isobornyl repeat units. The first one (7.5 mL) may contain the dead chains which transferred onto the PMDETA molecules. For the second peak (11.5 mL), it is more difficult to determine how the chains were produced. However considering the reaction time required to produce such macromolecules, which appear only at the end of the kinetic, it is conceivable that they are produced by controlled radical polymerization.

Figure 50 also shows the chromatogram overlay for the kinetic samples of polymer ATRP-1. Other than for the final product, separate peaks could not be identified but a broad elution region from 4.0 mL to 13.5 mL was observed. This region characterizes the broad chemical composition distribution which is not in agreement with an ATRP polymerization process. For the three kinetic samples the maximum intensity is observed at an elution volume of 5.9 mL, characteristic of block 1. Elution volumes shift towards higher values with increasing reaction time indicating the addition of isobornyl monomers to the already formed terpolymers. Considering the elution volume of PiBuA as the most polar species one would expect that elution starts at 5 mL. The earlier eluting parts could be an indication of the presence of oligomers due to the molar mass effect occurring when performing gradient HPLC. This effect is particularly strong for small molar mass macromolecules (see Figure 7).
The gradient analysis of the samples leads to a simultaneous elution of oligomers and polymers with different chemical composition. For this reason it is difficult to clearly interpret the results.

***b) Polymer ATRP-2***

The same kind of results was observed for the second synthesis even if the chromatograms are not completely identical. This is most probably due to the difference in the reaction characteristics: bulk synthesis in present case.
Figure 51 shows the overlaid chromatograms obtained for the kinetic and final samples of polymer ATRP-2. The final reaction product (black curve) presents three main peaks and a shoulder at the third peak. The elution volumes for these peaks are similar to those found for sample ATRP-1. The peak assignment is identical to that proposed for the previous sample but the relative intensity of each peak is quite different for the two samples. It seems that a smaller amount of block 1 remained after the synthesis of ATRP-2 and less binary copolymer of P(iBorM-*co*-iBorMA) is formed. However the amount of molecules eluted in peak 3

(elution volume 11.5 mL) appears to be much higher for sample ATRP-2. For the first kinetic sample ATRP-2 T1 (green curve), the peak maximum remains at 5.9 mL (elution volume of block 1) as already observed for the kinetic samples of polymer ATRP-1. However for ATRP-2 T2 the peak maximum of the HPLC trace shifted toward higher elution volumes, i.e. 7.2 mL. A peak is still visible at 5.9 mL indicating the presence of residual block 1 but the shift of the maximum confirms that the polymerization in case of sample ATRP-2 is faster than for ATRP-1: more terpolymer is formed. Comparing the sampling times of both kinetic samples confirms the assumption that the second polymerization was much faster. Traces of ATRP-1 T3 and ATRP-2 T1 are similar in terms of the chemical composition distribution. The first one corresponds to a polymerization time of 1360 min whereas the second is obtained only after 90 min.

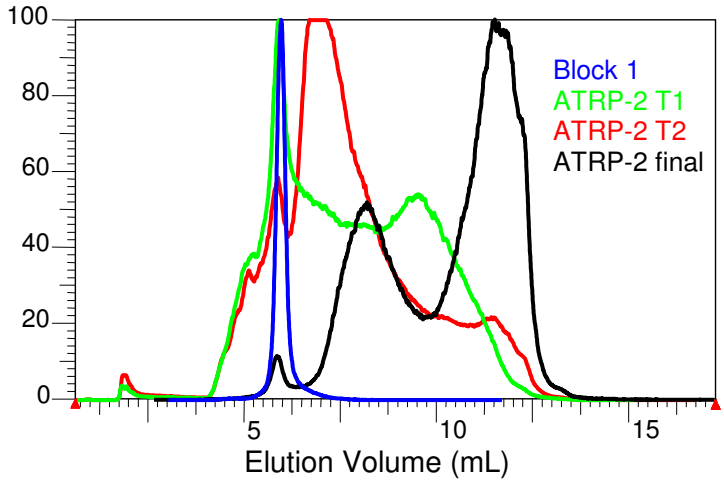


**Figure 51:** Overlay chromatograms of gradient chromatography experiments for polymer ATRP-2. Kinetic samples of copolymer ATRP-2 with block 1 and the final product. Stationary phase: PLRP-S (150 x 4.6 mm I.D., 5 µm); mobile phase: step gradient from methanol to THF as described. Flow rate 1 mL/min; detection: ELSD.

It has to be noted that the addition of solvent during the synthesis of polymer ATRP-2 occurred just before the second sampling time (ATRP-2 T2). It is thus difficult to give any conclusion on the role of the solvent on the polymerization. Nevertheless, the HPLC profiles of ATRP-2 T1 and T2 are significantly different which tends to indicate that the synthesis is very active between the two sampling times: a larger part of block 1 macromolecules seems to be activated to form copolymers (large peak at 5.9 mL) as well as the oligomers which tends to grow by adding iBor(M)A repeat units.

For polymer ATRP-2, the elution of the kinetic samples also begins before the elution volume of block 1 which again tends to indicate the presence of oligomers. For sample ATRP-2 the

reaction is much faster and a higher amount of block 1 chains is consumed during the second step.

According to these results it seems that the control over the chain growth follows the ATRP process but some transfer reactions occur which modify the chain composition of the final product. Undoubtedly the 2D-LC analyses of the samples will deliver much clearer information which will facilitate the understanding of the chemical heterogeneity of the samples.

.

### 2.1.3. 2D-LC analyses

For a better understanding of the process, coupling of gradient HPLC and SEC was performed. The 2D-LC system has been set up as follows:

| | | |
|---|---|---|
| 1st Dimension: | Column: | PLRP-S (150 x 4.6 mm I.D. 5 µm) |
| | Flow rate: | 0.075 mL/min |
| | Injected volume: | 50 µL |
| | Loop volume: | 100 µL |
| | Mobile phase: | gradient Methanol:THF |

The mobile phase gradient is described as follows:

| T (min) | 0 | 13,5 | 80 | 120 | 133,5 | 145 |
|---|---|---|---|---|---|---|
| % THF | 0 | 30 | 55 | 65 | 80 | 0 |

| | | |
|---|---|---|
| 2nd Dimension: | Column: | PL Rapide M (150 x 7.5 mm I.D.) |
| | Flow rate: | 3.0 mL/min |
| | Mobile phase: | THF |

***a) Block 1***

Figure 52 shows a very narrow spot in chemical composition (Y-axis) as well as in molar mass (X-axis) which is characteristic of a controlled homopolymer. Elution volume of the peak maximum is 6.1 mL which can be correlated to the elution volume of this polymer in gradient HPLC (5.9 mL). The molar mass of 55 000 g/mol is in good agreement with that obtained from direct SEC.

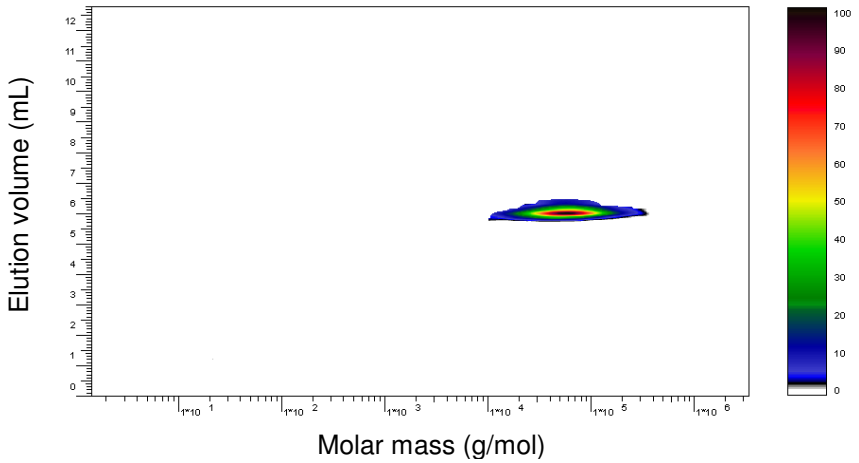


**Figure 52**: 2D-LC contour plot for block 1. 1st Dimension: step gradient HPLC MeOH:THF at 0.075 mL/min on PLRP-S 5 µm; 2nd Dimension: SEC with THF at 3.0 mL/min on PL Rapide M; Calibration: PMMA; Detection: ELSD

***b) ATRP-1 T1***

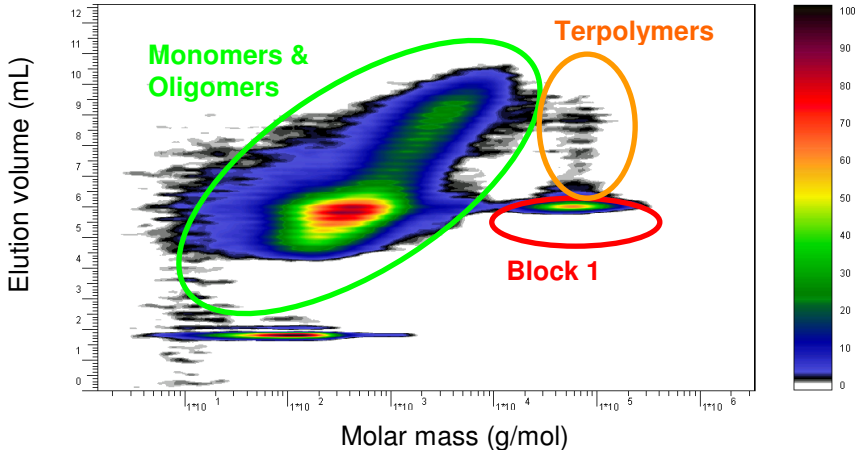


**Figure 53:** 2D-LC contour plot for polymer ATRP-1 T1, experimental conditions as given in Figure 52. Colored circles identify the different components present in the sample

This 2D-LC plot shows that after 160 min of polymerization large quantities of monomers and oligomers are still present whereas the amount of terpolymer is relatively low. As the detector ELSD gives different responses according to the molar mass of the analyte, it is difficult to quantitatively estimate the real amount of each product without a calibration. It appears, however, that the peak of block 1 is not the highest as observed in one-dimensional HPLC experiments. As we supposed, it elutes together with monomers and oligomers of iBor(M)A in gradient HPLC. 2D-LC, however, is able to discriminate all species.

***c) ATRP-1 T3***

In Figure 54 the molar mass dependence of gradient elution can be seen. This phenomenon has already been described in the one-dimensional gradient chromatography (Figure 50). This

molar mass dependence disappears for macromolecules with a molar mass larger than 20 000 g/mol. After this limit all macromolecules elute at the same volume appearing in Figure 54 in the spot called Block 2. These polymers are binary random copolymer of iBorA and iBorMA produced by the growth of the oligomers at the beginning of the synthesis. According to the low amount of detected block 2 at this stage of the reaction (22h40 of polymerization), it is conceivable that these macromolecules are formed according to the ATRP process transferred to the oligomers.

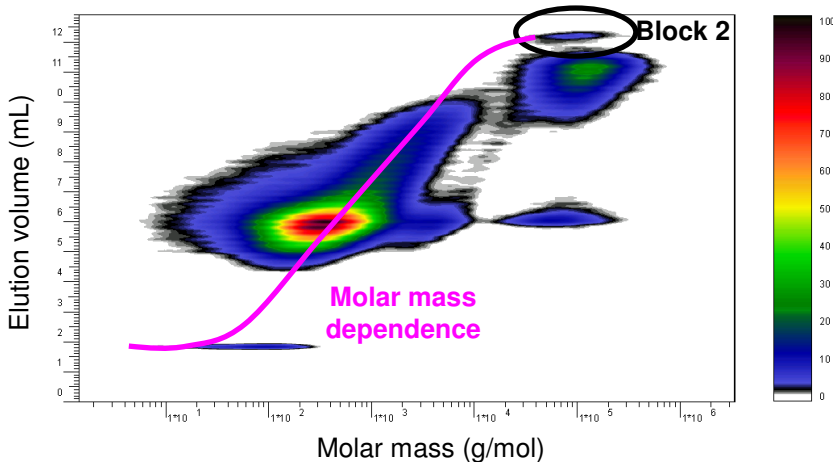


**Figure 54**: 2D-LC contour plot for polymer ATRP-1 T4, experimental conditions as given in Figure 52. Black circle identifies free chains of block 2 and pink curve shows the molar mass dependence in the gradient chromatography

***d) ATRP-1 final***

The 2D-LC plot of the final product (Figure 55) shows 4 different types of macromolecules. The first and last eluting fractions are the non-coupled blocks 1 and 2, respectively. The block 2 chains present a relative homogeneity, particularly a narrow distribution according to molar mass. This may be an argument to confirm the controlled synthesis of these chains. Between both blocks, two populations of terpolymers can be identified. The positions of these spots confirm that the fractions contain monomers of blocks 1 and 2. The molar masses for the two terpolymer fractions are larger than the molar masses of the non-coupled blocks confirming an association.

The majority of the ternary copolymers are rich in isobornyl repeat units (high elution volume along Y-axis related to a low polarity of the sample). The major part of these macromolecules is created in the last hours of the synthesis suggesting a relative low growth rate. This tends to indicate that they are produced under a controlled polymerization process by continuous addition of iBor(M)A monomers. However, as can be seen, the spot is relatively broad along

the Y-axis indicating a relatively broad chemical composition distribution in terms of block 2 length in the copolymers. It has to be noticed that a tailing of the main peak (11.5 mL) appears in the direction of lower molar masses and lower elution volume in gradient HPLC (i.e. higher polarity of the macromolecules. It corresponds to the chains containing less iBor(M)A repeat units than that those of the main peak. Indeed, less repeat units in the second block means a lower total molar mass and a higher polarity as the relative amount of iBuA (block 1 repeat units) in the copolymers is larger.

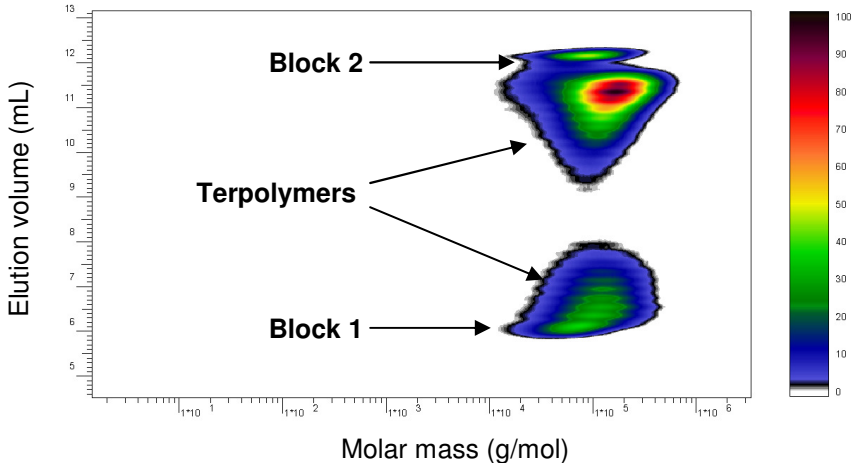


**Figure 55**: 2D-LC contour plot for ATRP-1 final product, experimental conditions as given in Figure 52

The terpolymer spot eluting close to the block 1 spot (6.5 mL along the Y-axis) is most probably composed of ternary copolymer chains terminated during the synthesis. According to the elution volume of the spot they contain all three kinds of repeat units but with a majority of that of block 1 (iBuA). The loss of the living character of these chains occurred either by transfer reactions as previously suggested or by termination reactions. The relative low intensity of the spot, in comparison with the other terpolymer spot, tends to confirm the hypothesis that these chains by-products of the reaction.

The results obtained for both syntheses were very much comparable. To have an overview of the results observed for the second synthesis, we present the 2D-LC plot of the kinetic sample ATRP-2 T2.

***e) ATRP-2 T2***

Same results as for polymer ATRP-1 are found for the present sample except that a large amount of terpolymers is already detected after 200 min of polymerization. In this case,

polymerization was faster due to the absence of solvent in the first part of the synthesis. Figure 56 shows the 2D-LC plot for a reaction time of 200 min of the synthesis of polymer ATRP-2.

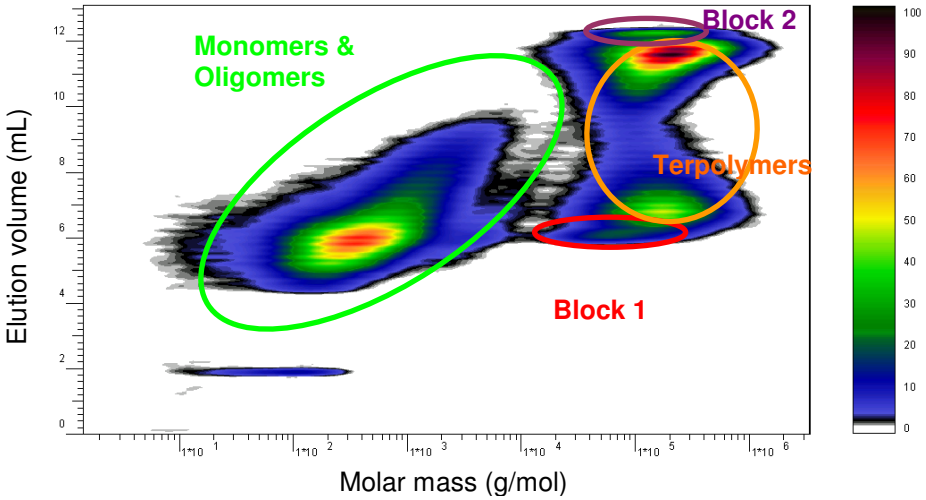


**Figure 56:** 2D-LC contour plot for polymer ATRP-2 T2, experimental conditions as given in Figure 52

In this kinetic sample we can see that both populations of terpolymer are formed simultaneously and throughout the reaction.

### 2.1.4. Conclusions

The ATRP process developed to produce ternary diblock copolymers seems to be only partly successful. The ternary copolymers were obtained apparently growing according to the controlled process but a significant number of by-products was also formed during the synthesis: non-reactivated block 1 chains, diblock copolymers with a low conversion of the second block and pure block 2 chains. These by-products were most probably produced due to the transfer reactions which apparently appeared at the beginning of the polymerization process. The main transfer agent seems to be the molecules of ligand (PMDETA). The oligomers formed seem to inherit the living character from the dead chains and thus are able to grow. It has to be noticed that even if the amount of oligomers appears very important the impossibility of direct quantification of the products with the detectors used prevent any comment on the importance of these side reactions in the global polymerization process.

## 2.2. Analysis of RAFT synthesized P(2EHA-*block*-MA)

The aim of the synthesis work was to design well-defined block copolymers of 2-ethylhexyl acrylate and methyl acrylate P(2EHA-*block*-MA) that form micelles, to be further used directly in the dispersant isododecane medium [18,111]. For an industrial application of the final dispersion, the direct formation of such nanoparticles in a selective solvent appeared to be the most appropriate process. For that purpose, controlled free-radical polymerization was used to prepare the samples. The synthesis was a RAFT-mediated dispersion polymerization of methyl acrylate (MA) in isododecane using poly(2-ethylhexyl acrylate) (P2EHA) as a soluble macromolecular reversible chain transfer agent [112].The reaction was initiated with *tert*-butyl peroxy-2-ethylhexanoate (T21S) and the RAFT agent used was the *tert*-butyl dithiobenzoate (DTB) (see Figure 57). The polymerization mechanism is shown in Figure 58.


**Figure 57:** Chemical structure of the initiator T21S (a) and the RAFT agent (b)

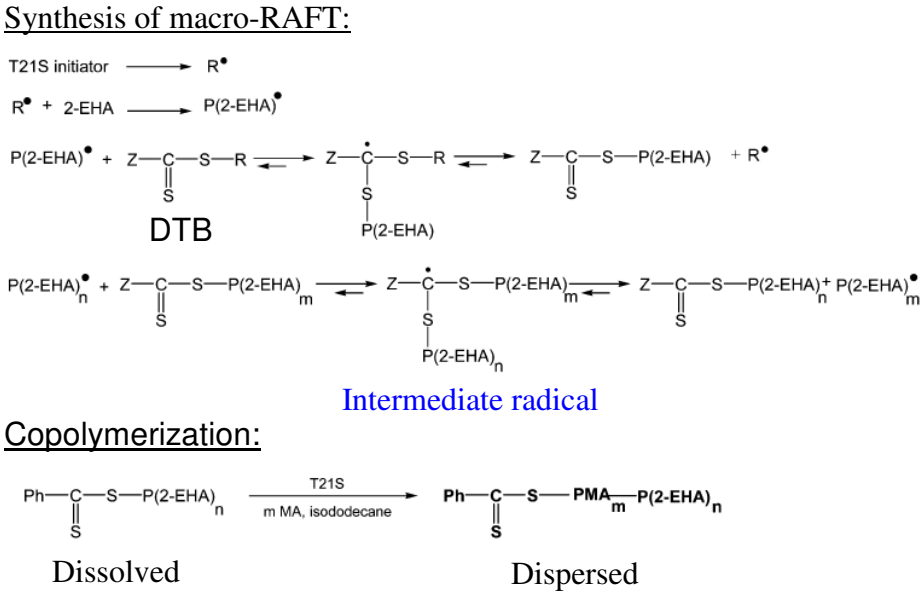


**Figure 58:** RAFT copolymerization mechanism for preparation of P(2EHA-*block*-MA) [18]

The copolymerization allowed stable particles with very small hydrodynamic diameter to be produced. However, these particles were found to be polydisperse. Polymerization characteristics were affected: strong rate retardation and very poor control over the polymer structure were observed together with an incomplete consumption of the macro-RAFT agent.

Such a result was quite surprising and in contradiction to the behavior of the P2EHA-DTB, when used as a macro-RAFT agent for polymerization either in bulk or in isododecane solution. Only a major influence of the dispersed state of the system could explain the difference in apparent reactivity of the macro-RAFT agents used in this work.

We analyzed samples which were taken in the first hours of a 20 hours synthesis performed under the described conditions. Samples were taken after 1, 2, 4 and 8 hours of synthesis. The monomer conversion is approximately 10 % after 4 hours of synthesis. These samples were interesting as the loss of control appears very early in the reaction.

In order to characterize the polymers as precisely as possible, we set up several chromatographic and spectroscopic techniques. Our main objective was to determine the molar mass and the chemical composition distributions which appeared during RAFT polymerization of MA to form the P(2EHA-*block*-MA) diblock copolymers.

### 2.2.1. Analysis of MMD using SEC

SEC analyses enabled to determine the molar mass distribution of kinetic samples. The chromatogram overlay of the macro-RAFT agent with four copolymer samples is shown in Figure 59. The average molar masses of these five samples are summarized in Table 21.

All samples were dissolved in THF for the analyses. It is a good solvent for both blocks which leads to a destruction of the micelles. This precaution was important to carry out chromatography on polymer chains and not on particles.

The chromatogram overlay shows a shift of the peak maximum in the direction of higher molar masses when the polymerization time increases. This clearly indicates that the polymerization process remained active during the whole synthesis. According to the polydispersity values, one can presume that the radical polymerization remained controlled except for the last sample which is bimodal and as a result has a polydispersity larger than 2. For the three other copolymers, as can be seen in the SEC chromatogram overlay, a shoulder at the higher molar mass side of the peaks appears. This shoulder is also present in the macro-RAFT agent. The shoulder is particularly noticeable for sample LH-239 4h. This tends to indicate that a part of the control was lost during the reaction and especially between two and four hours of the polymerization as the shoulder tends to increase with reaction time. It has also to be noticed that the molar mass determined for the shoulder is roughly twice the value

at peak maximum. The shoulder is most probably due to terminated chains formed by coupling of two macromolecules.

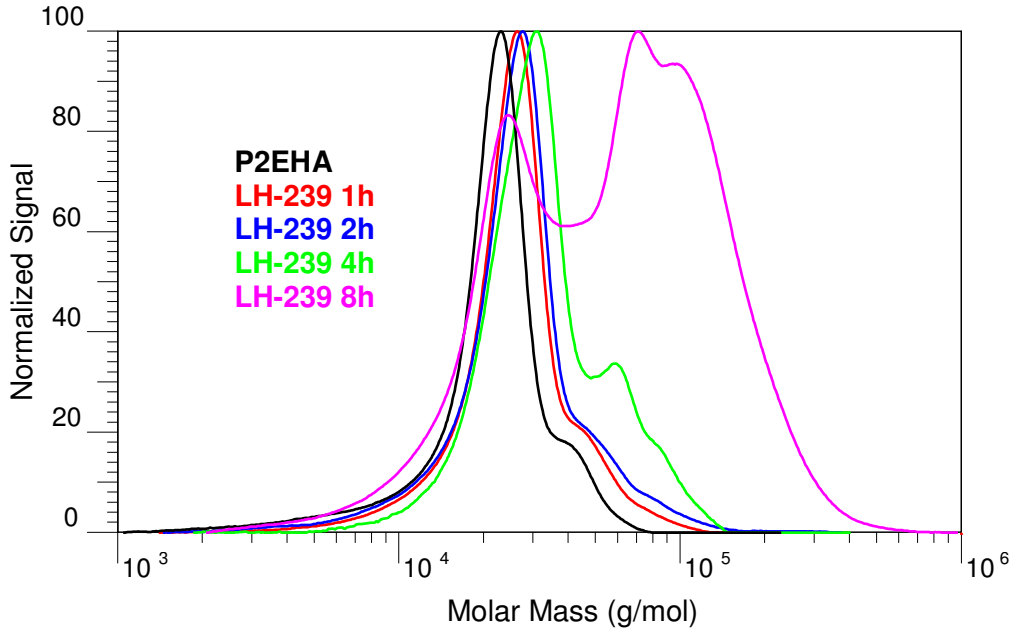


**Figure 59:** SEC chromatogram overlay of the macro-RAFT (black) with the three copolymers: LH-239 1h (red), LH-239 2h (blue), LH-239 4h (green) and LH-239 8h (pink). Columns: PSS SDV $10^3$, $10^4$, $10^5$ Å; mobile phase: THF at 1 mL/min; detection: RI; calibration: PMMA

**Table 21**: Average molar masses obtained after calibration of the system with PMMA standards for the macro-RAFT agent and the four kinetics samples

| | $\overline{M}_n$ (g/mol) | $\overline{M}_w$ (g/mol) | PDI |
|---|---|---|---|
| Macro-RAFT | 19 500 | 23 500 | 1.20 |
| LH-239 1h | 23 000 | 28 000 | 1.22 |
| LH-239 2h | 23 500 | 30 000 | 1.28 |
| LH-239 4h | 29 000 | 37 500 | 1.29 |
| LH-239 8h | 37 000 | 76 000 | 2.05 |

For the last sample it is difficult to find out which kinds of macromolecules were formed. It seems that macro-RAFT chains remain present in the sample which would explain the low molar mass peak. For the high molar mass peak, we can see that it is not completely symmetric. This could indicate that several kinds of binary copolymers were produced during the polymerization and thus suggest that the control of the polymerization was partially lost. This is confirmed by the high value of PDI for this sample.

For the first three samples 1h to 4h, the peaks of the copolymers still mostly overlay with the peak of the macro-RAFT agent. One could suppose that some non-reinitiated macro-RAFT chains remained present during the whole synthesis. No proof for this hypothesis could be found in the SEC experiments at least for the first three samples. To test this hypothesis and to characterize the copolymers according to the chemical composition, LAC and LC-CC experiments were performed on all samples.

### 2.2.2. Analysis of CCD using gradient LAC

Gradient liquid adsorption chromatography allows for the separation of polymers according to chemical composition. With this technique it should be possible to distinguish block copolymer molecules from remaining macro-RAFT and PMA homopolymer, if present. The discrimination of the various species in the samples is based on polarity and solubility differences. In the present case, PMA is more polar than P2EHA. Both can be dissolved in methanol-THF, however, PMA is soluble in methanol-THF mixtures with lower amounts of THF as compared to P2EHA.

To separate the macromolecules, first the complete sample was adsorbed on the stationary phase. We chose to carry out the separation on a non-polar column packing material composed of polystyrene cross-linked with divinylbenzene. To enhance adsorption on this stationary phase we conditioned it with a mobile phase constituted of a poor solvent of the polymer: methanol. As a result adsorption and/or precipitation of the macromolecules on the column material was achieved. The selective elution of the macromolecules according to their chemical composition is performed by linearly increasing the proportion of THF (as the good solvent) in the mobile phase. First the more polar macromolecules eluted containing higher proportions of methyl acrylate. These fractions were followed by macromolecules containing an increasing proportion of 2-ethylhexylacrylate. The expected order of elution is then: PMA followed by P(2EHA-*block*-MA) and finally P2EHA.

Figure 60 shows an overlay of the macro-RAFT agent with the four kinetic samples analyzed by gradient LAC. A uniform peak can be seen for P2EHA homopolymer (macro-RAFT) in the chromatogram at an elution volume of 12.8 mL. The narrow Gaussian form of the peak is characteristic for a homopolymer. On the contrary all copolymer chromatograms present two peaks and even a third peak can be seen for LH-239 8h. By analogy, the last eluted peak in all cases can be attributed to non-reinitiated macro-RAFT. It shows that initiation by the macro-RAFT agent is incomplete.

The other peaks eluted earlier which indicates that the detected macromolecules are more polar than P2EHA. The peaks not completely separated from the macro-RAFT agent are due to block copolymers containing a polar block of PMA. Peak maximum shifts towards lower elution volumes with increasing polymerization times, i.e. 12.4 mL for LH-239 1h to 12.0 mL for LH-239 8h. This is the result of the growth of the PMA block length.

Finally a peak eluting at $V_e$= 8.9 mL is detected for sample LH-239 8h which corresponds to the elution volume of PMA. Apparently a part of the polymerization occurs without the control of the RAFT agent and leads to formation of homopolymer chains of the second monomer.

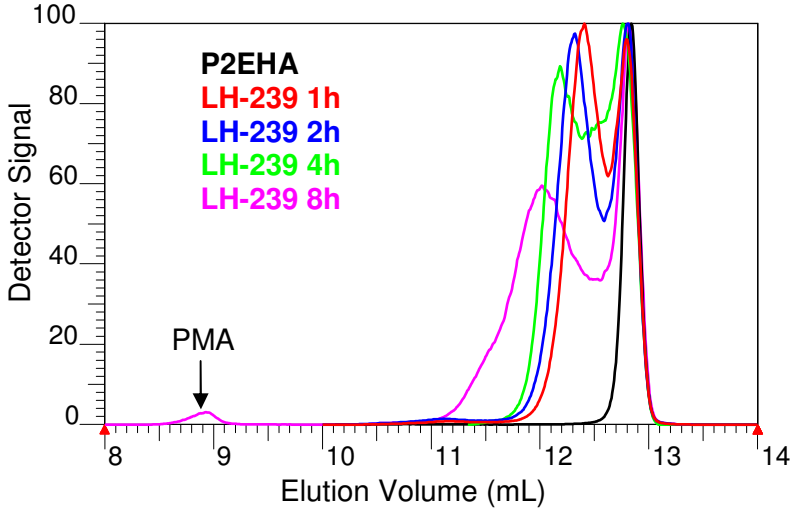


**Figure 60**: Gradient HPLC chromatogram overlay of the macro-RAFT (black) with the three copolymers: LH-239 1h (red), LH-239 2h (blue), LH-239 4h (green) and LH-239 8h (pink). Columns: 2 PLRP-S 8 µm; mobile phase: 10 min linear gradient from 0 to 70 % of THF in methanol; flow rate 1mL/min; detection: ELSD

For the kinetic samples taken at 1h and 2h, the copolymer peak remained symmetric and Gaussian. This reveals that the chemical composition distribution was still well controlled. However, it has to be noted that after 4 hours a certain peak deformation appeared. This is likely to be a consequence of the loss of control. This tendency is confirmed by the chromatogram of copolymer LH-239 8h. Copolymer peak maximum intensity decreased with polymerization time since the peaks became broader. It remains difficult at this stage to define the cause of the loss of control and the type of produced chains which were responsible for peak deformation. Further experiments such as 2D-LC were necessary to get more detailed information.

To study more in detail the copolymer and to analyze the distribution of the control agent on the polymer chains, we conducted the same gradient HPLC separation but this time using an

UV detector in addition to ELSD. The detection was done at a wavelength of 300 nm which is specific for the DTB molecule. The response is thought to be exclusively due to DTB as acrylates do not exhibit adsorption at such wavelength. Gradient HPLC chromatogram overlay for polymer LH-239 2h obtained with both detectors is presented in Figure 61.

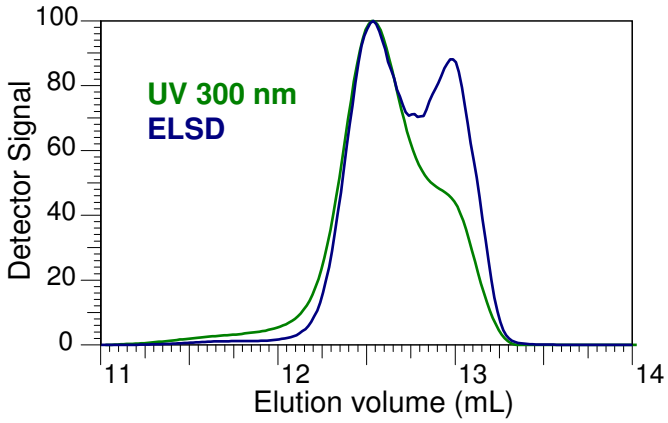


**Figure 61:** Gradient HPLC chromatogram overlay of the sample LH-239 2h. Columns: 2 PLRP-S 8 µm; mobile phase: 10 min linear gradient from 0 to 70 % of THF in methanol; flow rate 1mL/min; detection: UV 300 nm (green) and ELSD (blue)

As can be seen in Figure 61, there is a very good overlapping of both signals for the copolymer peak, $V_e$ = 12.5 mL. This would mean that living and terminated copolymers contain DTB molecules. This result gives then little credit to coupling of copolymers by termination reaction between two active chains. However, for the non-reinitiated P2EHA ($V_e$ = 13.2 mL), the UV signal is weaker than that of ELSD. This seems to indicate that a part of the P2EHA chains do not contain DTB molecules. These chains are not macro-RAFT agent but only non-functionalized homopolymers. This is the reason why they are unable to form block copolymer molecules as they have lost their living property.

### 2.2.3. 2D-LC gradient HPLC x SEC: combination of CCD and MMD information

2D-LC experiments where gradient LAC was coupled with SEC gave more comprehensive results for these samples. The 2D-LC contour plots for the macro-RAFT and the four polymer samples are presented in Figure 62. The SEC information appears on the X-axis and gradient LAC information on the Y-axis. The red lines indicate the peak integration limits. The relative volumes and average molar masses for each peak are given in Table 22 and the proposed macromolecule architectures for all peaks are given in Table 23. It has to be noticed that all

average molar mass estimations determined from 2D-LC experiments are very close to those given by SEC measurements.

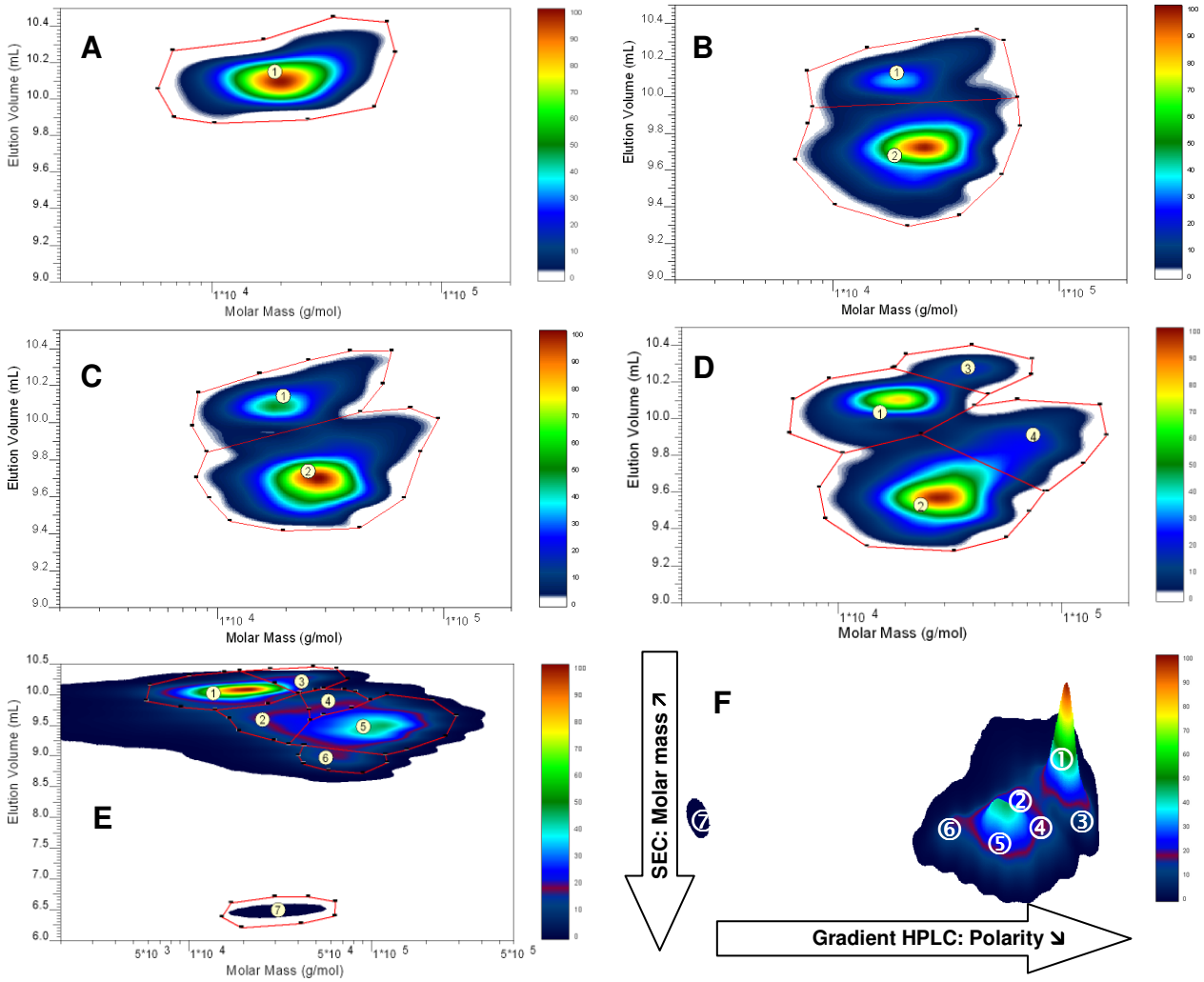


**Figure 62**: 2D-LC chromatograms of (A) P2EHA macro-RAFT, (B) LH-239 1h, (C) LH-239 2h, (D) LH-239 4h and (E) LH-239 8h. (F) is a rotation of 90° and inclination of 35° of 2D-LC plot from sample LH-239 8h. 1st Dimension: gradient LAC with 0 to 70 % THF in methanol in 200 min at 0.05 mL/min on PLRP-S 5 µm; 2nd Dimension: SEC with THF at 1.5 mL/min on PL HTS-C; Calibration: PMMA; Detection: ELSD

Figure 62A shows the 2D-LC plot of the macro-RAFT agent. As can be seen it is very narrowly distributed along the Y-axis, i.e. in chemical composition. Of course this has to be expected for a homopolymer. However, a deviation can be seen at the high molar mass side in the direction of higher elution volumes. This deviation can be related to the shoulder on the high molar mass side of the chromatogram detected in the SEC experiment of the macro-RAFT agent (black curve in Figure 59). It is also observable in the 2D-LC plots of the kinetic samples and particularly for sample LH-239 4h as a separate spot; see peak 3. This peak presumably corresponds to macromolecules formed by two coupled macro-RAFT chains

resulting from a termination reaction. One hypothesis could be formulated to explain the observed separation: the absence of DTB end group for the by-products and the doubled molar mass lead to a stronger adsorption on the stationary phase and thus a slightly delayed elution. The use of the UV detector was inefficient for these 2D-LC experiments as the polymer concentration is very low and the coupling products are by-products of the reaction and for this reason they represent only few percent of the total polymer sample.

The fact that a specific spot can be isolated only in sample LH-239 4h does not necessarily mean that the amount of these chains increased with reaction time. The intensity of the P2EHA peak increased for sample LH-239 4h as the intensity of the copolymer peak decreased as it was already mentioned in gradient LAC experiments. Even if it is difficult to obtain reliable results from ELSD without calibration, it is nevertheless possible to give approximations. This was done for the ratio of chains with doubled molar mass on the total of non-reinitiated P2EHA chains (ratio of the volume of spot 3 on the sum of volumes of spots 1 and 3) for samples LH-239 4h and 8h, Figure 62D and E respectively. Such calculations show that the volume of spot 3 is constant between 4 and 8 hours of polymerization and doubled molar mass chains correspond to ca 14 % of total non reinitiated chains. A calibration of the ELSD signal versus the mass of polymer injected should be made to confirm these results (see part IV.2.2.4.a).

Regarding the diblock copolymer peak which elutes in gradient LAC before the macro-RAFT agent, it is quite symmetric after the first hour of polymerization, see peak 2, but shows a deformation similar to that observed for macro-RAFT in the next samples (3C and 3D). This deformation appears as a tail towards higher molar masses and higher elution volumes (upper right) of the copolymer spot. It is identified as peak 4 in Figure 62D. Two hypotheses could be formulated to explain the formation of larger macromolecules during the RAFT polymerization: (1) chains are no more controlled and add a large amount of MA monomer; (2) two active chains are coupled either by termination reaction or by a coupling reaction involving one or two intermediate radicals. From these two assumptions, the second is more likely to be true for two main reasons. First one is the position of the tail. Indeed, tailing appears in the direction of higher elution volumes. This indicates that the macromolecules detected in the tail are less polar than the expected binary copolymer. The polymerization of the polar MA monomer increases the polarity of the chain. This phenomenon is confirmed by the shift of the binary copolymer peak in direction of lower elution volumes in comparison with the macro-RAFT agent. Thus, a decrease of polarity can only be obtained if 2EHA

repeat units are added to the macromolecules. This is undeniably the case if a coupling reaction occurs. The second reason can be deduced from the results given in Table 22. The comparison of the average molar masses of the copolymer peak (spot 2) and of the tail (spot 4) of Figure 62D indicates two times higher values for $\overline{M_n}$ and $\overline{M_w}$ in favor of spot 4. This is completely in agreement with the hypothesis of a linkage between two chains.

**Table 22:** Relative volumes and average molar masses obtained after calibration of the system with PMMA standards for each peak of the 2D-LC diagrams given in Figure 62

| Samples | Peak n° | Relative Peak Volume (%) | $\overline{M_n}$ (g/mol) | $\overline{M_w}$ (g/mol) | PDI |
|---|---|---|---|---|---|
| A: Macro-RAFT | 1 | 100 | 19 500 | 23 000 | 1.18 |
| B: LH-239 1h | 1 | 24 | 20 500 | 24 000 | 1.17 |
| | 2 | 76 | 23 000 | 27 000 | 1.17 |
| C: LH-239 2h | 1 | 26 | 19 500 | 23 000 | 1.18 |
| | 2 | 74 | 26 500 | 31 000 | 1.17 |
| D: LH-239 4h | 1 | 24 | 17 000 | 19 500 | 1.15 |
| | 2 | 59 | 28 000 | 32 500 | 1.16 |
| | 3 | 4 | 40 000 | 42 500 | 1.06 |
| | 4 | 13 | 64 500 | 72 500 | 1.12 |
| E: LH-239 8h | 1 | 31 | 16 500 | 18 500 | 1.12 |
| | 2 | 14 | 27 500 | 29 500 | 1.07 |
| | 3 | 5 | 38 500 | 40 500 | 1.05 |
| | 4 | 5 | 60 000 | 63 500 | 1.06 |
| | 5 | 39 | 89 500 | 107 000 | 1.20 |
| | 6 | 5 | 63 500 | 68 000 | 1.07 |
| | 7 | 1 | 29 000 | 32 500 | 1.12 |

A hypothesis can be formulated to explain the formation of macromolecules contained in peak 4. If we consider the initial conditions of polymerization, all species are soluble in isododecane: macro-RAFT agent, methyl acrylate monomer and initiator. When the reaction starts by decomposition of the initiator, few monomers of MA are polymerized until this chain reacts with a C=S bond from a present macro-RAFT to form a primary intermediate radical (P2EHA-DTB-PMA). After fragmentation, a homopolymer of P2EHA is released with an active center at its end. Copolymerization then occurs by addition of MA repeat units until the formation of a new intermediate radical. When the copolymer becomes dormant, it very

rapidly tends to segregate and form particles because of the poor solubility of PMA in isododecane. This full process happens as long as the initiator is present in the medium. From the three reactions occurring during polymerization: propagation, formation of intermediate radical by addition of propagating radical and fragmentation of the intermediate radical into dormant and active species, the latter is the limiting one as it has the lowest kinetic rate.

At one stage, it is conceivable that primary intermediate radicals have a sufficient life time to diffuse in the medium and join the particles. If this indeed happens, DTB molecules are situated and confined at the interface between particle and isododecane. It is then likely for two close radicals to react together forming a terminated product as presented in Figure 63. This coupling is likely to take place only at low conversion when low molar mass PMA is present in the medium and because of the poor solubility of these chains. The characteristics of such macromolecules correspond to that found with LC analyses:

- higher elution volume in comparison with the expected copolymer molecules as coupling products contain a higher percentage of 2EHA repeat units
- Molar mass two times that of the expected copolymers
- Presence of DTB molecule detected with UV response at 300 nm for these molecules.

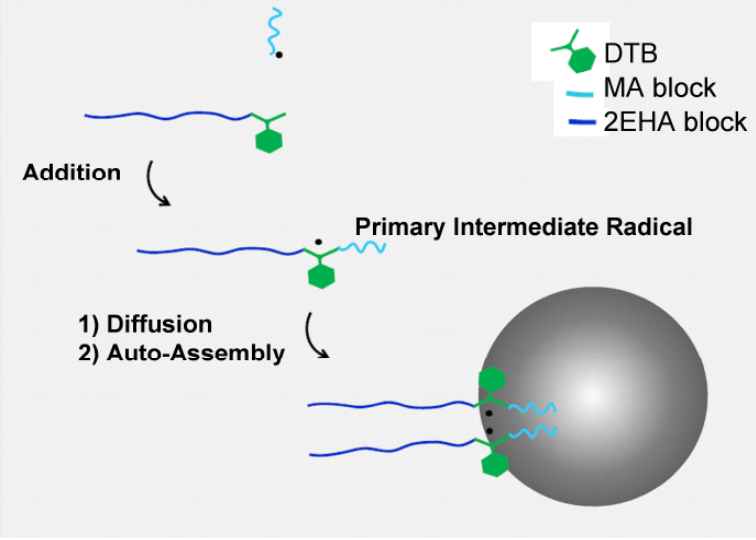


**Figure 63:** Scheme of the probable route for the formation of coupling product formed during the polymerization of MA in dispersion in isododecane in presence of P2EHA-DTB macro-RAFT agent. Such products elute as spot 4 in Figure 62D [111]

Because of the poor solubility of MA in isododecane it is possible that monomers as well as PMA blocks segregate in particles. This migration displaces the polymerization in the particles where some DTB end groups are present. It results in polymerization only in the dispersed phase and macro-RAFT agent still present in the continuous phase would no more

be initiated. This might be a reason why the entire macro-RAFT agent is not consumed in the present case of dispersion polymerization whereas it is usually consumed quantitatively in solution or bulk polymerization.

The interpretation of the 2D-LC plot of sample LH-239 8h is much more complex as at least four spots of copolymer can be detected. Spots 1 and 3 remain present and are (as previously) attributed to non-reinitiated P2EHA macromolecules. Spots 2 and 4 already detected in previous samples are also identified. Spot 4 was expected to be found as these chains are terminated and should remain present during the whole synthesis. Spot 2 corresponds more to a tail of the principal copolymer spot (spot 5). It most probably corresponds to terminated copolymer chains formed during polymerization as it occurs during the radical process.

Spot 5 constitutes the main part of copolymer. Its position in comparison with the previous main copolymer spot, spot 2 in LH-239 4h, Figure 62D, indicates that the copolymerization continues and addition of MA monomers still occurs: the increase of molar mass as well as polarity indicate addition of MA to the polymer chain. Nevertheless its form is not completely symmetrical and it is relatively broad along both axes. This suggests that all chains do not grow at the same rate and that the RAFT process does not allow a complete control over polymerization in the present synthesis.

A last kind of copolymer is detected and labeled as spot 6. Its elution in the first dimension gradient HPLC ($V_e$ = 9 mL) indicates that this copolymer contains more methyl acrylate repeat units than all other copolymers. Elution in the second dimension is equivalent to a PMMA standard with a molar mass of 63 500 g/mol, lower than the controlled diblock copolymer. The relative volume (5 %, see Table 22) and the chemical composition determined by HPLC suggest that this copolymer was not produced via the RAFT process. Some kind of side-reaction was responsible for its formation. According to these observations, a hypothesis of the structure of these chains can be formulated. The higher polarity (i.e. higher relative content of MA) combined with the smaller molar mass than spot 5 suggest that these macromolecules could be stars containing several MA arms. Such architecture is likely to be formed especially if the polymerization mostly takes place in the dispersed phase.

The poor quality of the control of the RAFT process over the polymerization is confirmed by the presence of PMA with a molar mass close to 30 000 g/mol (spot 7 on Figure 62E and F). It indicates that free radical polymerization occurred during the synthesis and more particularly between 4 and 8 hours of reaction.

The average molar mass values in Table 22 are in agreement with those calculated from SEC experiments. It should be reminded that molar mass values determined in 2D-LC conditions are less reliable than those obtained from direct SEC as column length is divided by a factor 6 and flow rate is increased from 1 to 1.5 mL/min. The molar masses of residual macro-RAFT, spot 1, remained constant during the polymerization process, whereas the molar masses for the diblock copolymer (spot 2 for samples LH-239 1h to 4h and spot 5 for sample LH-239 8h) increased with time, indicating the PMA block growth. The determination of the molar masses for spot 3 and 4 in Figure 62D was difficult since they appeared as shoulders of the main spots and not as separate peaks. However, the values are approximately two times higher than those of the main spots. This remark concerning the difficulty to integrate spots could also be applied to spots 2, 3, 4 and 6 for Figure 62E.

According to PDI values, it appears that the main peak of copolymer remains controlled between the 4$^{th}$ and the 8$^{th}$ hour of synthesis even if the PDI increases from 1.06 to 1.20.

Table 23 summarize all architecture hypotheses deducted from the analyses of the four samples by 2D-LC chromatography. The schemes represent the most probable hypothesis for each spot. It is very likely that more than only one kind of chain composes each 2D-LC spots.

**Table 23:** Hypotheses of the most probable chain architectures for each 2D-LC spots presented in Figure 62

| Spot 1 | Spot 2 | Spot 3 and 5 | Spot 4 | Spot 6 |
|---|---|---|---|---|
| 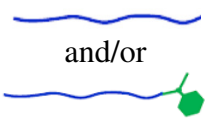  |  | 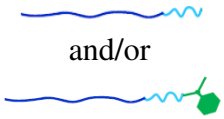  | 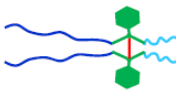 |  |
|  : DTB |  : 2EHA block | |  : MA block | |

### 2.2.4. Characterization of each block with LC-CC

As a baseline separation of the block copolymers and the residual macro-RAFT agent was not achieved, a chromatographic system was developed that operates at critical conditions for the P2EHA block. In such system, the P2EHA block is chromatographically “invisible” and all P2EHA homopolymer molecules elute at the same volume independently of chain length. Furthermore, the mobile phase was designed in such a way that it was a good solvent for the PMA block. Therefore, the PMA block was excluded from the stationary phase and, thus,

separation of the copolymers was only driven by the PMA block length. In other terms, the separation corresponded to a SEC-like experiment only based on the PMA block.

In this part we concentrated our efforts on the three samples taken during the first four hours of the polymerization. The results of these experiments are presented in Figure 64 as an overlay of the chromatograms from the first three kinetic samples and the macro-RAFT.

The macro-RAFT peak eluted at 3.27 mL which corresponded to the hold-up volume of the system. This is in agreement with the statement that the polymer eluting at critical conditions is "invisible" for the stationary phase. A comparison of Figure 60 and Figure 64 shows that a better separation of the copolymers and the residual macro-RAFT was obtained by LC-CC as compared to gradient HPLC. The copolymer fractions eluted before the void volume of the column indicating that elution takes place in the size exclusion region. As was expected, with increasing polymerization time the copolymer peak maxima shifted towards lower elution volumes, i.e. larger hydrodynamic volumes. This is caused by the growing PMA block length upon polymerization.

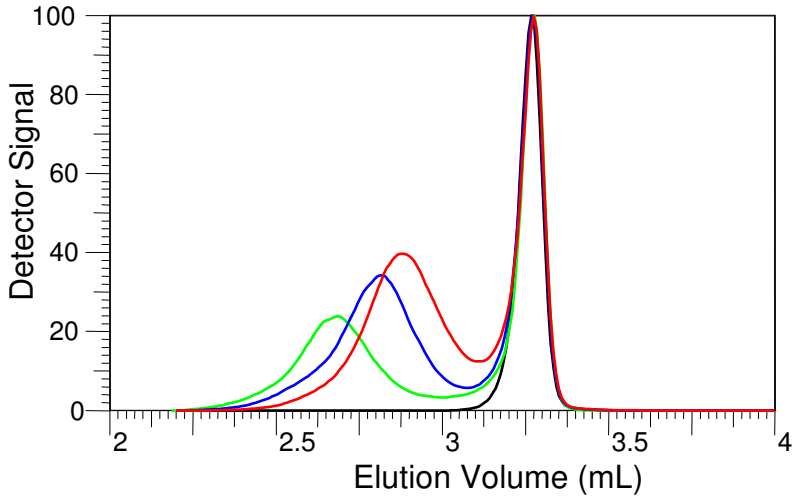


**Figure 64:** Chromatogram overlay of (black) P2EHA, (red) LH-239 1h, (blue) LH-239 2h, and (green) LH-239 4h at critical conditions of P2EHA; stationary phase: 2 x PLRP-S; mobile phase: ACN-THF 46:54 % by volume, flow rate 1 mL/min; 25°C; detection: ELSD

It should be noticed that the copolymer peaks for the samples taken during the first four hours of synthesis are symmetrical. Molar mass resolution in present case is much lower than that of the SEC experiment. This is the reason why the shoulders observed in Figure 59 are not seen in Figure 64. These copolymer peaks become larger with polymerization time which indicates that the distribution of PMA block lengths increases during the synthesis. This observation was already made when we compared PDI values determined from SEC measurements (see Table 21).

***a) Quantification of residual P2EHA***

The precise quantification of the non-reinitiated macro-RAFT is possible by calibrating the ELSD. For that reason, LC-CC experiments were conducted to quantify the amount of residual macro-RAFT. The calibration curve for P2EHA was obtained by injecting different masses of the macro-RAFT agent. The calibration curve, macro-RAFT peak area ($V_e$ = 3.27 mL) vs. mass of macro-RAFT injected, is shown in Figure 65. As expected for ELSD calibration, the best fit was achieved with a second order polynomial function. Equation parameters and $R^2$ value are also presented in Figure 65. According to these results the fit was sufficiently good to quantify residual macro-RAFT in the kinetic copolymer samples.

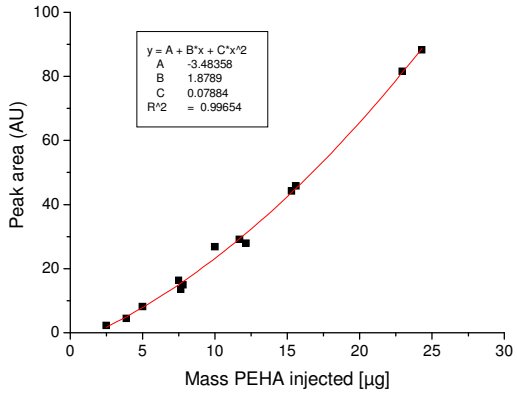


**Figure 65:** Calibration curve of ELSD detector response (peak area) vs. injected mass of macro-RAFT. Experimental conditions see Figure 64

The measurement of P2EHA peak area for the three kinetic samples allowed us to calculate the ratio of residual macro-RAFT mass to total injected mass of polymer (see 4$^{th}$ column of Table 24). With $^1$H-NMR analysis of the samples we were able to estimate the molar and mass proportions of 2EHA in the polymers. With these two values we estimated the percentage of 2EHA repeat units contained in macro-RAFT chains which were not reinitiated to produce copolymers. These results are summarized in Table 24.

As expected for a progressing polymerization, the amount of monomer from block 1 (macro-RAFT) decreases with synthesis time from 82.5 to 70.5 mol %. We converted these values into mass percentage using molar masses of MA (86 g/mol) and of 2EHA (184 g/mol).

From LC-CC measurements, we observed that the mass percentage of non-reinitiated macro-RAFT in total injected polymer decreased with reaction time from 38.4 to 34.7 mass %. This result was expected as the addition of MA repeat units to the polymer chains increase the total sample molar mass.

**Table 24**: Estimation of the amount of 2EHA repeat units contained in non-reinitiated macro-RAFT from 1H-NMR measurements and mass percentage of non-reinitiated chains

| Samples | Total 2EHA in polymer from $^1$H-NMR measurement (mol %) | Total 2EHA in polymer (mass %) | Non-reinitiated macro-RAFT in total polymer from LC-CC (mass %) | **Percentage of total 2EHA contained in non-reinitiated macro-RAFT (mass %)** |
|---|---|---|---|---|
| LH-239 1h | 82.5 | 90.9 | 38.4 | **42.2** |
| LH-239 2h | 79.0 | 88.6 | 35.9 | **40.5** |
| LH-239 4h | 70.5 | 83,2 | 34.7 | **41.7** |

Combining these two values allowed us to estimate the percentage of 2EHA contained in the non-reinitiated macro-RAFT chains from the total polymerized 2EHA. The comparison of the values given in the 5$^{th}$ column of Table 24 shows that this amount remained nearly constant during the whole polymerization: around 41.5 %. This means that approximately 59 % of the macro-RAFT chains were reactivated during the first hour of polymerization and that non-reinitiated chains remained inactive till the end of the reaction.

Bathfield et al. found similar results when polymerizing in dispersion n-butyl acrylate with poly(N-acryloylmorpholine) as macro-RAFT agent [113]. They analyzed the supernatant of the latex after centrifugation with $^1$H-NMR and found that 55 % of the introduced macro-RAFT agent was indeed involved in the formation of the particles. Their measurement was done after 89 % conversion. This makes of course a difference with the low conversion (< 10 %) for LH-239 4h, but we have seen that the quantity of non-reinitiated macro-RAFT agent remains constant during the first four hours of polymerization and should remain so during the whole process.

***b) Determination of MMD for MA block***

We used the new LC-CC method for further experiments on the kinetic samples. As mentioned before, LC-CC for P2EHA separates copolymers only according to PMA block length, assuming that the P2EHA block was “invisible” for the chromatographic system. We used this specificity to determine the average molar masses of the PMA blocks after calibrating the system with PMMA standards. PMMA is more polar than P2EHA and eluted similar to the PMA block in the exclusion mode. Figure 66 shows an overlay of copolymer peaks for the first three kinetic samples with a molar mass calibrated X-axis. Table 25 summarizes the average molar masses determined with this method.

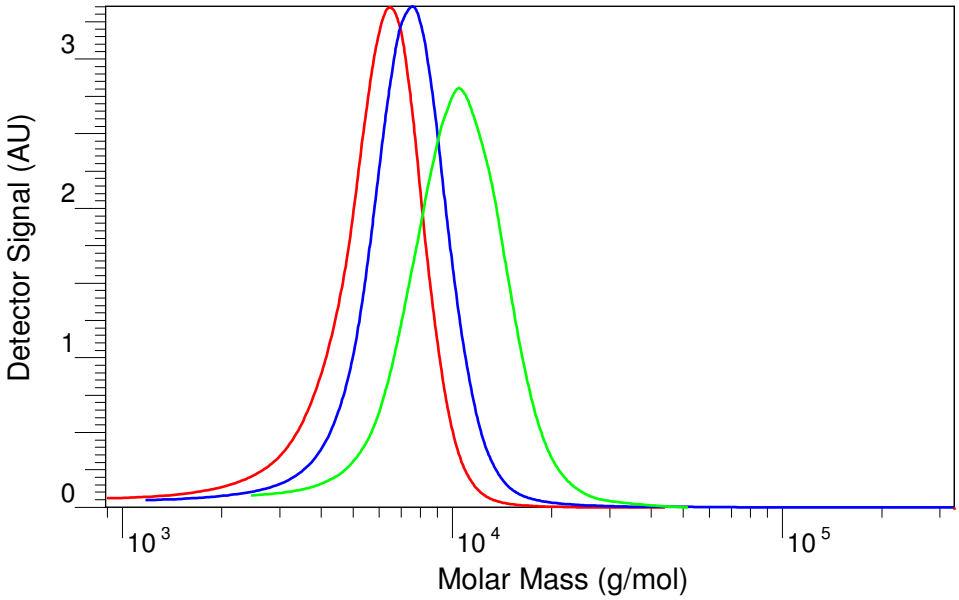


**Figure 66:** Copolymer peak overlay of (red) LH-239 1h, (blue) LH-239 2h, and (green) LH-239 4h at critical conditions of P2EHA. Experimental conditions see Figure 64; calibration: PMMA

**Table 25:** Average molar masses obtained after calibration of the system with PMMA standards of PMA blocks in binary copolymers determined from LC experiments at critical conditions for P2EHA

| | $\overline{M_n}$ (g/mol) | $\overline{M_w}$ (g/mol) | PDI |
|---|---|---|---|
| MA block of LH-239 1h | 4 500 | 5 800 | 1.29 |
| MA block of LH-239 2h | 6 200 | 7 900 | 1.27 |
| MA block of LH-239 4h | 8 800 | 12 000 | 1.36 |

The values given in Table 25 refer only to PMA block as copolymer chains eluted irrespective of the P2EHA block. The determined average molar masses for the PMA block by the LC-CC method are comparable to molar masses which could be calculated by subtracting the molar masses of the macro-RAFT from those of the copolymers in 2D-LC experiments. This confirms the separation mechanism and allows a more advanced characterization of the block copolymers as molar masses can be estimated for each block separately.

The molar mass distributions of the PMA blocks obtained with LC-CC are all monomodal. However, macromolecules resulting from coupling of two intermediate radicals are assumed to have two PMA blocks and should elute as if the PMA block was twice as long as that of expected diblock copolymers [114].These chains are thus included in the PMA molar mass calculations given in Table 25. This causes an overestimation of molar masses.

The lack of resolution results of the low efficiency in terms of size exclusion separation of the LC-CC system. In order to overcome this problem, we set up a 2D-LC system coupling SEC and LC-CC separations. Such system should first separate the macromolecules according to

their global size in solution (SEC) and thus fractions containing molecules with identical hydrodynamic volumes should be separated according to the length of their MA block length. The advantage of placing SEC in first dimension is that its resolution is better than that of LC-CC giving more homogeneous fractions.

### 2.2.5. 2D-LC SEC x LC-CC: Determination of molar mass for each species

With the previous analyses, we detected four kinds of macromolecules present in the kinetic polymer samples taken during the first four hours: non-reinitiated macro-RAFT, terminated macro-RAFT with doubled molar masses, the expected binary copolymer and terminated binary copolymer chains also with doubled molar masses. We developed a 2D-LC system coupling SEC and LC-CC for P2EHA in order to characterize all four species with regard to molar mass distribution and chemical composition and with regard to the average molar masses of the PMA blocks. In this case SEC separation was used as the first dimension. Each kind of chain eluted according to its hydrodynamic volume in THF. The separation was expected to be similar to that presented in Figure 59 except that the experiment time was increased since flow rate was decreased to 0.04 mL/min. The total mobile phase volume eluting from the SEC columns was transferred into the LC-CC system in fractions of 100 µL each. This second step was meant to discriminate P2EHA homopolymer from copolymer of identical hydrodynamic volume. Thanks to this method we were able to isolate all four polymer species present in the copolymer kinetic samples. Figure 67 shows 2D-LC chromatograms obtained with these conditions for samples LH-239 2h and 4h. Table 26 gives the quantification results obtained from these experiments.

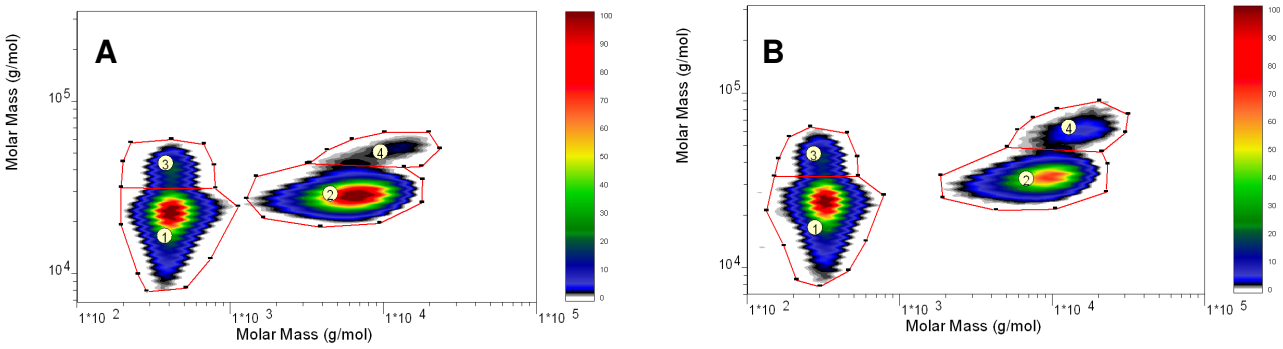


**Figure 67:** 2D-LC chromatograms of (A) LH-239 2h, (B) LH-239 4h. 1st Dimension: SEC in THF at 0.04 mL/min on PSS SDV $10^3$, $10^4$, $10^5$ Å. 2nd Dimension: LC-CC isocratic ACN:THF 46 54 % v/v at 1.0 mL/min on 2 x PLRP-S. Calibration: PMMA, Detection: ELSD

**Table 26:** Relative volume and average molar mass obtained after calibration of the system with PMMA standards for each peak of the 2D-LC diagrams given in Figure 67.

| | Peak n° | Relative peak volume (%) | $\overline{M_n}$ (g/mol) LC-CC | $\overline{M_w}$ (g/mol) LC-CC | PDI LC-CC | $\overline{M_n}$ (g/mol) SEC | $\overline{M_w}$ (g/mol) SEC | PDI SEC |
|---|---|---|---|---|---|---|---|---|
| LH-239 2h | 1 | 41 | - | - | - | 20 000 | 21 500 | 1.08 |
| | 2 | 51 | 6 100 | 7 200 | 1.18 | 28 000 | 28 500 | 1.02 |
| | 3 | 6 | - | - | - | 39 500 | 40 000 | 1.01 |
| | 4 | 2 | 10 100 | 11 900 | 1.18 | 52 000 | 52 500 | 1.01 |
| LH-239 4h | 1 | 50 | - | - | - | 21 000 | 22 500 | 1.07 |
| | 2 | 38 | 8 300 | 9 700 | 1.17 | 32 500 | 33 000 | 1.02 |
| | 3 | 7 | - | - | - | 42 000 | 43 000 | 1.02 |
| | 4 | 5 | 13 700 | 15 800 | 1.15 | 61 000 | 62 500 | 1.02 |

Figure 67A and Figure 67B illustrate the expected separation of the four polymer species. Spot assignment was done as follows:

- Spot 1 corresponds to non-reinitiated macro-RAFT. Average molar masses given in Table 26 fit well with previous SEC results already discussed.
- Spot 3 was attributed to terminated P2EHA by combination of two macro-RAFT chains. This hypothesis is confirmed by the estimated molar masses for this spot which are almost two times higher than those of spot 1. These two spots eluted at the system dead volume of the second dimension.
- Spot 2 is expected to be the binary copolymer of 2EHA and MA. An increase of the molar masses can be noticed from sample LH-239 2h to LH-239 4h. This indicates the growth of the PMA block. The polydispersity calculated from SEC measurements is very low indicating that these chains grew under controlled RAFT conditions. For this spot we also determined the average molar masses for the PMA blocks through LC-CC experiments. The molar mass values, given in Table 26, roughly correspond to the difference found between non-reinitiated macro-RAFT and binary copolymer molar masses. The molar masses from LC-CC experiments are, as previously mentioned, less reliable than those obtained from SEC experiments but are completely in agreement with the expected values.
- Spot 4 was attributed to terminated copolymer species formed by combination of two binary copolymer chains. Average molar masses obtained from SEC (first dimension) again confirm the idea of chain termination by combination as molar masses are doubled

from spot 2 to spot 4. For both samples, the polydispersity for spot 4 remained very low as well. This tends to indicate that macromolecules forming this peak resulted from controlled polymerization. Uncontrolled growth of the PMA block should have led to copolymers with higher polydispersity. The PMA block average molar masses determined for this spot are lower than expected. This might be caused by the architecture of the macromolecules which could be seen as triblock copolymers with a PMA block enclosed by two P2EHA blocks. Therefore, it is likely that, even if these latter blocks should have been chromatographically invisible, they played a role and slightly increased retention time, i.e. decreased molar masses of the PMA blocks.

Thus the peak assignment corresponds to that done in Figure 62. The schematic representations of the most probable polymer architecture for each spot can be found in Table 23.

It should be reminded that the relative peak volumes given here are determined from ELSD detection which is dependent on elution volume and chemical composition of the polymers. Only a comparison of the peak volumes for chemically identical species (spot 1 with 3 and spot 2 with 4) seems to be pertinent. Doing so reveals that approximately the same amount of terminated macro-RAFT chains was present in both samples, relative to the total amount of non-reinitiated P2EHA. This amount was estimated to be 12 % of P2EHA homopolymer. On the contrary, the comparison of Figure 67A and Figure 67B shows an increase of terminated copolymer chains during polymerization. We estimated the amount of terminated copolymer to the total amount of copolymer at 4 % for sample LH-239 2h and at 12 % for LH-239 4h.

Combining the results obtained with LC-CC after the calibration of the ELSD and by 2D-LC, the shoulder found in the SEC experiments (Figure 59) for sample LH-239 2h could be estimated to be 7 % of the total sample: around 4.5 % of terminated macro-RAFT agent and only 2.5 % of terminated copolymers. For sample LH-239 4h the shoulder should be composed of approximately 4.2 % terminated P2EHA homopolymer and 7.8 % of terminated copolymers which make roughly 12 % of total sample and explain the enlargement of the shoulder. These two steps were complementary to properly estimate the amount of terminated chains in both kinetic samples.

### 2.2.6. SEC-NMR: determination of chemical composition

Finally, to get more information on macromolecules constituting the shoulder of the SEC chromatograms, we performed SEC analyses coupled on-line with a Bruker 400 MHz NMR spectrometer.

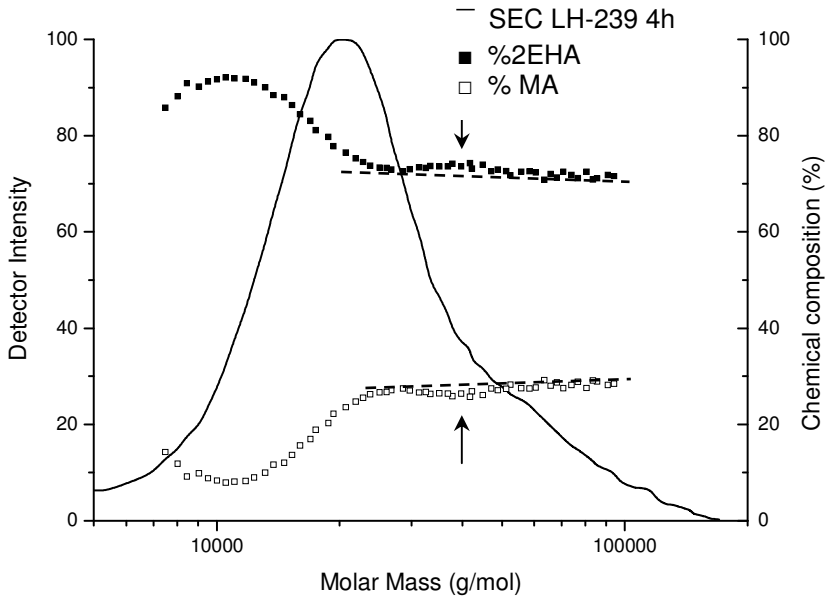


**Figure 68:** Chromatogram of polymer LH-239 4h (red) presented with calculated chemical composition from NMR measurements. Columns: PSS SDV $10^4$, $10^5$ Å and PL gel mixed-D; mobile phase: $CHCl_3$; detection: Bruker NMR 400 MHz; calibration: PMMA

By monitoring the intensity profiles of the O-CH signals at 3.90 ppm (characteristic for 2EHA) and the O-$CH_3$ signals at 3.64 ppm (characteristic for MA) as a function of elution volume, we were able to determine the chemical composition of the eluting peaks during the SEC separation. The SEC separation was performed in chloroform instead of THF to avoid any overlap of sample and solvent NMR signals. Even though the column set was not as efficient as the previous one and the new eluent impeded separation efficiency (decrease of solvent quality) a shoulder could nevertheless be seen. Figure 68 presents the SEC chromatogram of sample LH-239 4h. The chemical composition is plotted as a function of molar mass.

According to Figure 68 small molecules contain a higher amount of 2EHA as compared to large molecules. This likely corresponds to the non-reinitiated macro-RAFT which overlaps with the last eluting part of the copolymer.

As can be seen in Figure 68, for molecules larger than 25 000 g/mol average chemical composition remains nearly constant, i.e. approx. 70 mol % of 2EHA and 30 mol % of MA,

even for the largest molecules. This tends to indicate that molecules constituting the shoulder in SEC traces are terminated chains formed by coupling a growing chain with a dormant one. Only in this case, the ratio of 2EHA and MA monomers in the large macromolecules could be respected. Indeed an uncontrolled growth of the PMA block would have inversed the chemical composition in favor of MA and no 2EHA monomers are present at this stage of the reaction to maintain the ration constant.

We expected a certain increase of the 2EHA percentage at a molar mass of around 40 000 g/mol, corresponding to the terminated macro-RAFT made from combination of two macro-RAFT chains. In Figure 68, a small increase of the 2EHA content and a small decrease of the MA percentage can indeed be observed in this region which is stressed by the two arrows. This again proves the formation of such chains during the RAFT polymerization.

From the same experiment we determined the number of 2EHA and MA repeat units present in macromolecules for each molar mass. Combining these values with the total intensity of NMR spectra (chemigram) we were able to calculate the percentage of chains containing a given number of each repeat unit. We plotted the number of repeat units versus the cumulative percentage (see Figure 69). Calculating the derivatives and finding their maximum gave us the quantity of each monomer which is found in the majority of the macromolecules.

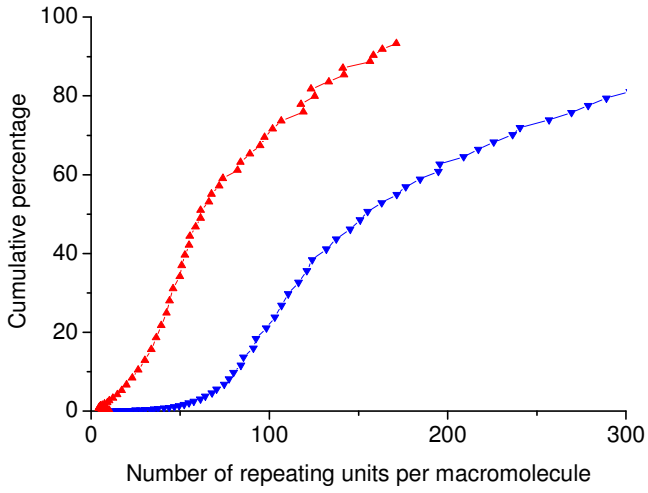


**Figure 69:** Number of repeat units (blue) 2EHA and (red) MA versus cumulative percentage determined from SEC-NMR experiment

Maximum of derivatives from the plots presented in Figure 69 were found to be 106 of 2EHA and 49 of MA repeat units. It could be interpreted as follow: the majority of the chains contain ~ 105 2EHA repeat units and the chains containing MA (PMA homopolymer if present as such macromolecule was not detected, and all kind copolymers) have ~ 50 of these repeat units.

These values are close to those theoretically expected in case of a completely controlled RAFT polymerization: 114 repeat units of 2EHA and 50 of MA. However, we have seen that polymerization in dispersion produces a large variety of products. This is confirmed by the plots in Figure 69, as the increase of the sigmoid is not abrupt as it should be if all molecules would have had the same chemical composition.

### 2.2.7. Conclusions

RAFT copolymerization in dispersed media allows in-situ production of polymer particles to be directly used in cosmetic formulations. Analysis of the particle size distribution showed that the control over the polymerization procedure was not totally efficient during the entire time of the synthesis. It is then assumed that side reactions occurred forming various kinds of by-products. An analytical strategy has been set up to comprehensively characterize the kinetic samples in order to better understand the deviations which occurred. SEC and gradient HPLC experiments already revealed certain heterogeneities of the products in terms of molar mass and chemical composition, respectively. Coupling these two techniques in a 2D-LC system gave us more precise information on these by-products. Non-reactivated macro-RAFT agents as well as terminated copolymers with doubled molar masses were detected. The position of the spot of these latter molecules in the 2D-LC plots informed us more precisely on their chemical composition. With such information and knowing the conditions of the synthesis it was possible to give a hypothesis of the formation of these by-products.

Using LC-CC separation it was possible, after calibration of the ELSD, to quantify the amount of non-reactivated macro-RAFT. Combining these results with chemical composition quantifications obtained from $^{1}$H-NMR, it was possible to determine the percentage of 2EHA present in the copolymers.

A second 2D-LC method coupling SEC and with this LC-CC separation was developed. After molar mass calibrations of both dimensions it was possible to characterize precisely all four components identified in the first kinetic samples.

Finally on-line coupling of SEC with $^{1}$H-NMR allowed us to determine the average chemical composition as a function of the molar mass. This was of great interest to confirm the previous results.

# V. Experimental Part

***a) Chromatographic equipment:***

Separations were carried out on a Shimadzu system (Kyoto, Japan) comprising a DGU-14A degasser, a FCV-10ALvp solvent mixing chamber, a LC-10ADvp pump and a SL 10ACvp auto sampler. The temperature was regulated with a column oven model K4 from Techlab. For detection, an evaporative light scattering detector, ELSD 1000 (Polymer Laboratories, Church Stretton, England) and/or a UV detector UV-2000 (Thermo Scientific, Waltham, MA, USA) and/or a differential refractive index detector Waters 450 (Waters, Milford, MA, USA) was used. For data collection and processing the software package "WinGPC-Unity" software v. 7.0" (Polymer Standards Service GmbH, Mainz, Germany) was used.

For two-dimensional chromatography, sample fractions from the first dimension were transferred to the second dimension column via an electronically controlled eight-port valve system (type EHC8W, VICI Valco instruments, Houston, Texas, USA), with two 100 µL loops. The second dimension consisted of a Shimadzu LC-10ATvp pump.

A HPLC system Agilent 1100 (Santa Clara, CA, USA) consisting of a degasser, a quaternary gradient pump and an auto sampler, was used for the SEC-NMR measurements. The volume injected was 50 µL.

***b) Chromatographic columns:***

*SEC*:

- set of three columns **PSS SDV $10^3$, $10^4$, $10^5$ Å**, each 300 x 8 mm I.D. (Polymer Standards Service, Mainz, Germany)
- **PL HTS-C**, 150 x 7.5 mm I.D. (Polymer Laboratories, Church Stretton, England)
- **PL Rapide M**, 150 x 7.5 mm I.D. (Polymer Laboratories, Church Stretton, England)
- **PL Rapide M**, 100 x 10 mm I.D. (Polymer Laboratories, Church Stretton, England)

*Gradient HPLC and LC-CC*:

- **Chromolith C18**, 100 x 4.6 mm I.D. (Merck KGaA, Darmstadt, Deutschland)
- **PLRP-S**, 150 x 4.6 mm I.D., **5 µm** particle size (Polymer Laboratories, Church Stretton, England)
- **PLRP-S**, 150 x 4.6 mm I.D., **8 µm** particle size (Polymer Laboratories, Church Stretton, England)
- **Luna RP-18**, 30 x 4.6 mm I.D., 3 µm particle size (Phenomenex, Torrance, CA,USA)

***c) Solvents:***

Acetonitrile (ACN), methanol (MeOH), methylethylketone (MEK), cyclohexane (cHex) and toluene were purchased from VWR (West Chester, PA, USA) and are all HPLC grade.

Tetrahydrofuran (THF) was freshly distilled.

***d) Polymer standards:***

All narrow distributed polymer standards of poly(methyl methacrylate) (PMMA) or polystyrene (PS) are synthesized and distributed by Polymer Standards Service GmbH (Mainz, Germany)

***e) Samples:***

All samples were laboratory products from L'Oréal (Paris, Farnce).

***f) Molar mass analysis by MALDI-ToF-MS:***

Mass spectra were realized with a Kompact MALDI IV MALDI-ToF-Mass Spectrometer (Kratos Analytical-Shimadzu, Kyoto, Japan). Spectra were recorded and integrated with the software Kompact.

Matrix was composed of dihydroxybenzoic acid dissolved in THF at a concentration of 10 g/L.

***g) LC-FTIR interface and FTIR spectrometer:***

LC-FTIR coupling was made possible using a LC-Transform 600XY system (LabConnections, Carrboro, NC, USA). After evaporation of the mobile phase samples were deposited on square Germanium plates (55 x 55 mm).

Sample FTIR analyses were carried out on a Nicolet Protégé 460 FTIR spectrometer (Thermo Scientific, Waltham, MA, USA). FTIR spectra were obtained after double pass of the laser beam through the samples, the energy being reflected by an Aluminium layer on the lower surface of the Germanium plate. Spectra were recorded between 800 and 4000 $cm^{-1}$ each 2 mm along the sample deposit. Each data point consisted of 32 scans.

Data acquisition and treatment were performed with the software Omnic developed by the spectrometer manufacturer.

***h) NMR:***

NMR experiments were executed on a 400 MHz spectrometer AVANCE (Bruker Biospin GmbH, Rheinstetten, Germany).

Direct 1H-NMR spectra were measured in 5 mm tubes on samples dissolved in deuterated chloroform ($CDCl_3$) (Euriso-Top, Saint-Aubin, France).

LC-NMR measurements were performed with a flow probe containing a 60 µL flow cell. The probe was a $^{1}H$ {$^{13}C$} inverse detection probe equipped with a shielded pulsed field-gradient coil. The gradient strength was 53 G/cm. The 90° $^{1}H$ pulse was 4.6 µs. WET solvent suppression was applied to $CHCl_3$. One frequency was suppressed. Sixteen scans per free induction decay (FID) were acquired with an acquisition time of 1.1 s (16 K data points) and a relaxation delay of 0.1 s.

# VI. Summary and Conclusions

The fast growing cosmetic market and the need for innovative products with new or combined properties lead to the development of a large variety of new complex polymer materials. The variations which can be achieved by modifying the monomer composition or the method of synthesis are very useful to produce (co)polymers with peculiar properties. The demand in characterization is then very important to understand the molecular structure of these new products in order to relate them with the observed properties aiming at the establishment of structure-property relationships. Such knowledge allows for optimization of the parameters of the synthesis and consequently the final application properties.

The aim of this work was to develop analytical methods and tools to comprehensively characterise the heterogeneities of acrylate- and methacrylate-based copolymers. The focus of the method development was on multidimensional chromatographic techniques that allow the different parameters of molecular heterogeneity (e.g. molar mass distribution, MMD, chemical composition distribution, CCD) to be described quantitatively.

The copolymers under investigation were different with regard to their monomer composition and the polymerization process used for their synthesis. The first set of samples was prepared according to a two-step free radical polymerization (FRP) process. The first step consisted of the random copolymerization of two monomers. A third monomer was then added during the second step to form a complex terpolymer. Five different monomers were combined: isobornyl acrylate (iBorA), isobornyl methacrylate (iBorMA), isobutyl acrylate (iBuA), isobutyl methacrylate (iBuMA) and 2-ethylhexyl acrylate (2EHA).

The second set of samples consisted of two kinds of diblock copolymers obtained by controlled radical polymerization (CRP). The first one was synthesized using Atom Transfer Radical Polymerization (ATRP) using a two-step process. During the first step, a homopolymer of iBuA was produced exhibiting a narrow MMD. This first block was used during the second step as an ATRP macro-initiator to copolymerize iBorMA and iBorA, these two monomers forming the second block. The second diblock copolymer was also formed by a two-step process but this time according to the Reversible Addition Fragmentation Chain Transfer (RAFT) process. The first block was composed of 2EHA having the controlling dithiobenzoate (DTB) function at its end. Using the living character of the RAFT

polymerization, the second block was produced by adding methyl acrylate (MA) monomers after re-activation of the macro-RAFT agent.

The results of the present thesis can be summarized as follows:

1\ Chromatographic methods were developed to characterize the polymers synthesized according to the two-step FRP process. The SEC method gave access to the molar mass distributions of the samples. As expected with FRP, the distributions were very broad since no control was possible over the synthesis. Moreover, the two-step process increased the polydispersity of the samples. Nevertheless it was observed in all cases that the distributions remained monomodal. Gradient HPLC was employed to analyze the chemical composition distributions of the samples. The method allowed for the separation and identification of all the species present in the samples. The by-products in the terpolymers were isolated and identified as being homopolymers of the third added monomer and binary copolymers of the first step monomers. Integrating the chromatographic peak areas gave a first approximation of the quantity of each kind of macromolecules present in the samples. The proportion of each kind of the three species was very dependent on the nature of the monomers used. All these results were valuable to understand the heterogeneity of the samples but were nevertheless insufficient to completely describe polymer complexity. For this reason, 2D-LC methods were developed where chemical composition separation was combined with molar mass separation. Indeed 2D-LC experiments enabled direct combination of information on these two different distributions of the samples. It was then possible to attribute average molar masses to the three kinds of macromolecules present in the samples. Developing a fast 2D-LC system was also one of our concerns. Such method could give a fingerprint of the samples prepared according to specific process. It could then be used as a quality control tool for polymers synthesized with the same process.

2\ In order to validate the peak assignment and to get more precise and quantitative information on the CCD of the samples, the developed chromatographic methods were coupled off-line with a FTIR detector. A LC-Transform device was used to spray the separated macromolecules locally separated on a Germanium disk. After evaporation of the solvent the polymer fractions are present on the disk as thin solid films that can subsequently be analyzed. FTIR spectra of these fractions were then measured. The coupling technique was used to analyze samples containing iBorMA, iBorA (first step) and iBuA (second step) at different percentages. The construction of a calibration curve with reference polymers allowed to determine the average chemical composition as a function of the molar mass when

SEC was coupled with FTIR. The analysis of the different types of chains (homopolymers, binary or ternary copolymers) was done by using coupled gradient HPLC-FTIR. As was shown a linear fit could be found between the iBorA + iBorMA monomer content and the ratio of selected FTIR absorption bands. SEC-FTIR confirmed the presence of binary copolymers in the samples, originating from the first synthesis step. By gradient HPLC-FTIR coupling it was possible to estimate the amount of iBor(M)A repeating units in the terpolymers. Large differences were observed depending on the amount of monomer added in the second step used for the synthesis. It was also possible to determine the average chemical composition at the terpolymer peak maxima. This could be considered to be the chemical composition of the most abundant terpolymer macromolecules.

3\ It has been demonstrated that changing the polarity of the stationary phase in gradient HPLC leads to an inversion of the polymer elution order. This was interesting for the characterization of the residual binary copolymers present as by-products in the terpolymers containing iBorMA, iBorA (first step) and iBuA (second step) at different percentages. We developed a system in which the residual binary copolymers are eluted in the SEC mode whereas all the macromolecules containing iBuA were retained on the stationary phase (cyano-modified silica). This system ensured a complete separation of the different chains. For the calibration of the Evaporative Light Scattering Detector (ELSD) signal, reference binary copolymers at different concentrations were used. By plotting the detected peak areas as a function of the injected mass of binary copolymer the mass percentage of the samples corresponding to residual binary copolymers were determined. Combining these results with the total amount of iBorA and iBorMA present in the samples determined by $^{1}$H-NMR, we were able to determine the mass percentage of these monomers present in the terpolymers. These results were very valuable to understand the polymerization process as they tend to indicate that copolymerization of iBuA is favored during the second step in comparison to the terpolymerization.

4\ For the ternary diblock copolymers synthesized by ATRP it was possible to use the chromatographic systems developed for the FRP samples since they were produced with the same kind of monomers. These samples being produced by CRP, which suppose a control of the addition of the monomers to the chains, it was anticipated that the SEC trace would be a narrow Gaussian peak. This was indeed the case for the products of the first polymerization step (homopolymer of iBuA). However, bimodal distributions for the kinetic samples were observed with one peak for low molar masses and one for high molar masses and a broad asymmetrical peak for the final products. This, of course, indicated a loss of control during

the reaction. This hypothesis was confirmed by the gradient HPLC and the 2D-LC measurements. It appeared that oligomers were formed in the first phase of the second synthesis step (copolymerization of iBorA and iBorMA). Their formation was supposed to be the consequence of transfer reactions onto the metal ligand used for the synthesis. It appeared that the bromine atom, regulator of the ATRP synthesis, was transferred to these oligomers. Indeed, the amount of these species tended to decrease with polymerization time and larger binary and ternary copolymers were progressively formed. In the case of transfer reactions followed by FRP, no oligomers would have been found and high molar mass products would have been detected in the early stage of the second polymerization step. Once again, it was confirmed how useful the chromatographic characterization is to explain and understand the synthesis process. In the present case 2D-LC was a very precious tool as unexpected results were obtained in each one-dimensional experiment (SEC and gradient HPLC). The direct combination of both separations enabled to elucidate the different reactions which occurred during the whole synthesis.

5\ The monomers used to produce the last kind of samples were slightly different from those used in the previous synthesis: 2EHA and MA. These monomers were copolymerized using a two-step RAFT procedure to form diblock copolymers which are able to auto-assemble during the synthesis to form particles. 2EHA was polymerized first forming a macro-RAFT agent followed by the addition of MA during the second step. The chromatographic methods used for the previous samples needed to be adapted to these samples, especially the gradient HPLC method. The SEC results suggested a certain loss of control during the RAFT polymerization as shoulders at the main peak or bimodal distributions were observed. Optimized gradient HPLC analysis made clear that a large part of the P2EHA was not re-activated during the second step and remained as homopolymer. Using an UV detector allowed to show that these macromolecules lost their DTB (only molecule absorbing at 300 nm) end group which was responsible for the living character of the chains. Finally, analyzing kinetic samples with 2D-LC, combining gradient HPLC with SEC, it was possible to better understand the evolution of the products during the polymerization. According to the peculiar position of the by-product spot in the 2D-LC diagram (double molar mass and lower polarity than the expected diblock copolymer) it was possible to formulate a hypothesis for the most probable side-reaction being the recombination of intermediate radicals at the surface of the particles. Apparently, this latter kind of reaction and free radical polymerization (characterized by the presence of PMA after eight hours of synthesis), that simultaneously

occurred as the RAFT polymerization progressed, are likely to be responsible for the loss of control over the synthesis.

6\ LC-CC was of great interest to better characterize the RAFT synthesized diblock copolymers. By working at very specific conditions of temperature and mobile phase for a given stationary phase corresponding to the critical conditions for P2EHA, it was possible to elute the 2EHA block at the void volume of the system and elute the MA block in exclusion conditions. As expected the copolymer chains were eluted only as a function of the length of the PMA block irrespective of the chain length of the P2EHA block. In such conditions and after performing a molar mass calibration of the system, it was possible to determine the molar mass distribution of the PMA block as if it was a homopolymer although it is part of a copolymer. This method showed that the size of the PMA block increased with increasing reaction time. We took advantage of this separation to quantify the amount of 2EHA repeating units present in the non re-activated chains. This was possible by calibrating the ELSD with P2EHA references. These results were combined with the total amount of 2EHA contained in the samples obtained by $^{1}$H-NMR measurements. It was thus possible to calculate the mass percentage of 2EHA repeating units present in the diblock copolymers. It appeared that this amount remained constant within four hours of synthesis. This would suggest that all P2EHA chains located in the copolymers were formed during the first hour of polymerization. This had to be related to the fact that the diblock copolymers form particles at a relative early stage of the synthesis. From this point on, it was likely that the polymerization only (or mainly) took place in the particles and no more in the continuous phase. Nevertheless, it was insufficient to properly characterize the MA block since the chromatographic system was not able to separate the active diblock copolymers from the terminated (recombined) copolymers. To realize this separation we set up a 2D-LC system combing SEC with the LC-CC separation. This method, after calibration, allowed to determine the average molar masses for each block of all of the four types of macromolecules identified.

7\ An on-line coupling of the SEC separation with $^{1}$H-NMR was developed for the RAFT synthesized copolymers. Such technique was expected to provide a direct quantification of the average chemical composition as a function of molar mass. It is interesting as it delivers results without the need of a calibration curve. Nevertheless a lot of efforts had to be made for setting up the method and there were a number of limitations for the implementation of the method. The main difficulty was the set-up of a solvent suppression method due to the necessity to change the mobile phase from THF to chloroform to avoid a signal overlapping between the signal and the large amount of sample which must be injected to obtain an

efficient signal. This had a significant effect on the quality of the separation. The results obtained for the RAFT synthesized products were nevertheless interesting. It was possible to plot the average content of 2EHA in the chains as a function of the molar mass directly and without any calibration. The peak corresponding to the non-reactivated homopolymer was clearly observable and even the terminated P2EHA chains with a doubled molar mass were detected.

In conclusion, it has been demonstrated that a significant variety of different separation and analysis tools is required to fully understand the molecular heterogeneity of complex copolymers. Even products that apparently are prepared by well-defined synthetic procedures exhibit a remarkable complexity in chemical composition and molar mass. The most feasible approach is the (if possible) on-line combination of different chromatographic methods and the hyphenation of liquid chromatography with FTIR and $^{1}$H-NMR. These complex analytical tools, however, require the development of dedicated experimental procedures.

# VII. List of Abbreviations and Symbols

| | |
|---|---|
| 2D-LC | Two-Dimensional Liquid Chromatography |
| 2EHA | 2-ethylhexyl acrylate |
| ACN | Acetonitrile |
| $A_i$ | Light absorption by the component i |
| APCI | Atmospheric Pressure Chemical Ionization |
| ATRP | Atom Transfer Radical Polymerization |
| *c* | Interaction parameter |
| C | Sample concentration |
| CCD | Chemical Composition Distribution |
| cHex | cyclohexane |
| CN | Cyano modified silica column |
| CRP | Controlled Radical Polymerization |
| *D* | Diameter of the stationary phase pores |
| *d* | Path length (distance that the IR irradiation travels through the material |
| DP | Degree of Polymerization |
| DTB | *tert*-butyl dithiobenzoate |
| ELSD | Evaporative Light Scattering Detector |
| erf | Error function |
| ESI | Electro-Spray Ionization |
| *F* | Mobile phase flow rate |
| FRP | Free Radical Polymerization |
| FTIR | Fourier Transform Infra Red |
| HPLC | High Performance Liquid Chromatography |
| I.D. | Internal Diameter |
| iBor(M)A | isobornyl methacrylate and acrylate |
| iBorA | isobornyl acrylate |
| iBorMA | isobornyl methacrylate |
| iBuA | isobutyl acrylate |
| iBuMA | isobutyl methacrylate |
| *k'* | Retention factor |

| | |
|---|---|
| $k'_0$ | Initial value of the retention factor |
| $K_d$ | Distribution coefficient |
| $K_{LAC}$ | Contribution of adsorption to distribution coefficient |
| $K_{SEC}$ | Contribution of size exclusion to distribution coefficient |
| $k'_{train}$ | Retention factor of a sequence of identical adsorbing repeat units |
| $k'_u$ | Retention factor of an adsorbing unit in a train |
| LAC | Liquid Adsorption Chromatography |
| LALLS | Low Angle Laser Light Scattering |
| LC | Liquid Chromatography |
| LC-CC | Liquid Chromatography at Critical Conditions |
| LRP | Living Radical Polymerization |
| MA | methyl acrylate |
| MALDI | Matrix Assisted Laser Desorption/Ionization |
| MALLS | Multiple Angle Laser Light Scattering |
| MEK | methylethylketone |
| MeOH | Methanol |
| MMA | methyl methacrylate |
| MMD | Molar Mass Distribution |
| $\overline{M_n}$ | Number average molar mass |
| MP | Mobile Phase |
| $\overline{M_w}$ | Weight average molar mass |
| $N$ | Number of bonds in a polymer chain |
| $n$ | Number of adsorbing repeat units in a train |
| NMP | Nitroxide Mediated Polymerization |
| NMR | Nuclear Magnetic Resonance |
| P2EHA | poly(2-ethylhexyl acrylate) |
| PCM | Polymer Chromatographic Model |
| PDI | Polydispersity Index |
| PEG | poly(ethylene glycol) |
| PiBor(M)A | poly(isobornyl methacrylate and acrylate) |
| PiBorA | poly(isobornyl acrylate) |
| PiBorMA | poly(isobornyl methacrylate) |
| PiBuA | poly(isobutyl acrylate) |

| | |
|---|---|
| PiBuMA | poly(isobutyl methacrylate) |
| PMA | poly(methyl acrylate) |
| PMDETA | N,N,N',N'',N''-pentamethyldiethylenetriamine |
| PMMA | poly(methyl methacrylate) |
| PS | polystyrene |
| $R$ | Gas constant |
| RAFT | Reversible Addition Fragmentation chain Transfer |
| $R_g$ | Polymer radius of gyration |
| RI | Refractive Index Detector |
| RP | Reverse Phase |
| SEC | Size Exclusion Chromatography |
| SP | Stationary Phase |
| $T$ | Absolute temperature |
| T21S | *tert*-butyl peroxy-2-ethylhexanoate |
| $T_g$ | Glass transition temperature |
| THF | Tetrahydrofuran |
| ToF-MS | Time-of-Flight Mass Spectrometer |
| $t_r$ | Retention time |
| $V_0$ | Hold-up volume of the system |
| $V_1$ | Total system volume |
| $V_{dw}$ | Dwell volume of the system |
| $V_e$ | Elution volume |
| $V_i$ | Column interstitial volume |
| $V_p$ | Pore volume of the HPLC column |
| WET | Water suppression through T1 effects (NMR solvent suppression technique) |
| $\Delta G$ | Free Gibbs energy difference |
| $\Delta H$ | Change in interaction enthalpy |
| $\Delta S$ | Change in conformational entropy |
| $\varepsilon_{i,j}$ | Extinction coefficient for component i at the wavelength j |
| $\lambda$ | Light wavelength |
| $\Phi$ | Mobile phase composition |
| $\Phi_0$ | Mobile phase composition in initial gradient conditions |
| $\Phi_e$ | Mobile phase composition at elution |
| $\omega_i$ | Molar fraction of component i |

# VIII. Bibliographic References

[1] INTERNATIONAL COSMETIC INGREDIENT DICTIONARY AN HANDBOOK, vol. 1-3, Cosmetic, Toiletry, and Fragrance Association, Washington, 7th edition, 1997

[2] Jachowicz J, ANALYSIS OF POLYMERS FOR COSMETICS, International Federation of the Societies of Cosmetic Chemists, 2004

[3] Pasch H, Trathnigg B, HPLC OF POLYMERS, SPRINGER, Berlin, 1998

[4] Glöckner G, GRADIENT HPLC OF COPOLYMERS AND CHROMATOGRAPHIC CROSS-FRACTIONATION, Springer, Berlin, 1991

[5] Chang T, *J Polym Sci Pol Phys*, 43 (2005), 1591

[6] Cools PJCH, Maesen F, Klumpermann B, van Herk AM, German AL, *J Chromatogr A*, **736** (1996), 125-130

[7] Mori S, Taziri H, *J Liq Chromatogr R T*, **17** (1994) 3055-3068

[8] Mass V, Bellas V, Pasch H, *Macromol Chem Phys*, **209** (2008), 2026-2039

[9] Im K, Kim Y, Chang T, Leeb K, Choi N, *J Chromatogr A*, **1103** (2006), 235-242

[10] Kilz P, *Labor Praxis*, **6** (1993), 64

[11] Kilz P, *Chromatographia*, **59** (2004), 3-14

[12] Adrian J, Esser E, Hellmann GP, Pasch H, *Polymer*, **41** (2000), 2439-2449

[13] Pasch H, Mequanint K, Adrian J, *e-polymers,* **2002**, 005

[14] Gao H, Min K, Matyjaszewski K, *Macromol Chem Phys*, **207** (2006), 1709–1717

[15] Matyjaszewski K, *Materials Today*, **8** (2005), 26-3

[16] Moad G; Solomon DH, THE CHEMISTRY OF FREE-RADICAL POLYMERIZATION; Pergamon: Oxford, England 1995

[17] Mayo FR, Lewis FM, *J Am Chem Soc*, **66** (1944), 1594–1601

[18] Houillot L, Bui C, Save M, Charleux B, Farcet C, Moire C, Raust J-A, Rodriguez I, *Macromolecules*, **40** (2007), 6500 -6509

[19] Kowalewski T, McCullough RD, Matyjaszewski K, *Eur Phys J E*, **10** (2003), 5-16

[20] Braunecker WA, Matyjaszewski K, *Prog Polym Sci,* **32** (2007), 93-146

[21] Braunecker WA, Matyjaszewski K, *Prog Polym Sci*, **33** (2008), 165

[22] Matyjaszewski K, Davis TP, HANDBOOK OF RADICAL POLYMERIZATION, Wiley-Interscience, Hoboken, NJ, 2002

[23] Moad G, Solomon DH, THE CHEMISTRY OF FREE RADICAL POLYMERIZATION, 2ND, Elsevier, Amsterdam, 2006

[24] Hawker CJ, Bosman, AW, Harth E, *Chem Rev*, **101** (2001), 3661

[25] Kamigaito M, Ando T, Sawamoto M, *Chem Rev*, **101** (2001), 3689

[26] Matyjaszewski K, Xia J, *Chem Rev*, **101** (2001), 2921

[27] Moad G, Rizzardo E, Thang SH, *Aust J Chem*, **58** (2005), 379

[28] Monteiro MJ, *J Polym Sci Pol Chem*, **43** (2005), 3189

[29] Favier A, Charreyre, MT, *Macromol Rapid Commun*, **27** (2006), 653

[30] Hadjichristidis N, Iatrou H, Pitsikalis M, Mays J, *Prog Polym Sci*, **31** (2006), 1068-1132

[31] Qiua J, Charleux B, Matyjaszewski K, *Prog Polym Sci*, **26** (2001), 2083-2134

[32] Matyjaszewski K, Coca S, Gaynor SG, Wei M, Woodworth BE, *Macromolecules*, **31** (1998), 5967-5969

[33] Matyjaszewski K, *Prog Polym Sci*, **30** (2005), 858-875

[34] Matyjaszewski K, Shipp DA, McMurtry GP, Gaynor SG, Pakula T, *J Polym Sci Pol Chem*, **38** (2000), 2023-2031

[35] Richard RE, Schwarz M, Ranade S, Chan AK, Matyjaszewski K, Sumerlin B, *Biomacromolecules*, **6** (2005), 3410-3418

[36] Liu S, Armes SP, *Langmuir*, **19** (2003), 4432-4438

[37] Nicolas J, Couvreur P, Charleux B, *Macromolecules*, **41** (2008), 3758-3761

[38] Garnier S; Laschewsky A; Storsberg J, *Tenside Surfact Det*, **43** (2006), 88-102

[39] Charleux B, Farcet C, Burguiere C, Vairon J-P, *NATO Science Series II: Mathematics, Physics and Chemistry,* **175** (2004), 39-46

[40] Riess G, HANDBOOK OF INDUSTRIAL WATER SOLUBLE POLYMERS, 174-238, Blackwell Publishing (2007)

[41] Matyjaszewski K, Ziegler MJ, Arehart SV, Greszta D, Pakula T, *J Phys Org Chem*, **13** (2000), 775-786

[42] Norman G, Gaylord J, *J Macromol Sci A*, **26** (1989), 1211-1229

[43] Kowalewski T, McCullough RD, Matyjaszewski K, *Eur Phys J E*, **10** (2003), 5-16

[44] Ejaz M, Yamamoto S, Ohno K, Tsujii Y, Fukuda T, *Macromolecules*, **31** (1998), 5934-5936

[45] Kolb HC, Finn MG, Sharpless KB, *Angew Chem Int Edit*, **40** (2001), 2004-2021

[46] Opsteen JA, Van Hest JCM, *Chem Commun*, **1** (2005), 57-59

[47] Sumerlin BS, Matyjaszewski K, *Macromolecules*, **38** (2005), 7540-7545

[48] Asif A, Huang C, Shi W, *Colloid Polym Sci*, **283** (2004), 200-208

[49] Nowers JR, Broderick SR, Rajan K, Narasimhan B, *Macromol Rapid Commun*, **28** (2007), 972-976

[50] Pasch H, *Adv Polymer Sci*, **157** (2000), 1-66

[51] Albrecht A, Brüll R, Macko T, Sinha P, Pasch H, *Macromol Chem Phys*, **209** (2008), 1909-1919

[52] Guiochon G, *J Chromatogr A*, **1126** (2006), 6–49

[53] Neue UD, *J Chromatogr A*, **1079** (2005), 153-161

[54] Snyder LR, Dolan JW, Gant JR, *J Chromatogr*, **165** (1979), 3-30

[55] Martin AJC, *Biochem Soc Symp*, **3** (1949) 4

[56] Skvortsov A, Trathnigg B, *J Chromatogr A*, **1015** (2003), 31-42

[57] Stalcup AM, Martire DE, Wise SA, *J Chromatogr*, **442** (1988) 1-14

[58] Skvortsov AM, Fleer GJ, *Macromolecules*, **35** (2002), 8609-8620

[59] Bashir M, Radke W, *J Chromatogr A*, **1131** (2006) 130–141

[60] Casassa EF, Tagami Y, *Macromolecules*, **2** (1969), 14

[61] Bashir M, Radke W, *J Chromatogr A*, **1163** (2007), 86-95

[62] Mori S, Barth HD, SIZE EXCLUSION CHROMATOGRAPHY, Springer, 1999

[63] Grubisic-Gallot Z, Lingeiser J-P, Gallot Y, *Polym Bull*, **23** (1990), 389-395

[64] Kok SJ, Wold CA, Hankemeier Th, Schoenmakers PJ, *J Chromatogr A*, **1017** (2003) 83–96

[65] Hatada K, Kitayama T, NMR SPECTROSCOPY OF POLYMERS, Springer, 2007

[66] Glöckner G, van den Berg JHM, *J Chromatogr*, **550** (1991), 629-638

[67] Augenstein M, Müller MA, *Makromol Chem*, **191** (1990) 2151

[68] Gorbunov AA, Vakhrushev AV, *J Chromatogr A*, **1064** (2005) 169-181

[69] Trathnigg B, Maier B, Gorbunov A, Skvortsov A, *J Chromatogr A*, **791** (1997), 21-35

[70] Philipsen HJA, *J Chromatogr A*, **1037** (2004), 329–350

[71] Quarry MA, Stadalius MA, Mourey TH, Snyder LR, *J Chromatogr*, **358** (1986) 1-16

[72] Stadalius MA, Quarry MA, Mourey TH, Snyder LR, *J Chromatogr,* **358** (1986) 17-37

[73] Brun Y, Alden P, *J Chromatogr A*, **966** (2002), 25-40

[74] Falkenhagen J, Much H, Stauf W, Müller AHE, *Macromolecules*, **33** (2000), 3687-3693

[75] Jiang W, Khan S, Wang Y, *Macromolecules*, **38** (2005), 7514-7520

[76] Skvortsov AM, Gorbunov AA, *J Chromatogr*, **507** (1990), 487-496

[77] Orelli S, Jiang W, Wang Y, *Macromolecules*, **37** (2004), 10073-10078

[78] Macko T, Hunkeler D, *Adv Polym Sci*, **163** (2003), 61-136

[79] Baschir M, Brüll A, Radke W, *Polymer*, **46** (2005), 3223–3229

[80] Van der Horst A, Schoenmakers PJ, *J Chromatogr A*, **1000** (2003), 693–709

[81] Kilz P, Krüger RP, Much H, Schulz G, *ACS Adv Chem*, **247** (1995) 223-241

[82] Siewing A, Lahn B, Braun D, Pasch H, *J Polym Sci Polym Chem*, **41** (2003), 3143-3148

[83] Jiang X, van der Horst A, Lima V, Schoenmakers PJ, *J Chromatogr A*, **1076** (2005), 51-61

[84] Raust JA, Brüll A, Moire C, Farcet C, Pasch H, *J Chromatogr A*, **1203** (2008), 207-216

[85] Graef SM, van Zyl AJP, Sanderson RD, Klumperman B, Pasch H, *J Appl Polym Sci*, **88** (2003), 2530–2538

[86] Guiochon G, Marchetti N, Mriziq K, Schalliker RA, *J Chromatogr A*, **1189** (2008), 109-168

[87] Schoenmakers PJ, Vivó-Truyols G, Decrop WMC, *J Chromatogr A*, **1120** (2006), 282-290

[88] Ludlow M, Louden D, Handley A, Taylor S, Wright B, Wilson ID, *J Chromatogr A*, **857** (1999), 89-96

[89] Kok SJ, Hankemeier T, Schoenmakers PJ, *J Chromatogr A*, **1098** (2005), 104

[90] Willis JN, Dwyer JL, Liu MX, *Intl J Polym Anal Ch*, **4** (1997), 21-29

[91] Hiller W, Brüll A, Argyropoulos D, Hoffmann E, Pasch H, *Magn Reson Chem*, **43** (2005), 729-735

[92] Hiller W, Sinha P, Pasch H, *Macromol Chem Physic*, **208** (2007), 1965-1978

[93] Smallcombe SH, Patt SL, Keifer PA, *J Magn Reson Ser A*, **117** (1995), 295–303

[94] Kulkarni AS, Beaucage G, *J Polym Sci Pol Phys*, **44** (2006), 1395-1405

[95] Oppenheimer LE, Mourey TH, *J Chromatogr*, **323** (1985), 297-304

[96] Mourey TH, *Intl J Polym Anal Ch*, **9** (2004), 97-135

[97] Pasch H, Schrepp W, MALDI-TOF MASS SPECTROMETRY OF SYNTHETIC POLYMERS, Springer, 2003

[98] Spriestersbach KH, Rode K, Pasch H, *Macromol Symp,* **193** (2003), 129-141

[99] http://www.biochem.arizona.edu/classes/bioc471/pages/Lecture23/Lecture23.html

[100] Weidner S, Falkenhagen J, Krueger RP, Just U, *Anal Chem*, **79** (2007), 4814-4819

[101] Trimpin S, Weidner SM, Falkenhagen J, McEwen CN, *Anal Chem*, **79** (2007), 7565-7570

[102] Wilczek-Vera G, Yu1 Y, Waddell K, Danis PO, Eisenberg A, *Rapid Commum Mass Spectrom,* **13** (1999), 764–777

[103] van Herk AM, *Macromol Rapid Commun*, **22** (2001), 687-689

[104] Pasch H, Rode K, Chaumien N, *Polymer*, **37** (1996) 4079-4083

[105] Jiang X, van der Horst A, Schoenmakers PJ, *J Chromatogr A*, **982** (2002) 55

[106] Krämer I, Pasch H, Händel H, Albert K, *Macromol Chem Phys*, **200** (1999), 1734-1744

[107] Pasch H, Hiller W, *Macromolecules*, **29** (1996), 6556-6559

[108] Dervaux B, van Camp W, van Renterghem L, du Prez FE, *J Polym Sci Pol Chem*, **46** (2007), 1649-1661

[109] Corner T, *Adv Polym Sci*, **62** (1984), 95-142

[110] Huang J, Pintauer T, Matyjaszewski K, *J Polym Sci Pol Chem*, **42** (2004), 3285-3292

[111] Houillot L, PhD Thesis, POLYMERISATION PAR VOIE RAFT EN DISPERSION ORGANIQUE. SYNTHESE DE COPOLYMERES A BLOCS ET AUTO-ASSEMBLAGES SIMULTANES, Université Paris VI Jussieu, 2008

[112] Farcet C, French Patent FR 2881648, 2006

[113] Bathfield M, D'Agosto F, Spitz R, Charreyre M-T, Pichot C, Delair T, *Macromol Rapid Commun*, 28 (15) (2007), 1540-1545

[114] Guttman CM, Di Marzio EA, Douglas JF, *Macromolecules*, **29** (1996) 5723-5733

# Jacques-Antoine RAUST

**Geburtsdatum:** 30. November 1980
**Geburtsort:** Nîmes, Frankreich
**Staatsangehörigkeit:** französisch
**Familienstand:** verheiratet

## Ausbildung

**Baccalauréat** (entspricht dem deutschen Abitur) 1998, in Nîmes, Frankreich

**Docteur d'état en Pharmacie** (entspricht dem deutschen Diplom-Pharmazeut und Apotheker)
Université Montpellier (Sept. 1998-Juni 2000) und Paris XI (Sept. 2000-Juni 2005)
Diplomarbeit zum Pharmazeuten**:** *„Isolierung und Identifikation von Abbauprodukten des 3,4-Diaminopyridins"*
Vertiefte Kenntnisse in der „Formulierung und Bioverfügbarkeit von Wirkstoffen" und in „Qualitätskontrolle und -management".

**Diplom-Ingenieur Chemie an der „Ecole Nationale Supérieure de Chimie de Paris"**
(Sept. 2003-Juni 2005)
Diplomarbeit zum Ingenieur: *„Analyse der Copolymerzusammensetzung durch Gradienten HPLC"*
Chemie der Wirkstoffe in Medizin und Kosmetik: katalysierte Synthesen, Simulation und Analyse von industriellen, chemischen Reaktoren, analytische Methoden (präparative und analytische Chromatographie, Gel- und Kapillar- Elektrophorese, Spektralanalyse).

**Master of Polymer Science** an der Universität Paris VI (Sept. 2005-Jan. 2006)
Synthese von Polymeren und Charakterisierung der mechanischen, physikalischen und chemischen Eigenschaften.

**Promotion am Deutschen Kunststoff-Institut** (DKI) in Darmstadt in Kooperation mit L'Oréal, Paris (seit Feb. 2006)
Doktorarbeit: *„Entwicklung von mehrdimensionalen, chromatographischen Methoden für die Analyse komplexer Kunststoffe aus (Meth-)Acrylat Monomereinheiten"*.

Eidesstattliche Erklärung

Ich erkläre hiermit an Eides Statt, dass ich meine Dissertation selbständig und nur mit den angegebenen Hilfsmitteln angefertigt und noch keinen Promotionsversuch unternommen habe.

Darmstadt, den 17. Oktober 2008,

Jacques-Antoine Raust